Interference Management and Exploitation in Emerging Wireless Networks

by

Yi Xu

A dissertation submitted to the Graduate Faculty of
Auburn University
in partial fulfillment of the
requirements for the Degree of
Doctor of Philosophy

Auburn, Alabama
May 10, 2015

Keywords: Cellular Networking, Cognitive Radio Networks, Interference Management

Approved by

Shiwen Mao, McWane Associate Professor
Prathima Agrawal, Ginn Distinguished Professor of Electrical and Computer Engineering
Jitendra Tugnait, James B Davis Professor of Electrical and Computer Engineering
Ming Liao, Professor of Mathematics and Statistics

Abstract

In the past decade, with the prevalence of smart phones, the main use of cellphones has been shifted from phone call to multimedia access. This paradigm shift has resulted in the demand for higher and higher transmission rate. Many sophisticated physical layer techniques, such as IDMA (interleave division multiple access), OFDM (orthogonal division multiple access), MIMO (multiple input multiple output), IA (interference alignment) and massive MIMO) have been proposed to cater for this demand. Meanwhile, cognitive radio networks and femtocell networks are proposed to strengthen the cellular networks.

Given these new exciting techniques, how to incorporate them into current wireless networks is one of the main issues need to be addressed. Moreover, taking a close look at these techniques, how to manage interference so that the throughput can be enhanced is one of the most important problems.

The first part of this dissertation investigates how to incorporate IDMA into two-tier femtocell networks so that the throughput of femtocell networks can be enhanced. Based on the computational capability of the femtocells, three schemes are proposed for the femtocell networks.

The second part of this dissertation addresses the problem of incorporating interference alignment to OFDM and MIMO-OFDM system. We firstly prove the upper bound of the throughput with an integer programming formulation. Then considering practical constraints of the (MIMO) OFDM system, effective algorithms are proposed to approach the theoretical bounds.

In the third part of this dissertation, how will the primary user and secondary users equipped with multiple antennas behave in cognitive radio networks is studied. With a Stackelberg game formulation, we derive the unique Stackelberg game equilibrium for the primary user and secondary users. The proposed scheme is also shown to outperform the non-spectrum-leasing scheme and a cooperative scheme in the literature.

In the fourth part the this dissertation, the problem of incorporating massive MIMO to FDD system is addressed. To reduce the cost of acquiring channel state information, two-stage precoding was proposed. The problems of user grouping and user scheduling thus arise. Three user grouping schemes and a greedy user scheduling scheme are proposed and validated. The problem of load balancing when the number of user is small is studied as well. Effective algorithm is proposed to solve this load balancing problem.

In summary, this dissertation aims to enhance the throughput of current or future wireless systems by managing interferences among different data streams or different users or different base stations. In-depth analysis and comprehensive results are also provided. Some of the findings may shed light on how to put emerging techniques into real applications.

Acknowledgments

This dissertation could never have been finished without the guidance of my advisory committee, support from my family, and help from my friends.

First and foremost, I would like to express my deepest gratitude to my major advisor, Dr. Shiwen Mao, who provided me with excellent guidance, thoughtful care and persistent support. Dr. Mao led me into the research area of wireless networking, taught me many useful techniques, and gave me valuable advice on how to be a successful researcher. I will benefit from all these throughout my life. In addition, I want to thank Dr. Mao's wife, Dr. Yihan Li for her hospitality.

I would also like to thank my committee members, Dr. Prathima Agrawal, Dr. Jitendra Tugnait and Dr. Ming Liao. I learnt a lot from their courses and benefited so much from the discussions with them. I also give my special thanks to Dr. Guosen Yue from Broadcom, who offered me the opportunity for internship in the summer of 2013 and provided me with numerous advice thereafter.

I'm also indebted to Dr. Nedret Billor, who supervised my Master in Probabilities and Statistics, Dr. Peng Zeng and Dr. Asheber Abebe, who served as my committee members for my Master in Probabilities and Statistics.

I appreciate so much the friendship with my fellow students, including Dr. Donglin Hu, Dr. Yingsong Huang, Jing Ning, Yu Wang, Dr. Hui Zhou, Zhifeng He, Zhefeng Jiang, Xuyu Wang, Mingjie Feng, Yu Wang, Ningkai Tang, Lingjun Gao, and many others. We have spent such a happy and memorable time together in this lovely village.

I also want to thank my parents and grandparents. They inspired me to pursue the doctorate. Without their encouragement and support throughout my life, I could achieve nothing. Last, I want to thank my wife, Qiuyan Peng. She was always there and stood by me through the good times and the bad.

At last, this dissertation work was supported in part by the U.S. National Science Foundation (NSF) under Grants CNS-0953513, CNS-1247955, and CNS-1320664, and through the NSF Broadband Wireless Access & Applications Center (BWAC) at Auburn University. Any opinions, findings, and conclusions or recommendations expressed in this material are those of the author(s) and do not necessarily reflect the views of the NSF.

Table of Contents

List of Figures

List of Tables

Chapter 1

Introduction

The past decade has witnessed drastic increase of wireless data traffic, largely due to the so-called "smart phone revolution." As wireless data traffic is explosively increasing, the capacity of existing and future wireless networks will be greatly stressed. Many advanced physical layer techniques have been designed and proposed such as IDMA (interleave division multiple access), OFDM (orthogonal division multiple access), MIMO (multiple input multiple output), IA (interference alignment) and massive MIMO.

IDMA is essentially a multiple access scheme. Different from conventional TDMA (time division multiple access) and FDMA (frequency division multiple access), IDMA uses different interleaver to distinguish different users so that time and frequency can be multiplexed. OFDM divides the frequency band into small pieces of sub-bands, to combat the multi-path effect of the time disperse wireless channel so that the system throughput can be enhanced. The key idea of MIMO is to support multiple data streams while suppressing the interferences among different streams. Interference alignment manages interference in a different perspective. It suppresses the interferences into half of the signal space (or time, or frequency, et al.) of the receiver and keeps the other half free from interference. The base station of massive MIMO system is equipped with hundreds or even thousands of antennas. Users can be distinguished by their spatial locations. With that many antennas, the system throughput can be roaringly boosted. We can see that the key ideas of these transmission techniques to enhance system throughput is to support multiple data streams while keeping interferences under control.

Meanwhile, due to the tremendous increase in wireless data, radio spectrum is quickly depleted. However, according to the FCC report [1], while some licensed bands are overcrowded, many others are underutilized. Under traditional fixed spectrum allocation policy, when licensed

users (or, *primary users*) are not active, the channels assigned to them are wasted (termed as *spectrum opportunities*). Cognitive radio networks (CRN) are proposed as a new wireless paradigm for exploiting such spectrum opportunities, to enable flexible and efficient access to radio spectrum. In CRN, unlicensed users (or, *secondary users*) are allowed to access the licensed band opportunistically, while primary users gain by collecting revenue for spectrum leasing. Such a CR (cognitive radio) paradigm has been shown to have high potentials to enhance spectrum efficiency [2].

Moreover, femtocell, which is also called home base station, has also been proposed. Femtocell typically serves as an access point for use in home or small business. It is usually installed by wireless users for backhauling data to the service provider through a broadband gateway such as digital subscriber line (DSL), cable, et al. The most prominent feature of femtocell is that the transmission distances between wireless network infrastructure and users are greatly reduced, compared with that in traditional cellular networks. This brings about many benefits such as enhanced link quality, better signal to interference noise ratio (SINR), improved cellular capacity, and greatly reduced transmission power, among others.

A huge amount of wireless access networks/base stations (BS) or Femtocell base stations (FBS) are deployed every year to accommodate the compelling need for more capacity. Given the increasing wireless data volume, the increasingly crowded BS deployment and the potential interferences from the Secondary Users (SU) in CRN, interferences are becoming the major factor that limits wireless network performance.

To study the interference and throughput issues of cellular or cognitive radio networks so that the system throughput and the user experience can be enhanced are the main motivation of this dissertation.

Main contributions of this dissertation are summarized as follows.

- Taking the computational capabilities of femtocell into consideration, this dissertation studies how to apply IDMA to two-tier femtocell networks so that all kinds of interference are under well control. Three effective schemes are proposed to enhance the system throughput.

- Most of the existing works of interference alignment focus on structureless wireless channel. However, wireless channel with structure such as diagonal channel is very important. This dissertation considers the problem of applying interference alignment to OFDM and MIMO-OFDM system. Performance bounds for the multi-user (MIMO) OFDM system with interference alignment are derived. Efficient algorithms are proposed to approach these bounds for OFDM and MIMO-OFDM system.

- In future wireless systems, all the base stations and users will be equipped with multiple antennas. With the development of MIMO and distributed interference alignment, how will the primary users and secondary users behave is of great importance. By modeling the behaviors of the primary user and secondary users using Stackelberg game theory, this dissertation derives the unique Stackelberg Equilibrium and shows that the proposed scheme outperforms the non-spectrum leasing scheme and a cooperative scheme in the literature.

- To ultimately boost the system throughput, massive MIMO system would be adopted in the near future, where many antennas are deployed at the base station. Existing researches mainly focus on the TDD (Time Division Duplex) system due to the advantage of exploiting channel reciprocity. However, there are much more FDD (Frequency Division Duplex) systems deployed worldwide. This dissertation considers how to reduce the channel estimation overhead and proposes effective schemes for enhancing system throughput. The problem of load balancing in massive MIMO system is also investigated. An effective algorithm to solve the optimization problem is proposed and validated.

- Besides massive MIMO system, in the future wireless systems, small cells such as femtocell or picocell will be densely deployed. To investigate the user association problem in such heterogeneous networks is of great importance for system throughput enhancement. From the centralized and distributed perspective, this dissertation investigates how to obtain the optimal user association scheme under different scenarios.

Chapter 2

Applying IDMA to Two-Tier Femtocell Networks: the Uplink Case

2.1 Introduction

A recent study [3] shows that more than 50% of the voice traffic and more than 70% of the data traffic are generated by indoor users. Considerable research efforts from both industry and academia have been made to meet such compelling demands and provide satisfactory services to end users. A number of novel technologies and network structures have been proposed, among which femtocell is particularly a highly promising one under this context.

A femtocell is a user installed small base station at homes or small businesses, which are connected to the service provider via broadband wireline connections. Licensed users of femtocell could access the wireless network via the femtocell base station (FBS) directly, other than through the remote cellular base station (BS). In this way, the distance between femtocell users and the core wireless network is greatly reduced, which brings about numerous benefits including extended cell coverage, reduced transmission, enhanced capacity, and reduced energy consumption, etc. Although some of these benefits could be achieved by deploying more BS's, deploying FBS is a much more economical choice, especially for indoor users.

One of the technical challenges stands in the way of harvesting the envisioned benefits of femtocells is how to manage all kinds of interferences [3] in femtocell networks. Here we consider the uplink of a two-tier femtocell network consisting of one macro base station (MBS) and multiple FBS's. An authorized user can connect to either the MBS (i.e., as a macrocell user) or a close-by FBS (i.e, as a femtocell user). For the uplink in such a two-tier femtocell network, five types of interference may exist.

1. A femtocell user's signal may be interfered by a macrocell user's signal in the vicinity.

2. The femtocell user's signal may cause interference to the macrocell user's signal when it is close to the MBS.

3. A femtocell user's signal in one femtocell may interfere the signals in neighboring femtocells.

4. Signals within a femtocell may interfere with each other due to multipath propagation or carrier frequency offset.

5. Signals within a macrocell may interfere with each other due to multipath propagation or carrier frequency offset.

The first two types of interference can be classified as cross-tier interference [4], while the last three types of interference can be classified as intra-tier interference.

Existing researches for interference management in femtocell networks include [4–9]. Most of these works focus on the cross-tier interference. Here we address the interference management problem of femtocell from a multi-access and iterative multi-user detection perspective. In particular, we propose to adopt IDMA [10] for the uplink transmission of two-tier femtocell networks. The main feature of IDMA is that it distinguishes users by assigning different interleavers to each of them. So with IDMA, in the uplink, each user employs a unique interleaver to interleave its data before transmission. The base stations receives the mixed signal from all the users and then uses an iterative decoding and interference cancellation technique to separate and decode the signals (more details in section 2.2.2).

Since for IDMA, most of the signal processing is conducted at the receiver, the requirement of the transmitter computational capability is very loose. Thus, the transmitter can be easily designed. Moreover, IDMA is highly suitable for the uplink of the two-tier femtocell network, in which the BS (with comparatively high computational capability) performs most of the computations and users are thus relieved from this burden. Compared with traditional multiple access techniques such as TDMA and FDMA, IDMA does not require precise time synchronization or frequency calibration among the users [10]. Therefore the design of user device can be further simplified.

IDMA also allows concurrent transmissions of multiple users, and does not require the use of guard times to deal with different propagation delays of users. Therefore, higher utilization of wireless resources can be achieved. Compared with code division multiple access (CDMA), IDMA represents a new form of orthogonality that can be integrated with CDMA. For example, users can be divided into groups, each sharing a CDMA spreading sequence; users within the same group are then distinguished with unique interleavers. Thus the network capacity can be greatly enhanced.

In this chapter, we discuss how to adopt IDMA for the uplink of two-tier femtocell networks, as motivated by the above observations. In particular, we propose three IDMA-based schemes: (i) Femtocell Decode, where each FBS decodes the signals locally for the users within its coverage; (ii) Femtocell Forward, where the FBS's forward the received signals to the MBS, which then decodes the signals for all users; and (iii) Femtocell Select, where the FBS performs local decoding if the number of users it serves does not exceed a threshold, and forwards received signals to the MBS otherwise. We evaluate the performance of the proposed schemes, and compare them with conventional TDMA and IDMA without the use of femtocells in simulations. We focus on the case where all the users share a common spreading sequence (since the advantage of integrating IDMA with CDMA is obvious). Our simulation study shows that the proposed IDMA-based schemes can achieve considerable throughput gains over traditional schemes and are highly suited for the uplink of two-tier femtocell networks.

The remainder of this chapter is organized as follows. Section 2.2 describes the background of femtocell and the general principle of IDMA. We examine the use of IDMA in femtocell networks and propose three schemes in Section 2.3. The proposed schemes are evaluated in Section 2.4. We review related work in Section 2.5 and Section 2.6 concludes the chapter.

2.2 Background and Preliminaries

2.2.1 Femtocell Networks

A femtocell, also called home base station, typically serves as an access point for use in home or small business. It is usually installed by wireless users for backhauling data to the service

provider through a broadband gateway such as digital subscriber line (DSL), cable, et al. The most prominent feature of femtocell is that the transmission distances between wireless network infrastructure and users are greatly reduced, compared with that in traditional cellular networks. This brings about many benefits such as enhanced link quality, better signal to interference noise ratio (SINR), improved cellular capacity, and greatly reduced transmission power, among others.

Despite of these envisioned advantages, there are many technical challenges need to be addressed, such as interference management and mitigation [3, 6]. For the uplink case, conventionally, Time Division Multiple Access (TDMA) or Frequency Division Multiple Access (FDMA) are used to coordinate the transmissions of users. Under the presence of multipath propagation or carrier frequency offset, however, both intra-tier and cross-tier interferences exist. Moreover, by using TDMA or FDMA, the precious time and frequency resources may not be fully exploited, since only one user can transmit at a time or within a frequency band, and due to the use of guard times or guard bands. Given these facts, it is natural to think about better ways for interference mitigation in femtocell networks that can make more efficient use of wireless network resources. We consider IDMA as one of such options in this chapter.

2.2.2 Interleave Division Multiple Access

The essence of IDMA is to distinguish signals from different users according to their unique interleavers. IDMA represents a new form of orthogonality, such that multiple users can transmit in the same time slot using the same frequency band. The transmitter and receiver architecture of IDMA are shown in Fig. 2.1 [11]. We briefly review the operation of IDMA in this section.

For the uplink case, assume that there are K users in a cell. The signals of each user, i.e., d_1, d_2, $\cdots$, d_K, are coded, interleaved and then transmitted simultaneously to the BS. In IDMA, each user employs a unique interleaver. Therefore, the users can transmit signals simultaneously, occupy the same portion of spectrum, and employ the same coding scheme, in which ways the traditional resources can be better utilized.

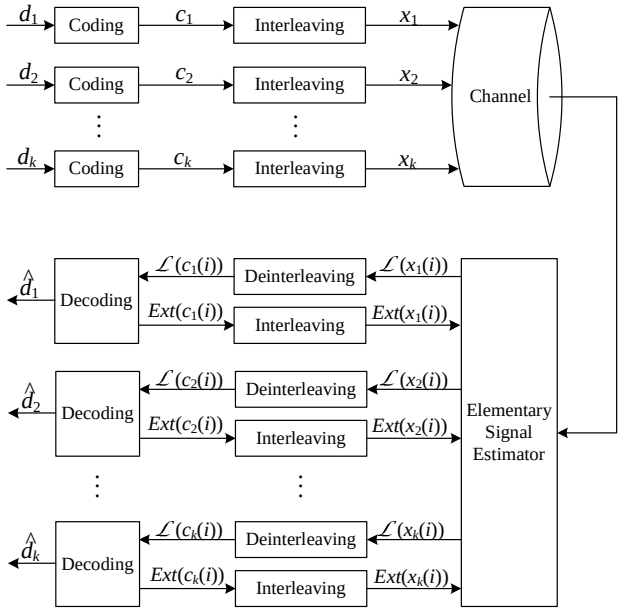

Figure 2.1: The transmitter and receiver architecture of IDMA.

At the BS, the received signal is the superposition of the signals from all the users. The BS then performs an iterative bit by bit decoding, as shown in Fig. 2.1. To simplify discussion, synchronous BPSK system is considered. The channel is assumed to be time-invariant with only one path. However, it is shown in [10] that the decoding algorithm can be extended to more general cases, such as asynchronous system with high order constellation, or time-variant multi-path channels.

At the BS, the i-th received signal $r(i)$ is:

$$r(i) = \sum_{k=1}^{K} h_k x_k(i) + n(i), \quad i = 1, 2, \cdots, L, \tag{2.1}$$

where h_k is the channel gain of the k-th user, $x_k(i)$ is the i-th transmitted signal from the k-th user, $n(i)$ is the zero mean additive white Gaussian noise with variance σ^2, and L is the coded length. It is also assumed that the channel state information is known at the BS through some channel estimation techniques. To examine the signal from the k-th user, we can rewrite (2.1) as:

$$r(i) = h_k x_k(i) + \xi_k(i), \quad i = 1, 2, \cdots, L. \tag{2.2}$$

In (2.2), $\xi_k(i)$ represents the interference plus noise with respect to the signal of the k-th user, which can be written as:

$$\xi(i) = \sum_{k'=1,k'\neq k}^{K} h_{k'} x_{k'}(i) + n(i), \quad i = 1, 2, \cdots, L, \tag{2.3}$$

or

$$\xi(i) = r(i) - h_k x_k(i), \quad i = 1, 2, \cdots, L. \tag{2.4}$$

According to the Central Limit Theorem, $\xi_k(i)$ in (2.3) can be approximated by a Gaussian random variable when K is sufficiently large, with mean

$$\mathrm{E}(\xi(i)) = \mathrm{E}(r(i)) - h_k \mathrm{E}(x_k(i)), \quad i = 1, 2, \cdots, L, \tag{2.5}$$

and variance

$$\mathrm{Var}(\xi(i)) = \mathrm{Var}(r(i)) - |h_k|^2 \mathrm{Var}(x_k(i)), \quad i = 1, 2, \cdots, L, \tag{2.6}$$

where

$$\begin{cases} \mathrm{E}(r(i)) = \sum_{k=1}^{K} h_k \mathrm{E}(x_k(i)), & i = 1, 2, \cdots, L \\ \mathrm{Var}(r(i)) = \sum_{k=1}^{K} |h_k|^2 \mathrm{Var}(x_k(i)) + \sigma^2, & i = 1, 2, \cdots, L. \end{cases} \tag{2.7}$$

The Elementary Signal Estimator in Fig. 2.1 computes the *Logarithm Likelihood Ratios (LLRs)* of each bit as [10]:

$$\begin{aligned} \mathcal{L}(x_k(i)) &= \log\left(\frac{p(r(i)|x_k(i) = +1)}{p(r(i)|x_k(i) = -1)}\right) \\ &= \frac{2h_k(r(i) - \mathrm{E}(\xi(i)))}{\mathrm{Var}(\xi(i))}, \text{ for all } i, k. \end{aligned} \tag{2.8}$$

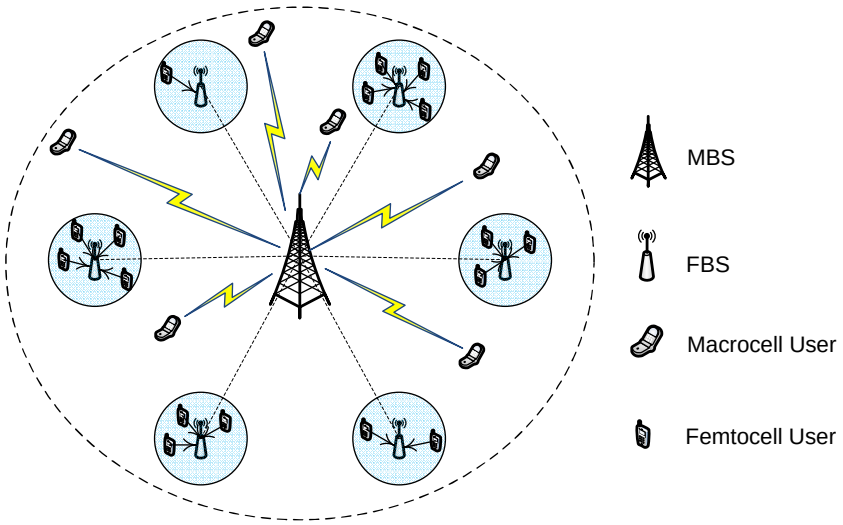

Figure 2.2: The uplink case in a two-tier femtocell network.

Then the *LLRs* are deinterleaved and decoded to produce estimations $\hat{d}_k(i)$ of the original signals, for all i, k. To further mitigate the interferences between different users, the estimations $\hat{d}_k(i)$, for all i, k are then coded, and interleaved to update the $\mathrm{E}(x_k)$ and $\mathrm{Var}(x_k)$. Based on the updated $\mathrm{E}(x_k)$ and $\mathrm{Var}(x_k)$, the Elementary Signal Estimator then recalculates the $\mathcal{L}(x_k)$, and so forth. This procedure is repeated for a prescribed number of iterations. The estimations $\hat{d}_k(i)$'s will be progressively improved and finally the BS can decode all the signals from all the users.

2.3 Adopting IDMA in Two-Tier Femtocell Networks

Figure 2.2 illustrates the uplink of a two-tier femtocell network, where an MBS can serve users in the entire network and each FBS serves authorized users within its coverage. To simplify the discussion, it is assumed that the femtocells are evenly deployed. Using IDMA, users inside or outside the femtocells simultaneously transmit signals to the FBS or MBS, respectively, using the same frequency band.

As discussed above, the greatest merit of femtocell is bringing users much closer to the wireless network infrastructure. Here we propose three IDMA-based schemes for the uplink of the two-tier femtocell network.

2.3.1 FBS Decode

The first scheme is that each FBS decodes the received signals locally, and then sends the decision results to the MBS. We call this scheme FBS Decode for short. It is demonstrated in [12] that the performance for each user depends on its Signal to Interference plus Noise Ratio (SINR) $sinr_k$, which can be written as:

$$sinr_k = \frac{p_k|h_k|^2}{\sum_{k'=1,k'\neq k}^{K} p'_k|h'_k|^2 f(\gamma'_k) + \sigma^2}, \quad \text{for all } k, \tag{2.9}$$

where p_k is the transmit power of each user k, and $f(x)$ is a function representing the amount of interference canceled at each decoding iteration, which has no close form expression but can be obtained through Monte Carlo simulation [11].

If all the users transmit at the same power, since there are little differences in the channel gains for all the users (i.e., due to closeness to the FBS), the sum of the SINR of all the users would be quite high. That is to say, from the perspective of the system performance, this scheme is expected to perform better than the other two schemes introduced later in this section. However, since the user number served by each FBS may be large, this scheme may put a stringent requirement for the computational capability of the FBS's.

2.3.2 FBS Forward

If the computational capability of the FBS is not strong, the FBS could directly forward all the received signals to the MBS. Then the MBS will decode the signals from all the users. We call this scheme FBS Forward for short. Since the users served by the FBS enjoy high quality channels, while cell edge users suffer from the bad ones, in the light of (2.9), the SINR of an FBS user is usually very high, but the SINR of an edge user is usually very low. The consequence is that although the throughput of the FBS users could be high, the overall system throughput may be degraded due to the bad performance of edge users.

2.3.3 FBS Select

This is a hybrid scheme that provides a trade-off between FBS Decode and FBS Forward. FBS Select is useful for the case when the computational capability of the FBS is not sufficiently strong. In particular, an FBS can directly forward the received signals to the MBS, if the number of users being served is greater than a predefined threshold η. Otherwise, the FBS decodes the signals locally and sends the decoded data to the MBS. We call this scheme FBS Select for short. The performance of this scheme is expected to lie between those of FBS Decode and FBS Forward.

It will be shown in the next section that by applying IDMA to femtocell networks, considerable throughput gains can be achieved at comparatively low cost over traditional TDMA and IDMA schemes.

2.4 Performance Evaluation

We present our simulation study of the proposed IDMA-based schemes in this Section. In the following, we first describe the simulation settings, and then present the simulation results and discussions.

2.4.1 Simulation Settings

Monte Carlo simulations are conducted to evaluate the performance of the proposed schemes and to verify the benefits brought about by adopting IDMA in the uplink of two-tier femtocell networks. Since power consumption is a critical factor for battery life and CO_2 emission, we focus on the performance at the low power region. Since it is a general assumption that femtocells are deployed at hotspots, 80% of the users are served by the femtocells in our simulation. For fair comparison, we simply use spreading as the channel coding scheme, and all the users share the same spreading sequence. Let the spreading sequence be $g = \{+1, -1, \cdots\}$, with length G. Then

it follows that [10]

$$\hat{d}_k(i) = \sum_{j=1}^{G} g(j)\mathcal{L}(c_k((i-1)\times G+j)),\ i = 1, 2, \cdots, L, \tag{2.10}$$

$$Ext(c_k(i)) = g(i)\hat{d}_k(i) - \mathcal{L}(c_k(i)),\ i = 1, 2, \cdots, L. \tag{2.11}$$

Thus the mean and variance of $x_k(i)$ can be updated as [10, 13]:

$$\mathrm{E}(x_k(i)) = \tanh\left(\frac{Ext(x_k(i))}{2}\right),\ i = 1, 2, \cdots, L \tag{2.12}$$

$$\mathrm{Var}(x_k(i)) = 1 - \mathrm{E}^2(x_k(i)),\ i = 1, 2, \cdots, L. \tag{2.13}$$

The path gain is modeled as [14]:

$$h_k = A_k/d_k^{\alpha}, \tag{2.14}$$

where the A_k's are all independent and identically distributed (i.i.d.) log-normal random variables with 0 dB mean and 8 dB variance, d_k is the distance between the user and the BS it connects to (could be either the MBS or an FBS), $\alpha = 4$ for outdoor users, and $\alpha = 2$ for indoor users. When d_k approaches to 0, h_k approaches to infinity, which is impossible in practical systems. We simply let $h_k = 1$ if $d_k \leq 1$. This can be interpreted as when the user is close enough to the MBS or an FBS, the channel between them becomes perfect.

As for user locations, we first generate uniformly distributed random locations for 20% of the users, which are served by the MBS. Considering the height of the MBS and its geographic impact, these users are located outside the unit circle that is centered at the MBS. Their locations are uniformly distributed under the coverage of the MBS. Next, the remaining 80% users are randomly scattered in the femtocells. Within the coverage of each femtocell, the users are uniformly distributed. This user location generation process is performed 10,000 times in each simulation. Each point in the figures is the average of 10,000 simulation results. Fig. 2.3 illustrates one of the realizations of random user locations.

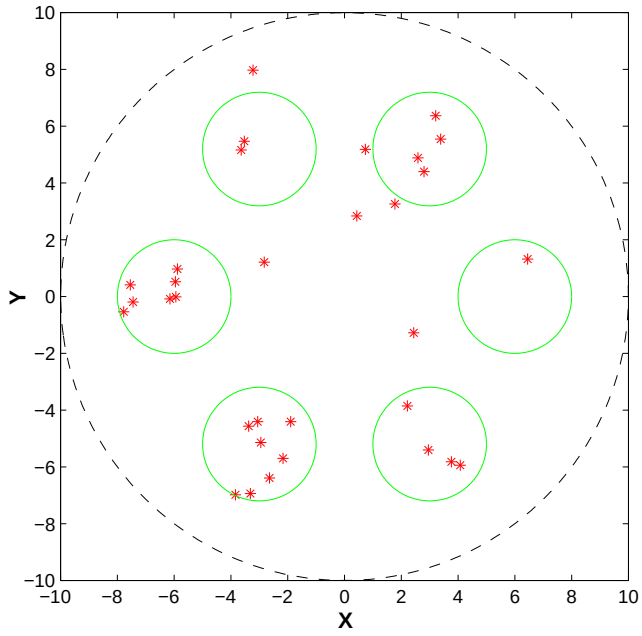

Figure 2.3: Generation of random user locations.

Table 2.1: System Parameters Used in the Simulations of IDMA and Femtocell Networks

Description	*Value*
Number of users	32
Number of femtocells	6
Coverage radius of MBS (normalized)	10
Coverage radius of FBS (normalized)	2
Distance between MBS and FBS (normalized)	6
Number of decoding iterations	5
FBS Select threshold η	5

The proposed schemes are implemented with MATLAB. The system parameters used in the simulations are specified in Table 2.1. For comparison purpose, we also simulated the traditional IDMA scheme without the use of femtocells (termed IDMA w/o Femtocells), where all the users in the cell directly transmit to the MBS, and the signals are decoded at the MBS. In addition, we also simulated the conventional TDMA scheme. With TDMA, each user is assigned with an equal and non-overlapping portion of the total time for signal transmission. We assume perfect synchronization for all the users with zero guard times, so as to obtain an upper bound on the TDMA performance.

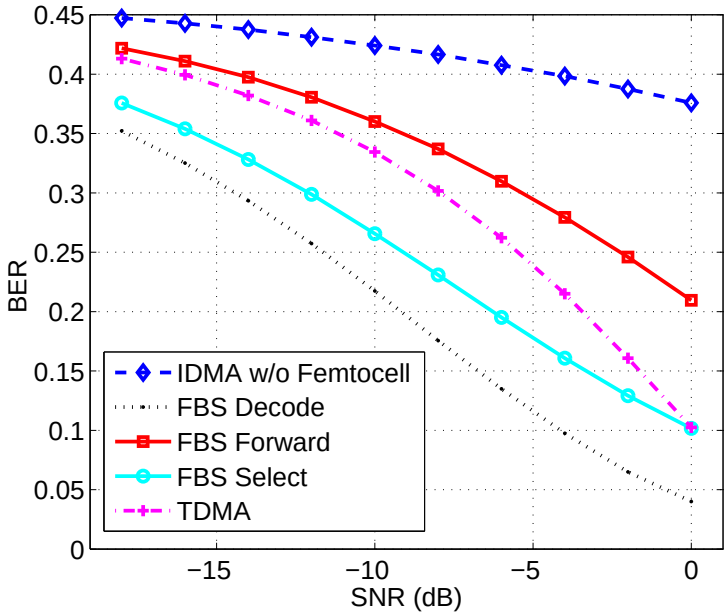

Figure 2.4: Throughput of the five schemes vs. SNR.

2.4.2 Simulation Results and Discussions

We first compare the throughput performance of the five schemes under different signal-to-noise-ratios (SNRs). The throughput is measured by the error-free bits received and normalized by the bandwidth (B) and time slot duration (T).

Fig. 2.4 shows the achieved throughput at different SNRs. It is obvious that by deploying femtocells, considerable throughput gains can be achieved over the IDMA w/o Femtocells scheme. It can also be observed that FBS Decode has the highest throughput performance among all the five schemes. Under FBS Forward, the channel gain differences between the FBS users and the MBS users are so large that the SINR of FBS users are extremely high while their MBS counterparts are extremely low. Actually, it can be examined that the bit error rate (BER) of high quality channel users is close to zero, while the BER of edge users is so high that the system performance is greatly affected. As expected, FBS Select's throughput performance lies in-between those of FBS Decode and FBS Forward. It is important to note that both FBS Decode and FBS Select strictly outperform TDMA, while the throughput of FBS Forward is close to that of TDMA. The relatively lower throughput of FBS Forward is due to the low quality channels of the edge users.

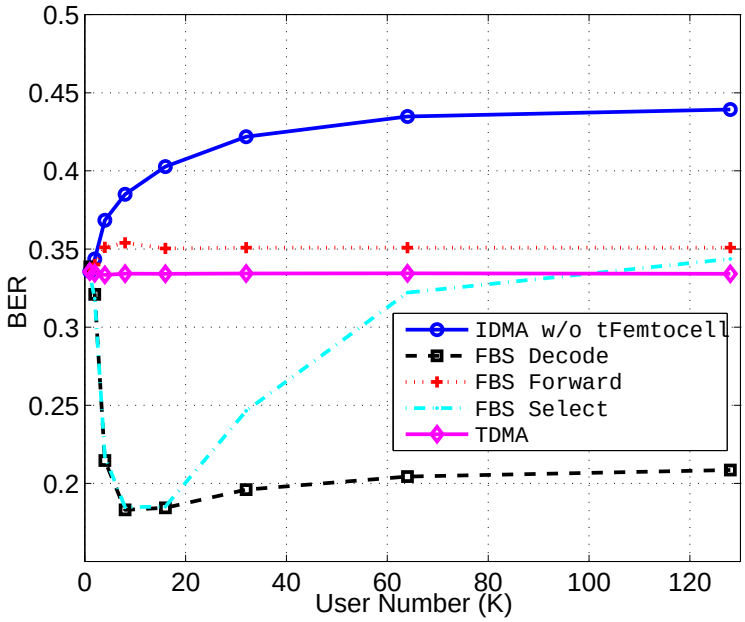

Figure 2.5: Throughput of the five schemes vs. number of users.

We next compare the five schemes under different numbers of users. Most of the system parameters are still the same as given in Table 2.1, except that the SNR is set to -10 dB and the user number is varied. The simulation results are presented in Fig. 2.5. It can be observed that similar conclusions drawn from Fig. 2.4 still hold true here. FBS Decode has the best performance; the FBS Select outperforms TDMA when the user number is less than 90; and FBS Forward achieves a performance close to that of TDMA.

From Figs. 2.4 and 2.5, we conclude that if the FBS has the capability of local decoding for the signals from a certain amount of users, which is the usual case of femtocell applications, considerable throughput gains can be achieved by adopting IDMA for the uplink of femtocell networks. Even if the femtocell works in signal forwarding mode, the throughput performance is still close to that of TDMA and better than that of IDMA w/o Femtocells.

Since IDMA adopts an iterative decoding procedure (see Fig. 2.1), it would be interesting to investigate how fast the decoding procedure converges under the uplink two-tier femtocell network scenario. Our simulations show that the IDMA decoding algorithm can converge very fast. The simulation results are presented in Fig. 2.6 for the three IDMA-based schemes. We still follow

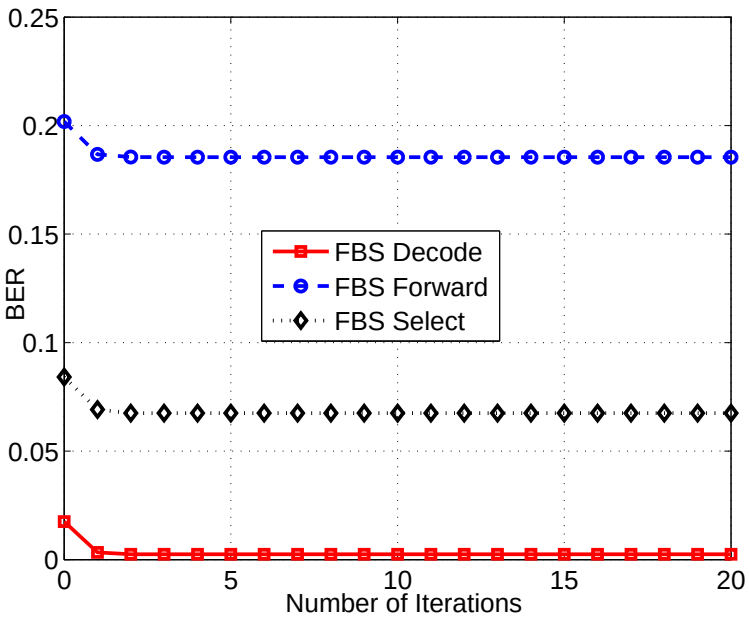

Figure 2.6: Throughput of the three IDMA-based schemes vs. number of iterations.

the system parameters given in Table 2.1, except that the SNR is fixed to 0 dB and the number of iterations is varied. It can be observed that the FBS Decode scheme converges after two iterations, FBS Forward converges after three iterations, and FBS Select converges after three iterations. Therefore, the computational complexity and processing delay incurred from the turbo iterative decoding algorithm are negligible; the throughput gains are achieved at relatively low cost.

2.5 Related Work

Femtocell is designed to cater for the ever-increasing demand of high speed wireless data transmissions. By significantly reducing the distance between the service provider and the service users, great capacity gain can be obtained. A comprehensive survey of femtocells is provided in [3]. Even though the femtocell has the great potential of creating dual benefits to both network operator and users, there are many challenges to be addressed. It was pointed out in [3] that interference management is one of the key factors for the success of femtocell. Considerable research have been conducted in this problem area [4–9]. In [4], the authors studied the impact of the cross-tier

interference on the system outage probability, analyzed the uplink capacity, and proposed an interference avoidance strategy. To suppress the cross-tier interference below an adaptive threshold and compensate for the uplink throughput, open-loop and closed-loop interference mitigation strategies were proposed in [6]. In [5], the authors considered the cochannel interference incurred by frequency reuse, and proposed a femtocell based distributed antenna system for uplink interference cancellation. In [7], the authors proposed a coordinated user scheduling combined with transmit beamforming scheme to alleviate the inter-femtocell interference problem. We adopted successive interference cancellation for downlink data multicast in two-tier femtocell networks in [9], and examined medium grain scalable videos streaming over femtocell cognitive radio networks in [8]. However, the uplink case was not fully considered in these papers.

IDMA has been shown to support multiple transmissions at the same time using the same frequency [10]. The quality of service (QoS) issue in IDMA-based networks was examined in [15]. An IDMA QoS architecture and an interleave division slotted-ALOHA (IDSA) are proposed and shown to be effective. Applying the large-system performance approximation and the extrinsic information transfer (EXIT) chart, Li, Wang, and Li [11] analyzed and optimized the BER of IDMA communication systems. From a game theoretical view, a decentralized power allocation algorithm for the uplink IDMA system was proposed in [12]. The optimal transmission power for the spread spectrum uplink IDMA channels was derived in [16]. In [17], a fully-analytical approach was developed to predict the rate allocation scheme of IDMA system, and a modified linear programming method is proposed to get the best rate profile.

It can be seen from the above discussions that the interference issue is of great importance for femtocell networks, which needs to be addressed before we could fully harvest the potentially high benefits of femtocells. To this end, an interference cancellation or mitigation approach provides highly effective solutions. In this chapter, we address the interference issue from an iterative multi-user detection point of view, and introduce three IDMA-based schemes to enhance the system throughput performance. The proposed schemes are shown to be quite effective and to achieve the design goals.

2.6 Conclusions

In this chapter, we investigated the problem of interference management in the uplink of two-tier femtocell networks. To enhance the uplink throughput performance for low power transmissions, we introduced IDMA to allow concurrent transmissions from all users and cancel the intra and cross-tier interference with iterative decoding and interference cancellation. We proposed three IDMA-based schemes, namely, FBS Decode, FBS Forward, and FBS Select, for the uplink of two-tier femtocell networks based on the processing capability of femtocells. Simulation results demonstrated that considerable throughput gains can be achieved under FBS Decode and FBS Select over conventional TDMA and IDMA schemes at comparatively low costs.

Chapter 3

Interference Alignment Improves the Capacity of OFDM Systems

3.1 Introduction

Many advanced wireless communication technologies, such as Orthogonal Frequency Division Multiplexing (OFDM) and Multiple Input Multiple Output (MIMO), are widely adopted to enhance the system capacity, while a huge amount of wireless access networks/base stations (BS) are deployed every year to accommodate the compelling need for larger capacity. Given the increasing wireless data volume and the more and more crowded BS deployment, interference is becoming the major factor that limits wireless network performance.

Traditionally, interference is considered harmful and often treated as background noise. As the performance of point-to-point transmission techniques is approaching Shannon capacity, there is now considerable interest on exploiting interference for further capacity gains. It is shown that when interference is large, it can be decoded and canceled from the mixed signal (as in interference cancellation), while when interference is comparable, interference alignment can be adopted to enable concurrent transmissions. Although interference is harmful in many cases, it could be beneficial for enhancing system throughput as long as the interference can be aligned. We call this kind of interference beneficial interference.

Interference alignment was first proposed in [19], and the feasibility condition was investigated in [20]. Since in a large network, there are many users but limited dimensionality, the authors in [21] proposed the concept of "best-effort" interference alignment, and adopted an iterative algorithm to optimize it. However, how to use interference alignment to enhance the throughput in practical OFDM system was not fully considered. Shi et al. in [22] also considered the problem of interference alignment in multi-carrier interference networks. But it is not clear if the approach can be extended to the general case of a large number of subcarriers. In [25], the authors proposed

two schemes to adopt interference alignment in multi-cell MIMO OFDM systems. In the first scheme, interference alignment was used to remove the inter-cell interference, while zero-forcing precoding was used to suppress the intra-cell interference. In the second scheme, interference alignment was also used for inter-cell interference removal, while the OFDMA access scheme was applied for intra-cell interference cancellation. However, the fundamental performance bound of multi-user MIMO OFDM system with interference alignment has not been discussed. In [26], the authors derived the necessary and sufficient conditions for the three-user OFDM system with interference alignment in the time domain. However, these conditions cannot be applied to system with more users or under other conditions. Ayach et al. in [27] investigated the feasibility problem MIMO-OFDM system with interference alignment over measured channels, while in this chapter, we mainly concern about the theoretical bound when interference alignment is incorporated in the OFDM system.

Interference alignment also finds many applications in practical wireless networks. In [28], a cognitive interference alignment scheme was presented to suppress both cross-tier and co-tier interferences in OFDM-based two-tier networks. In [29,30], the authors investigated the behaviors of primary users and secondary users under a Stackelberg game theory framework, where distributed interference alignment is adopted to enable spectrum leasing in the cognitive radio network. To achieve better error rate performance, a novel interference alignment based precoder design was presented in [31] for OFDM system.

There are also some existing studies that aim to adopt interference alignment in more advanced systems. In [32], the authors extended the traditional interference alignment scheme to a general algorithm for multi-hop mesh networks. The authors in [33] considered combining interference alignment and interference cancellation to further enhance the system throughput. In [34], the authors proposed to use multimode MIMO antennas instead of the typical omni-directional antennas to improve the performance of MIMO OFDM system with interference alignment, while in [35], the impact of antenna spatial correlation on the performance of interference alignment systems was investigated.

As claimed in [36], there are not many studies about interference alignment with structured channels. In [37], the authors aimed to show how interference alignment works in OFDM system under practical constraints. To further address this problem, here in this chapter, we consider the problem of incorporating interference alignment in multi-user (MIMO) OFDM systems. Specifically, we first examine the fundamental characteristics and practical constraints on adopting interference alignment in a multi-user OFDM system. We show that, for a K user N subcarrier OFDM system, $KN/2$ concurrent transmissions that is achievable for generic structureless channels [19], cannot be achieved for a practical multi-user OFDM network with diagonal channels and a limited number of subcarriers. We then investigate effective schemes to exploit interference in multi-user OFDM systems. With an integer programming problem formulation, we derive the maximum efficiency of the Multi-user OFDM/interference alignment system. We also show how to achieve the maximum efficiency with a decomposition approach, and derive the closed-form precoding and decoding matrices. Finally, we extend the above analysis to the multiple antennas scenarios. All the proposed schemes are evaluated with simulations and their superior performance is validated.

Notation: in this chapter, a capital bold symbol like $\mathbf{H}$ denotes a matrix, a lower case symbol with an arrow on top like $\vec{v}$ denotes a vector, and a lower case letter like v denotes a scalar. $[\cdot]^T$ means *transpose* and $[\cdot]^{-1}$ means *inversion*. $\mathbf{H}_{ij}$ and h_{ij} are the channel gain matrix and channel gain from the i-th transmitter to the j-th receiver, respectively. $\mathbf{V}_i$ is the precoding matrix for transmitter i; $\vec{v}_i^j$ is the j-th column of $\mathbf{V}_i$. $\mathbf{U}_i$ denotes the interference cancellation matrix for the i-th receiver, while $\vec{u}_i^j$ is the j-th column of $\mathbf{U}_i$. Let h, v, u denote the entries of $\mathbf{H}$, $\mathbf{V}$, and $\mathbf{U}$, respectively.

Note that with these notations, the entries of $\mathbf{H}_{ij}$ takes slightly different ordering from conventional ones. For instance, if transmitter 1 and receiver 2 are both equipped with M antennas, the channel gain is:

$$\mathbf{H}_{12} = \begin{pmatrix} h_{11} & h_{21} & \cdots & h_{M1} \\ h_{12} & h_{22} & \cdots & h_{M2} \\ \vdots & \vdots & \ddots & \vdots \\ h_{1M} & h_{2M} & \cdots & h_{MM} \end{pmatrix}. \tag{3.1}$$

The rest of this chapter is organized as follows. Section 3.2 describes the background and preliminaries. Section 3.3 investigates how to adopt interference alignment in multi-user OFDM system. Section 3.4 extends the analysis to the multiple antennas scenario. Simulation results are presented in Section 3.5. Section 3.6 concludes the chapter.

3.2 Background and Preliminaries

3.2.1 Orthogonal Frequency Division Multiplexing

While higher data rates can be achieved by reducing symbol duration, severe inter-symbol-interferences (ISI) will be caused over time dispersive channels. OFDM is an effective approach to allow transmissions at a high data rate and combat the destructive effect of channel. By dividing the channel into narrow bands, in which the signal experiences flat fading, OFDM can effectively mitigate ISI and maintain high data rate transmissions. Interested reader are referred to [18, 38, 39] and the references therein for details.

3.2.2 Multiple Input and Multiple Output

With the single antenna transmission technique being well developed, it is natural to extend to multiple antenna systems. The MIMO transmission techniques have been evolving rapidly since last decades. Generally speaking, multiple antennas or an antenna array can be used to attain the *diversity gain*, *multiplexing gain*, or *antenna gain*, and thereby reduce the system error rate, enhance the system throughput, or strengthen the signal to interference and noise ratio (SINR) [23]. Given M_1 transmitting antennas and M_2 receiving antennas, the maximum multiplexing gain is known to be $\min\{M_1, M_2\}$. Throughout this chapter, we assume that channel state information is perfectly known at each transmitter and receiver as in prior works [19]. For how to acquire channel information, readers are referred to [40].

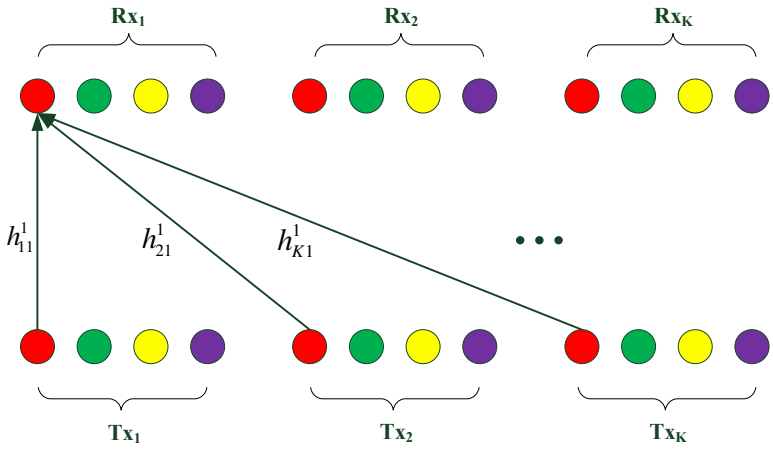

Figure 3.1: Multi-user OFDM using interference alignment.

3.2.3 Interference Alignment

It is shown in [19] that in a K user wireless network, with $(n+1)^q + n^q$ symbol extensions, totally $K/2$ normalized *degrees of freedom* (DoF) can be achieved using interference alignment, where $q = (K-1)(K-2) - 1$ and $n \in \mathbb{N}$. In single antenna systems, the normalized DoF is 1. With interference alignment, the system throughput is enhanced by a factor of $K/2$ for $K \geq 2$. Note that there is no interference if there is only one user occupying the time or frequency resource.

Observation 1: The system throughput could be improved if alignable interference is introduced among users.

This observation is useful for OFDM systems, where the channel gain matrix is diagonal. Since the gain of interference alignment is proportional to K, we should have more users transmit at the same time slot or frequency band if the transmitted vectors can be aligned. That is why we call this kind of interference *beneficial interference* in this chapter.

3.3 Multi-user OFDM with Interference Alignment

In this section, we investigate the problem of interference alignment in multi-user OFDM systems. We first examine fundamental characteristics and practical constraints, and then demonstrate how to exploit interference in multi-user OFDM systems. We derive the maximum throughput

when interference alignment is adopted, as well as closed-form precoding and decoding matrices to achieve the maximum throughput.

3.3.1 Subcarriers versus Antennas

In traditional interference alignment, deploying multiple transmitting antennas allows us to precode data packets and align them at the receiver. Deploying multiple receiving antennas provides multidimensional signal space, so that interference can be aligned into a sub signal space that is orthogonal to the desired signal. Therefore, deploying multiple antennas can provide the needed freedom in the signal space.

In OFDM, we observe that subcarriers can function in the same way as antennas in MIMO/interference alignment systems. To some extent, subcarriers can be regarded as a counterpart of antennas. However, there is a distinguishing difference between the two systems: there is no cross-talk among different subcarriers in OFDM.

3.3.2 Precoding in OFDM

The main idea of interference alignment is to compress the interference space to no more than half of the total received signal space at each receiver, leaving the remaining part of the space for desired signals [19]. This goal is achieved through precoding at every transmitter and zero forcing interference cancellation at every receiver.

In OFDM, data is transmitted on multiple carriers, as shown in Fig. 3.1. Suppose there are N subcarriers. Ignoring noise, the received signal $\vec{y}$ is an $N \times 1$ vector given by:

$$\vec{y} = \mathbf{H}\vec{x}, \tag{3.2}$$

where $\vec{x}$ is the desired signal in the form of an $N \times 1$ vector, and $\mathbf{H}$ is the $N \times N$ channel gain matrix between the transmitter and receiver. Since different subcarriers have different frequencies, the channel gain matrix is *diagonal* if there is no severe frequency shift. It can be seen from later

discussions that this property makes interference alignment in OFDM system quite different from the general channel case.

Going one step further, we can precode the data before transmission. If d packets are to be transmitted in an N subcarrier OFDM system, an $N \times d$ *precoding matrix* $\mathbf{V}$ should be used. The system equation is as follows.

$$\vec{y} = \mathbf{HV}\vec{x}. \tag{3.3}$$

If we let $d = N$ and $\mathbf{V} = \mathbf{I}_N$, where $\mathbf{I}_N$ is an $N \times N$ identity matrix, (3.3) is reduced to (3.2).

In general, we could control what to be transmitted on the subcarriers by adjusting the precoding vector accordingly. For a single user single antenna OFDM system with N subcarriers, the maximum number of packets can be transmitted is N. Note that, here N is normalized by the QAM (Quadrature Amplitude Modulation) modulation level. However, inspired by the idea of interference alignment, we show that a throughput higher than N can be achieved in the following subsections.

3.3.3 Interference Alignment in a K-User OFDM System

As discussed, we consider the problem of interference alignment in multiuser OFDM systems. Basically, we aim to answer the following questions.

(i) What are the practical constraints for adopting interference alignment in such systems?

(ii) What is the maximum throughput that can be achieved?

(iii) How to achieve the maximum throughput (i.e., deriving closed-form precoding and decoding matrices)?

Dependence of Precoding and Decoding Vectors in Diagonal Channels

In this section, we show the difference on applying interference alignment between a diagonal channel and a general channel, as well as the challenges to adopt interference alignment in the former case.

It was shown in [20] that given M_1 transmitting antennas and M_2 receiving antennas in a K user interference channel, the DoF for each user, denoted by d, must satisfy

$$d \leq \frac{M_1 + M_2}{K + 1}. \tag{3.4}$$

For example, given two transmitting and receiving antennas in a three-user interference channel, (3.4) indicates that each user could transmit one packet simultaneously. With a generic structureless channel, the throughput $Kd = 3$ can be achieved as follows.

At each receiver, we align the signals from the other two users. Recall the channel gain matrices as defined in (3.1) and let the user i signal be $\vec{v}_i$, $i = 1, 2, 3$. It follows that

$$\mathbf{H}_{21}\vec{v}_2 = \mathbf{H}_{31}\vec{v}_3 \tag{3.5}$$

$$\mathbf{H}_{12}\vec{v}_1 = \mathbf{H}_{32}\vec{v}_3 \tag{3.6}$$

$$\mathbf{H}_{13}\vec{v}_1 = \mathbf{H}_{23}\vec{v}_2. \tag{3.7}$$

Solving (3.5), (3.6) and (3.7), we have

$$\vec{v}_1 = \text{eig}(\mathbf{H}_{12}^{-1}\mathbf{H}_{32}\mathbf{H}_{31}^{-1}\mathbf{H}_{21}\mathbf{H}_{23}^{-1}\mathbf{H}_{13}) \tag{3.8}$$

$$\vec{v}_2 = \mathbf{H}_{23}^{-1}\mathbf{H}_{13}\vec{v}_1 \tag{3.9}$$

$$\vec{v}_3 = \mathbf{H}_{32}^{-1}\mathbf{H}_{12}\vec{v}_1, \tag{3.10}$$

where $\text{eig}(\mathbf{A})$ stands for the eigenvector of matrix $\mathbf{A}$.

This scheme works well for generic structureless channels, but not for the case of diagonal channels. For instance, if 2 subcarriers (instead of two antennas) are used in OFDM, all the channel gain matrices in (3.8), (3.9) and (3.10) are diagonal. Since the product of diagonal matrices is still diagonal, we have from (3.8) that

$$\vec{v}_1 = \begin{pmatrix} 1 \\ 0 \end{pmatrix} \text{ or } \begin{pmatrix} 0 \\ 1 \end{pmatrix}.$$

If $\vec{v}_1 = [1, 0]^T$, we derive $\vec{v}_2 = [a, 0]^T$ from (3.9) and $\vec{v}_3 = [b, 0]^T$ from (3.10), where a and b are scalars. To cancel the interference at receiver 1, the *cancellation vector* $\vec{u}_1$ must be $\vec{u}_1 = [0, c]^T$, where c is a scalar. However, the desired packet is also canceled since $\vec{u}_1$ is orthogonal to $\vec{v}_1$. Therefore, we cannot simultaneously transmit 3 packets in this system.

The reason behind is that for a diagonal channel, its eigenvectors have only one nonzero entry. If we align interferences at receiver r by letting $\mathbf{H}_{jr}\vec{v}_j = \cdots = \mathbf{H}_{ir}\vec{v}_i$, for $j \neq \cdots \neq i \neq r$, the precoding vectors are dependent to each other. Consequently, when interference is canceled at a receiver, the desired packet will also be canceled.

Interference Alignment with Multi-user OFDM–Performance Bound

It is shown in [19] that in a K user system with $(n+1)^q + n^q$ symbol extensions, totally $K/2$ normalized DoF can be achieved using interference alignment, where $q = (K-1)(K-2)-1$ and $n \in \mathbb{N}$. In light of this result, one may think that $KN/2$ concurrent transmissions is achievable in a K-User, N subcarrier OFDM system. However, we will show that this is unachievable for large K in practical systems in the following.

It is worth noting that an assumption made in [19] is that the symbol extensions can be infinitely large. This assumption may not hold true in practical systems. Given a finite bandwidth, the number of subcarriers is the bandwidth divided by the subcarrier spacing. Typically, the value of subcarrier spacing is $10 - 20$ KHz. Then even for a 100 MHz bandwidth, we can have at most

10^4 subcarriers. For instance, in 802.16m and LTE, the maximum number of IFFT is 2,048, and maximum number of effective subcarriers is 1,200.

Therefore, the problem is to maximize system throughput given a finite number of subcarriers, denoted by N_{max}. It is shown in [19] that with $(n+1)^q+n^q$ symbol extensions, the total normalized DoF is $[(n+1)^q+(K-1)n^q]/[(n+1)^q+n^q]$. So we aim to maximize $(n+1)^q+(K-1)n^q$ and have the following formulation.

$$\max_{n,K} \quad (n+1)^q+(K-1)n^q \tag{3.11}$$

$$s.t. \quad q=(K-1)(K-2)-1 \tag{3.12}$$

$$(n+1)^q+n^q \leq N_{max}, n \in \mathbb{N} \tag{3.13}$$

$$K \geq 3, K \in \mathbb{N}. \tag{3.14}$$

In problem (3.11), all the variables are integers. Constraint (3.13) indicates that for practical systems, the number of subcarriers $N=(n+1)^q+n^q$ is upper bounded by N_{max}. Although this integer programming problem is NP-hard, by careful inspection, we can find the solution under practical constraints.

In particular, we find the feasible region is very small for practical N_{max} values. Also the objective value is monotone with respect to the two variables n and K. In problem (3.11), assuming $K=5$, we have $q=11$ from (3.12). For each value of n, we can derive the number of subcarriers needed, N_{max}, from (3.13) for the problem to be feasible, as well as the throughput of the system (i.e., the objective value of (3.11)). The corresponding degree of freedom, d, is the ratio of the throughput and the number of subcarriers required. These numbers are presented in Table 3.1.

Table 3.1 shows that if there are $K=5$ users, $2,049$ and $179,195$ subcarriers are needed when $n=1$ and $n=2$, respectively. As discussed, a practical system usually do not have more than 10^4 subcarriers. So n can only be 1 in this case, with efficiency $d_{max}=1.002$. Therefore, interference alignment is not useful in this case, since we can simply allow only one user to transmit over one time-slot or a particular frequency band to get $d=1$ (i.e., single user OFDM).

Table 3.1: System Efficiency

When $K = 5$ and $q = 11$			
n	*No. of subcarriers*	*No. of packets*	*Normalized DoF* d
1	2,049	2,052	1.002
2	179,195	185,339	1.03
When $K = 4$ and $q = 5$			
n	*No. of subcarriers*	*No. of packets*	*Normalized DoF* d
1	33	35	1.06
2	275	339	1.23
3	1,267	1,753	1.38
4	4,149	6,197	1.49
When $K = 3$ and $q = 1$			
n	*No. of subcarriers*	*No. of packets*	*Normalized DoF* d
1	3	4	1.333
2	5	7	1.40
3	7	10	1.429
4	9	13	1.444
100	201	301	1.498
1000	2001	3001	1.4998

If there are $K = 6$ transmitters, we have $q = 19$. Even if $n = 1$, the number of subcarriers needed is $524,289$, which is not feasible for practical systems. Since the number of subcarriers $(n+1)^{(K-1)(K-2)-1} + n^{(K-1)(K-2)-1}$ grows exponentially with $(K^2 - 3K + 1)$, it can be readily concluded that K cannot be more than 4 for interference alignment to be beneficial in multi-user OFDM systems.

Since the objective value of (3.11) is an monotone increasing function of K, the maximum feasible value $K = 4$ is of particular interest. We have $q = 5$ when $K = 4$. Table 3.1 also shows that under this condition, the maximum efficiency for practical system is $d_{max} = 1.38$ for the practical case with at most $2,000$ subcarriers. When $K = 3$, we have $q = 1$. The objective function (3.11) becomes $3n+1$, and the constraint (3.13) becomes $2n+1 \leq N_{max}$. If the maximum number of subcarriers is $N_{max} = 2,001$, the system achieves its maximum efficiency $d_{max} = 1.4998$.

The above analysis can be summarized as follows.

Conjecture 3.3.1. *For a practical multi-user OFDM system with number of subcarriers less than* $2,002$*, the maximum efficient is* $d_{max} = 1.4998$*, which is achieved when there are* $K = 3$ *users using* $N = 2,001$ *subcarriers.*

However, in the later discussions, we will show that this conjecture does not hold true.

Interference Alignment with Multi-user OFDM–Realization

It is shown in [19] how to design the precoding matrices to transmit $3n + 1$ packets over $2n + 1$ symbol extensions in a three-user interference channel (i.e., for a three-user system, we have $q = 1$ and $N = (n + 1)^q + n^q = 2n + 1$). We will derive the precoding/decoding procedure for interference alignment with multi-user OFDM and prove its efficacy in this section.

The precoding matrices proposed in [19] for the case of three users are as follows.

$$\mathbf{V}_1 = \mathbf{A} \tag{3.15}$$

$$\mathbf{V}_2 = \mathbf{H}_{23}^{-1}\mathbf{H}_{13}\mathbf{C} \tag{3.16}$$

$$\mathbf{V}_3 = \mathbf{H}_{32}^{-1}\mathbf{H}_{12}\mathbf{B}, \tag{3.17}$$

where

$$\mathbf{A} = [\vec{w}\ \mathbf{T}\vec{w}\ \mathbf{T}^2\vec{w}\ \cdots\ \mathbf{T}^n\vec{w}] \tag{3.18}$$

$$\mathbf{B} = [\mathbf{T}\vec{w}\ \mathbf{T}^2\vec{w}\ \cdots\ \mathbf{T}^n\vec{w}] \tag{3.19}$$

$$\mathbf{C} = [\vec{w}\ \mathbf{T}\vec{w}\ \mathbf{T}^2\vec{w}\ \cdots\ \mathbf{T}^{n-1}\vec{w}] \tag{3.20}$$

$$\mathbf{T} = \mathbf{H}_{21}\mathbf{H}_{12}^{-1}\mathbf{H}_{32}\mathbf{H}_{23}^{-1}\mathbf{H}_{13}\mathbf{H}_{31}^{-1} \tag{3.21}$$

$$\vec{w} = [1\ 1\ \cdots\ 1]^T. \tag{3.22}$$

Thus, the received signal at receiver 1 is:

$$\vec{y}_1 = \mathbf{H}_{11}\mathbf{V}_1\vec{x}_1 + \mathbf{H}_{21}\mathbf{V}_2\vec{x}_2 + \mathbf{H}_{31}\mathbf{V}_3\vec{x}_3. \tag{3.23}$$

In the general case, since the data streams are independent of each other, the received mixed signal spans $3n+1$ dimensions of the space. In interference alignment with multi-user OFDM, the received signal spans only $2n+1$ dimensions of space. Solving these $2n+1$ equations will yield the desired packets. However, the challenge is, if $2n+1$ is too large, we may not be able to solve these equations efficiently (as can be seen from the later discussions). This problem can be addressed with a decomposition approach as given in the following theorem.

Theorem 3.1. *For an N subcarrier OFDM system, we can divide the subcarriers into $\lfloor N/(2n+1) \rfloor$ groups, where $n \in \mathbb{N}$, and precode and decode the groups separately to achieve the interference alignment gain.*

Proof. Recall that the channel gain matrix in OFDM is diagonal. Generally, if every user tries to transmit d packets over the N subcarriers, we have

$$\mathbf{HV} = \begin{pmatrix} h_1 & 0 & \cdots & 0 \\ 0 & h_2 & \cdots & 0 \\ \vdots & \vdots & \ddots & \vdots \\ 0 & 0 & \cdots & h_N \end{pmatrix} \begin{pmatrix} v_{11} & \cdots & v_{1d} \\ v_{21} & \cdots & v_{2d} \\ \vdots & \ddots & \vdots \\ v_{N1} & \cdots & v_{Nd} \end{pmatrix}.$$

The precoding vectors must satisfy the conditions given in (3.15)-(3.22). Let the precoding matrix assume the following form.

$$\mathbf{V} = \begin{pmatrix} \widetilde{\mathbf{V}}_1 & 0 & \cdots & 0 \\ 0 & \widetilde{\mathbf{V}}_2 & \cdots & 0 \\ \vdots & \vdots & \ddots & \vdots \\ 0 & 0 & \cdots & \widetilde{\mathbf{V}}_g \end{pmatrix}, \tag{3.24}$$

where $g = N/(2n+1)$ is the number of groups and $\widetilde{\mathbf{V}}_i$ is the precoding matrix for group i with dimensions $(2n+1) \times (n+1)$ or $(2n+1) \times n$ (i.e., user 1 sends $(n+1)$ packets, and each of the other users sends n packets over $(2n+1)$ subcarriers.) Without loss of generality, we assume N is dividable by $2n+1$. Rewriting **H** in the form of multiple diagonal sub-matrices with the same

dimensions, we have

$$\mathbf{HV} = \begin{pmatrix} \widetilde{\mathbf{H}}_1\widetilde{\mathbf{V}}_1 & 0 & \cdots & 0 \\ 0 & \widetilde{\mathbf{H}}_2\widetilde{\mathbf{V}}_2 & \cdots & 0 \\ \vdots & \vdots & \ddots & \vdots \\ 0 & 0 & \cdots & \widetilde{\mathbf{H}}_g\widetilde{\mathbf{V}}_g \end{pmatrix}. \tag{3.25}$$

For instance, when $N = 6$ and $n = 1$, we have for transmitter 1

$$\mathbf{HV} = \begin{pmatrix} h_1v_{11} & h_1v_{12} & 0 & 0 \\ h_2v_{21} & h_2v_{22} & 0 & 0 \\ h_3v_{31} & h_3v_{32} & 0 & 0 \\ 0 & 0 & h_4v_{41} & h_4v_{42} \\ 0 & 0 & h_5v_{51} & h_5v_{52} \\ 0 & 0 & h_6v_{61} & h_6v_{62} \end{pmatrix}. \tag{3.26}$$

If there are 3 users, we can let $\mathbf{H}_{21}\mathbf{V}_2 = \mathbf{H}_{31}\mathbf{V}_3$ at receiver 1 to get

$$\begin{pmatrix} h_{21}^{(1)}v_2^{(1)} & 0 & \cdots & 0 \\ h_{21}^{(2)}v_2^{(2)} & 0 & \cdots & 0 \\ h_{21}^{(3)}v_2^{(3)} & 0 & \cdots & 0 \\ 0 & h_{21}^{(4)}v_2^{(4)} & \cdots & 0 \\ 0 & h_{21}^{(5)}v_2^{(5)} & \cdots & 0 \\ 0 & h_{21}^{(6)}v_2^{(6)} & \cdots & 0 \\ \vdots & \vdots & \ddots & \vdots \\ 0 & 0 & \cdots & h_{21}^{(N-2)}v_2^{(N-2)} \\ 0 & 0 & \cdots & h_{21}^{(N-1)}v_2^{(N-1)} \\ 0 & 0 & \cdots & h_{21}^{(N)}v_2^{(N)} \end{pmatrix}$$

$$= \begin{pmatrix} h_{31}^{(1)} v_3^{(1)} & 0 & \cdots & 0 \\ h_{31}^{(2)} v_3^{(2)} & 0 & \cdots & 0 \\ h_{31}^{(3)} v_3^{(3)} & 0 & \cdots & 0 \\ 0 & h_{31}^{(4)} v_3^{(4)} & \cdots & 0 \\ 0 & h_{31}^{(5)} v_3^{(5)} & \cdots & 0 \\ 0 & h_{31}^{(6)} v_3^{(6)} & \cdots & 0 \\ \vdots & \vdots & \ddots & \vdots \\ 0 & 0 & \cdots & h_{31}^{(N-2)} v_3^{(N-2)} \\ 0 & 0 & \cdots & h_{31}^{(N-1)} v_3^{(N-1)} \\ 0 & 0 & \cdots & h_{31}^{(N)} v_3^{(N)} \end{pmatrix},$$

which indicates:

$$\begin{pmatrix} h_{21}^{(i)} v_2^{(i)} \\ h_{21}^{(i+1)} v_2^{(i+1)} \\ h_{21}^{(i+2)} v_2^{(i+2)} \end{pmatrix} = \begin{pmatrix} h_{31}^{(i)} v_3^{(i)} \\ h_{31}^{(i+1)} v_3^{(i+1)} \\ h_{31}^{(i+2)} v_3^{(i+2)} \end{pmatrix}, \ i = 1, 4, \cdots, N-2. \tag{3.27}$$

Since the above conditions can also be obtained by separately encoding the $N/(2n+1)$ groups of subcarriers, we could decompose the problem into a number of subproblems, one for each group, and precode and decode the groups separately.

It remains to show how to decode the packets for this scheme. Without loss of generality, we also assume $K = 3$. If this scheme is adopted, each time we sequentially take out $2n + 1$

subcarriers. The received signal at receiver 1 is:

$$\begin{aligned}
\vec{y}_1 &= \mathbf{H}_{11}\mathbf{V}_1\vec{x}_1 + \mathbf{H}_{21}\mathbf{V}_2\vec{x}_2 + \mathbf{H}_{31}\mathbf{V}_3\vec{x}_3 \\
&= \mathbf{H}_{11}\mathbf{V}_1\vec{x}_1 + \mathbf{H}_{21}\mathbf{H}_{23}^{-1}\mathbf{H}_{13}\mathbf{C}\vec{x}_2 + \mathbf{H}_{31}\mathbf{H}_{32}^{-1}\mathbf{H}_{12}\mathbf{B}\vec{x}_3 \\
&= \mathbf{H}_{11}\mathbf{V}_1\vec{x}_1 + \mathbf{H}_{21}\mathbf{H}_{23}^{-1}\mathbf{H}_{13}\mathbf{C}\vec{x}_2 + \mathbf{H}_{31}\mathbf{H}_{32}^{-1}\mathbf{H}_{12}\mathbf{T}\mathbf{C}\vec{x}_3 \\
&= \mathbf{H}_{11}\mathbf{V}_1\vec{x}_1 + \mathbf{H}_{21}\mathbf{H}_{23}^{-1}\mathbf{H}_{13}\mathbf{C}\vec{x}_2 + \mathbf{H}_{21}\mathbf{H}_{23}^{-1}\mathbf{H}_{13}\mathbf{C}\vec{x}_3 \\
&= \mathbf{H}_{11}\mathbf{V}_1\vec{x}_1 + \mathbf{H}_{21}\mathbf{H}_{23}^{-1}\mathbf{H}_{13}\mathbf{C}(\vec{x}_2 + \vec{x}_3) \\
&= (\mathbf{H}_{11}\mathbf{V}_1\ \mathbf{H}_{21}\mathbf{V}_2) \cdot \left(\vec{x}_1\ \vec{x}_2 + \vec{x}_3\right)^T. \qquad (3.28)
\end{aligned}$$

Taking the inverse of matrix $(\mathbf{H}_{11}\mathbf{V}_1\ \mathbf{H}_{21}\mathbf{V}_2)$ and discard the packets from transmitters 2 and 3, we can recover the desired packets $\vec{x}_1$. Note that we exploit the *commutative* property of diagonal matrices in (3.28).

At receiver 2, the received signal is:

$$\begin{aligned}
\vec{y}_2 &= \mathbf{H}_{12}\mathbf{V}_1\vec{x}_1 + \mathbf{H}_{22}\mathbf{V}_2\vec{x}_2 + \mathbf{H}_{32}\mathbf{V}_3\vec{x}_3 \\
&= \mathbf{H}_{12}(\vec{w}\ \mathbf{B})\vec{x}_1 + \mathbf{H}_{22}\mathbf{V}_2\vec{x}_2 + \mathbf{H}_{12}\mathbf{B}\vec{x}_3 \\
&= \mathbf{H}_{12}\vec{w}x_1^{(1)} + \mathbf{H}_{22}\mathbf{V}_2\vec{x}_2 + \mathbf{H}_{12}\mathbf{B}\begin{pmatrix} x_1^{(2)} + x_3^{(1)} \\ \vdots \\ x_1^{(n+1)} + x_3^{(n)} \end{pmatrix} \\
&= (\mathbf{H}_{22}\mathbf{V}_2\ \mathbf{H}_{12}\vec{w}\ \mathbf{H}_{12}\mathbf{B}) \cdot \\
&\quad \left(\vec{x}_2, x_1^{(1)}, x_1^{(2)} + x_3^{(1)}, \cdots, x_1^{(n+1)} + x_3^{(n)}\right)^T. \qquad (3.29)
\end{aligned}$$

Taking the inverse of matrix $(\mathbf{H}_{22}\mathbf{V}_2\ \mathbf{H}_{12}\vec{w}\ \mathbf{H}_{12}\mathbf{B})$, we get $\vec{x}_2$.

At receiver 3, the received signal is:

$$\begin{aligned}
\vec{y}_3 &= \mathbf{H}_{13}\mathbf{V}_1\vec{x}_1 + \mathbf{H}_{23}\mathbf{V}_2\vec{x}_2 + \mathbf{H}_{33}\mathbf{V}_3\vec{x}_3 \\
&= \mathbf{H}_{13}(\mathbf{C}\ \mathbf{T}^n\vec{w})\vec{x}_1 + \mathbf{H}_{13}\mathbf{C}\vec{x}_2 + \mathbf{H}_{33}\mathbf{V}_3\vec{x}_3 \\
&= \mathbf{H}_{13}\mathbf{C}\begin{pmatrix} x_1^{(1)} + x_2^{(1)} \\ \vdots \\ x_1^{(n)} + x_2^{(n)} \end{pmatrix} + \mathbf{H}_{13}\mathbf{T}^n\vec{w}x_1^{(n+1)} + \mathbf{H}_{33}\mathbf{V}_3\vec{x}_3 \\
&= (\mathbf{H}_{33}\mathbf{V}_3\ \mathbf{H}_{13}\mathbf{C}\ \mathbf{H}_{13}\mathbf{T}^n\vec{w}) \cdot \\
&\quad \left(\vec{x}_3, x_1^{(1)} + x_2^{(1)}, \cdots, x_1^{(n)} + x_2^{(n)}, x_1^{(n+1)}\right)^T. \qquad (3.30)
\end{aligned}$$

Taking the inverse of matrix $(\mathbf{H}_{33}\mathbf{V}_3\ \mathbf{H}_{13}\mathbf{C}\ \mathbf{H}_{13}\mathbf{T}^n\vec{w})$, we can decode $\vec{x}_3$. After decoding each group separately, we then combine the decoded data. The theorem is thus proved. □

Note that the proof of Theorem 3.1 also leads to an algorithm to achieve interference alignment gains for any large $N \in \mathbb{N}$.

Practical Issue of Large Channel Variance

Here we examine another practical problem of adopting interference alignment for multi-user OFDM.

A necessary condition to achieve interference alignment in OFDM is that the channel gain is drawn from a continuous distribution. As a result, if the variance of the channel is large, some of the channel gains can be very small in certain conditions, while some other channel gains can be very large. When precoding over all the subcarriers, after taking the inverse of the channel gain matrix, some entry of the precoding matrix could be 10^4 times (or even more) larger than some other ones. The result is that the power of one subcarrier could be 10^8 times (or even more) larger than that of another subcarrier. Given certain power constraints, the error performance of the system will suffer from great degradation, which makes interference alignment less useful.

In our proposed scheme, if the channel variance is large, there is also a certain chance that some entries of $\mathbf{T}$ can be much larger than the others, since $\mathbf{T} = \mathbf{H}_{21}\mathbf{H}_{12}^{-1}\mathbf{H}_{32}\mathbf{H}_{23}^{-1}\mathbf{H}_{13}\mathbf{H}_{31}^{-1} = \mathbf{H}_{21}\mathbf{H}_{32}\mathbf{H}_{13}\mathbf{H}_{12}^{-1}\mathbf{H}_{23}^{-1}\mathbf{H}_{31}^{-1}$. If we precode and decode over large n, since the last column of $\mathbf{V}_1$, $\mathbf{V}_2$ and $\mathbf{V}_3$ are all obtained by multiplying $\mathbf{T}^n$, the situation could be further exacerbated. The consequences are as follows.

(i) Since some of the entries can be extremely small, the decoding matrices can be close to singular. Thus the desired signal cannot be decoded.

(ii) Even if the decoding matrices is invertible, due to the transmitter power constraint, the system error performance could be rather poor.

In fact, even if $n = 1$, there is still a chance that some matrices are not invertible. These are the reasons why we cannot precode and decode for large N. This issue also demonstrate the importance of the proposed decomposition theorem (see Theorem 3.1).

Take $\mathbf{V}_1$ for instance. The constraint is the power on one subcarrier cannot be 10^a (e.g., $a = 3$) times larger than the power on another subcarrier. If the constraint is violated, the system is considered to be in the outage state. Let

$$\mathbf{T} = \begin{pmatrix} t_1 & 0 & \cdots & 0 \\ 0 & t_2 & \cdots & 0 \\ \vdots & \vdots & \ddots & \vdots \\ 0 & 0 & \cdots & t_{2n+1} \end{pmatrix}, \tag{3.31}$$

where $t_i = h_{21}^{(i)}h_{32}^{(i)}h_{13}^{(i)}/(h_{12}^{(i)}h_{23}^{(i)}h_{31}^{(i)}),\ i = 1, 2, \ldots, (2n+1)$. $t_1, t_2, \ldots, t_{2n+1}$ can be regarded as $i.i.d$ (independent identically distributed) random variables. Let t denote the common distribution of $t_1, t_2, \ldots, t_{2n+1}$. Define $t_{(1)}, t_{(2)}, \ldots, t_{(2n+1)}$ be the order statistics of $t_1, t_2, \ldots, t_{2n+1}$ with $t_{(1)} = \min_i t_i$, $t_{(2n+1)} = \max_i t_i$.

Let $\gamma = t_{(2n+1)}/t_{(1)}$. From (3.15)-(3.22), we have $\gamma^{2n} \leq 10^a$, thus

$$\gamma \leq 10^{a/(2n)}, \tag{3.32}$$

which means $t_{(2n+1)}$ cannot be $10^{a/(2n)}$ times larger than $t_{(1)}$.

On the other hand, since $\gamma_{max} = 10^{a/(2n)}$, we have

$$1 - \left(\Pr\left\{ t \geq \frac{t_{(2n+1)}}{10^{\frac{a}{2n}}} \right\} \right)^{2n+1} \leq \Pr\left\{ t_{(1)} \leq \frac{t_{(2n+1)}}{\gamma} \right\} \leq 1. \tag{3.33}$$

It can be seen that $\Pr\left\{ t \geq \frac{t_{(2n+1)}}{10^{\frac{a}{2n}}} \right\}$ is a decreasing function of n. With the power of $2n+1$, $\Pr\left\{ t_{(1)} \leq t_{(2n+1)}/\gamma \right\}$ will quickly converge to 1. That means, with large n, $P(t_{(2n+1)} \geq \gamma t_{(1)}) = 1$. Therefore, with large n the constraint (3.32) will not be satisfied.

Next, we show how large n could be for given constraint (3.32). The joint probability density function (PDF) of $t_{(1)}$ and $t_{(2n+1)}$ is found as follows.

$$f_{t_{(1)}t_{(2n+1)}}(x, y) = \frac{\partial^2 F_{t_{(1)}t_{(2n+1)}}(x, y)}{\partial x \partial y}, \tag{3.34}$$

where $F_{t_{(1)}t_{(2n+1)}}(x,y)$ is the joint cumulative distribution function (CDF) of $t_{(1)}$ and $t_{(2n+1)}$. By the definition of partial derivative, we have:

$$
\begin{aligned}
& f_{t_{(1)}t_{(2n+1)}}(x,y) \\
=& \frac{\partial}{\partial y}\{\lim_{\Delta x\to 0}[F_{t_{(1)}t_{(2n+1)}}(x+\Delta x,y)- \\
& F_{t_{(1)}t_{(2n+1)}}(x,y)]/\Delta x\} \\
=& \lim_{\Delta x\to 0,\Delta y\to 0}[F_{t_{(1)}t_{(2n+1)}}(x+\Delta x,y+\Delta y)- \\
& F_{t_{(1)}t_{(2n+1)}}(x,y+\Delta y)-F_{t_{(1)}t_{(2n+1)}}(x+\Delta x,y)+ \\
& F_{t_{(1)}t_{(2n+1)}}(x,y)]/(\Delta x\Delta y) \\
=& \lim_{\Delta x\to 0,\Delta y\to 0}[\Pr\{x\le t_{(1)}\le x+\Delta x, t_{(2n+1)}\le y+\Delta y\}- \\
& \Pr\{x\le t_{(1)}\le x+\Delta x, t_{(2n+1)}\le y\}]/(\Delta x\Delta y) \\
=& \lim_{\Delta x\to 0,\Delta y\to 0}\Pr\{x\le t_{(1)}\le x+\Delta x, \\
& y\le t_{(2n+1)}\le y+\Delta y)/(\Delta x\Delta y\}. \qquad (3.35)
\end{aligned}
$$

To calculate the probability of the last equality, for any $x<y$, we can divide the x axis into five disjoint intervals as: $I_1=(-\infty,x)$, $I_2=(x,x+\Delta x)$, $I_3=(x+\Delta x,y)$, $I_4=(y,y+\Delta y)$ and $I_5=(y+\Delta y,\infty)$. For each t_i, the probability it falls into each interval can be calculated as follows.

$$p_1=\Pr\{t_i\in I_1\}=F_t(x) \qquad (3.36)$$

$$p_2=\Pr\{t_i\in I_2\}=F_t(x+\Delta x)-F_t(x) \qquad (3.37)$$

$$p_3=\Pr\{t_i\in I_3\}=F_t(y)-F_t(x+\Delta x) \qquad (3.38)$$

$$p_4=\Pr\{t_i\in I_4\}=F_t(y+\Delta y)-F_t(y) \qquad (3.39)$$

$$p_5=\Pr\{t_i\in I_5\}=1-F_t(y+\Delta y). \qquad (3.40)$$

To make $(x \leq t_{(1)} \leq x+\Delta x, y \leq t_{(2n+1)} \leq y+\Delta y)$ happen, the statistics $\{t_1, t_2, \ldots, t_{2n+1}\}$ must have exactly 1 sample falling into interval I_2, 1 falling into interval I_4, $(2n-1)$ falling into interval I_3, and 0 elsewhere, which is a multinomial problem. So we have:

$$\begin{aligned}\Pr\{x \leq t_{(1)} \leq x+\Delta x, y \leq t_{(2n+1)} \leq y+\Delta y\} = \\ \binom{2n+1}{0,1,(2n-1),1,0} p_1^0 p_2^1 p_3^{(2n-1)} p_4^1 p_5^0. \end{aligned} \tag{3.41}$$

It follows that

$$\begin{aligned} & f_{t_{(1)}t_{(2n+1)}}(x,y) \\ = & \lim_{\Delta x \to 0, \Delta y \to 0} \left\{ \frac{(2n+1)!}{(2n-1)!} \frac{F_t(x+\Delta x) - F_t(x)}{\Delta x} \times \right. \\ & \left. \frac{F_t(y+\Delta y) - F_t(y)}{\Delta y} \times [F_t(y) - F_t(x+\Delta x)]^{2n-1} \right\} \\ = & (2n+1)(2n) f_t(x) f_t(y) [F_t(y) - F_t(x)]^{2n-1}. \end{aligned} \tag{3.42}$$

Since $t_i = h_{21}^{(i)} h_{32}^{(i)} h_{13}^{(i)} / (h_{12}^{(i)} h_{23}^{(i)} h_{31}^{(i)}),\ i = 1, 2, \ldots, 2n+1$, and each $h^{(i)}$ is a random variable, the distribution of t_i is difficult to be explicitly found. Here we continue our analysis by approximating t_i as a Uniform distributed or Rayleigh distributed random variable.

If t_i is approximated as a Uniform distributed random variable and $t_i \in (0,1)$, we have:

$$\Pr\left\{ t_{(1)} \leq \frac{t_{(2n+1)}}{\gamma} \right\} \tag{3.43}$$

$$= \int_0^1 \int_0^{\frac{y}{\gamma}} (2n+1)(2n)(y-x)^{2n-1} dx dy. \tag{3.44}$$

$$= \left[1 - \left(1 - \frac{1}{\gamma} \right)^{2n} \right] \tag{3.45}$$

$$\geq 1 - (1 - 10^{-\frac{a}{2n}})^{2n}, \tag{3.46}$$

where the last inequality is a direct result of (3.32). Taking derivative of (3.46), it can be found that $P_{outage} = \Pr\left\{ t_{(1)} \leq \frac{t_{(2n+1)}}{\gamma} \right\}$ is an increasing function of n. For $a = 3$, if $n = 1$, $P_{outage} = 0.0622$;

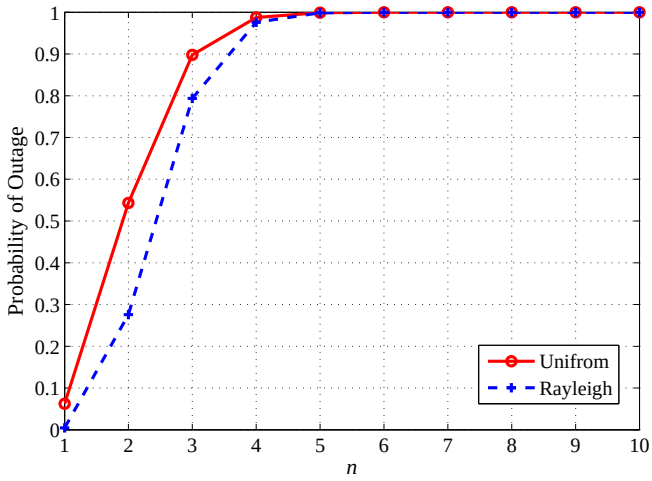

Figure 3.2: Probability of System Outage.

if $n = 2$, $P_{outage} = 0.5431$; and if $n = 3$, $P_{outage} = 0.8978$. For a system with many subcarriers, it indicates that we can only precode over $n = 1$.

If t_i is approximated as a Rayleigh distributed random variable with PDF $f(x \mid \sigma) = \frac{x}{\sigma^2} \exp(-\frac{x^2}{2\sigma^2})$, $x \geq 0$, then

$$f_{t_{(1)}t_{(2n+1)}}(x, y) = (2n+1)(2n)\frac{xy}{\sigma^4} \exp\left(-\frac{x^2+y^2}{2\sigma^2}\right) \cdot \left(\exp\left(-\frac{x^2}{2\sigma^2}\right) - \exp\left(-\frac{y^2}{2\sigma^2}\right)\right)^{2n-1}. \tag{3.47}$$

There's no closed-form solution of $\Pr\left\{t_{(1)} \leq \frac{t_{(2n+1)}}{\gamma}\right\}$ in this case. The numerical results are shown in Fig. 3.2. It can be seen that the conclusion still holds, i.e., we can only precode over $n = 1$.

Recall that Conjecture 3.3.1 tells us $d_{max} = 1.4998$ when $K = 3$ and $n = 1000$. Here we can see that this maximum DoF cannot be achieved under practical settings. So we have the following theorem.

Theorem 3.2. *For a practical multi-user OFDM system with number of subcarriers less than* 4149*, the maximum DoF is* $d_{max} = 1.33$*, which is achieved when there are three transmitter/receiver pairs precoding over* 3 *subcarriers each time.*

3.4 Multi-user MIMO OFDM with Interference Alignment

In previous sections, we have considered applying interference alignment to OFDM systems. Since MIMO transmission technique can also be adopted to enhance the system throughput, we consider incorporating interference alignment to MIMO-OFDM systems in this section.

Suppose we have M antennas at both the transmitter and receiver sides, and N subcarriers in total. The signals received at the i-th receiver on subcarrier n can be represented as:

$$\vec{y}_i(n) = \mathbf{H}_{ii}(n)\mathbf{V}_i(n)\vec{x}_i(n) + \sum_{j \neq i} \mathbf{H}_{ji}(n)\mathbf{V}_j(n)\vec{x}_j(n), \tag{3.48}$$

where $\mathbf{H}_{ij}(n)$, $\mathbf{V}_i(n)$, and $\vec{x}_i(n)$ are the channel matrix from transmitter i to receiver j, precoding matrix at transmitter i, and data at transmitter i, respectively; and all of them are at subcarrier n. From (3.48), we can see that, the signals received can be represented as a matrix, with each column being the signals received from each subcarrier, i.e., $\mathbf{Y}_i = [\vec{y}_i(1)\ \vec{y}_i(2)\ \ldots\ \vec{y}_i(n)]$. Or we could vectorize this matrix so that we get the following simpler form.

$$\vec{y}_i = \mathbf{H}_{ii}\mathbf{V}_i\vec{x}_i + \sum_{j \neq i} \mathbf{H}_{ji}\mathbf{V}_j\vec{x}_j. \tag{3.49}$$

Since each antenna pair could operate on any subcarrier and there is no crosstalk between subcarriers, the wireless channel $\mathbf{H}_{ij}$ between transmitter i and receiver j is of the form as shown in (3.50).

Theorem 3.3. *For a MIMO-OFDM system with N subcarriers and M antennas at each transmitter and receiver side, we can divide the subcarriers into $\lfloor N/(2n+1) \rfloor$ groups, where $n \in \mathbb{N}$, and precode and decode the groups separately to achieve the interference alignment gain.*

Proof. In Theorem 3.1, we have actually established that for a system of diagonal channels, we could separately precode and decode each group of subcarriers. Now consider the case when all the devices are equipped with multiple antennas. We can still divide the subcarriers into different

$$\mathbf{H}_{ij} = \begin{pmatrix} h_{ij}^{1,1} & 0 & 0 & \cdots & h_{ij}^{N+1,1} & 0 & \cdots & h_{ij}^{(M-1)N+1,1} & 0 & \cdots \\ 0 & h_{ij}^{2,2} & 0 & \cdots & 0 & h_{ij}^{N+2,2} & \cdots & 0 & h_{ij}^{(M-1)N+2,2} & \cdots \\ \vdots & \vdots & \ddots & \vdots & \vdots & \ddots & \vdots & \vdots & \ddots & \vdots \end{pmatrix}. \quad (3.50)$$

$$\mathbf{H}_{ij} = \begin{pmatrix} h_{ij}^{1,1} & \cdots & h_{ij}^{M,1} & 0 & \cdots & 0 & \cdots & 0 \\ \vdots & \ddots & \vdots & 0 & \cdots & 0 & \cdots & 0 \\ h_{ij}^{1,M} & \cdots & h_{ij}^{M,M} & 0 & \cdots & 0 & \cdots & 0 \\ \vdots & \vdots & \vdots & \ddots & \cdots & \vdots & \vdots & \vdots \\ \cdots & \cdots & \cdots & \cdots & \ddots & \cdots & \cdots & \cdots \\ 0 & \cdots & \cdots & 0 & \cdots & h_{ij}^{M(N-1)+1,M(N-1)+1} & \cdots & h_{ij}^{MN,M(N-1)+1} \\ \vdots & \vdots & \vdots & \vdots & \cdots & \vdots & \ddots & \vdots \\ 0 & \cdots & \cdots & 0 & \cdots & h_{ij}^{M(N-1)+1,MN} & \cdots & h_{ij}^{MN,MN} \end{pmatrix}. \quad (3.51)$$

groups, then precode and decode them separately, since we are able to distinguish the signals from different antennas and different subcarriers. In other words, upon receiving a signal, the receiver has the knowledge of from which antenna and which subcarrier it gets the signal. So by properly adjusting the order of the data transmitted, the channel is essentially of the form in (3.51). We can readily identify that (3.51) is actually in the block diagonal form with the i-th block corresponding to the channels associated with the i-th subcarrier. Within each block, we have standard MIMO channels. Letting V, with dimension $MN \times d$, assume the form of (3.24), by similar arguments as in Theorem 3.1, we could precode and decode the groups separately to achieve the interference alignment gain. □

Lemma 1. *All the channel matrices and matrix T are invertible.*

Proof. As shown in (3.52), the inverse of a block matrix can be found by calculating the inverse of each block. Since for each block, we have a standard MIMO channel matrix and each of its entry is drawn from a continuous random distribution, each block is invertible with probability 1. So each channel matrix is invertible. Since the product of invertible matrices is still invertible, according to

(3.21), matrix T is invertible.

$$\begin{pmatrix} B_1 & 0 & 0 \\ 0 & B_2 & 0 \\ 0 & 0 & B_3 \end{pmatrix}^{-1} = \begin{pmatrix} B_1^{-1} & 0 & 0 \\ 0 & B_2^{-1} & 0 \\ 0 & 0 & B_3^{-1} \end{pmatrix}. \tag{3.52}$$

□

Theorem 3.4. *For a MIMO-OFDM system with N subcarriers and M antennas at each transmitter and receiver side, the maximum gain is $\frac{4}{3}M$.*

Proof. According to Theorem 3.3, we could precode and decode over groups of subcarrier. Also, according to our previous results, we can only precode and decode over 3 subcarriers. So subcarrier-wise, the normalized DoF is $4/3$.

We next show that $\frac{4}{3}M$ is the maximum achievable DoF. Firstly, we notice that by dividing the subcarriers into groups of 3, taking $\mathbf{H}_{11}$ for instance, it is transformed from (3.53) to (3.54). With the establishment of Lemma 1, following the proof of Theorem 3.1, and replacing the scalars with blocks, we readily have the maximum gain of $\frac{4}{3}M$.

$$\mathbf{H}_{11} = \begin{pmatrix} h_{11}^{11} & 0 & 0 & h_{11}^{41} & 0 & 0 \\ 0 & h_{11}^{22} & 0 & 0 & h_{11}^{52} & 0 \\ 0 & 0 & h_{11}^{33} & 0 & 0 & h_{11}^{63} \\ h_{11}^{14} & 0 & 0 & h_{11}^{44} & 0 & 0 \\ 0 & h_{11}^{25} & 0 & 0 & h_{11}^{55} & 0 \\ 0 & 0 & h_{11}^{36} & 0 & 0 & h_{11}^{66} \end{pmatrix}. \tag{3.53}$$

$$\mathbf{H}_{11} = \begin{pmatrix} h_{11}^{11} & h_{11}^{21} & 0 & 0 & 0 & 0 \\ h_{11}^{12} & h_{11}^{22} & 0 & 0 & 0 & 0 \\ 0 & 0 & h_{11}^{33} & h_{11}^{44} & 0 & 0 \\ 0 & 0 & h_{11}^{34} & h_{11}^{44} & 0 & 0 \\ 0 & 0 & 0 & 0 & h_{11}^{55} & h_{11}^{65} \\ 0 & 0 & 0 & 0 & h_{11}^{56} & h_{11}^{66} \end{pmatrix}. \tag{3.54}$$

□

We next show how to achieve this gain. We design $\mathbf{V}_1$, $\mathbf{V}_2$, and $\mathbf{V}_3$ as follows.

$$\mathbf{V}_1 = \mathbf{A} \tag{3.55}$$

$$\mathbf{V}_2 = \mathbf{H}_{23}^{-1}\mathbf{H}_{13}\mathbf{C} \tag{3.56}$$

$$\mathbf{V}_3 = \mathbf{H}_{32}^{-1}\mathbf{H}_{12}\mathbf{B}, \tag{3.57}$$

where

$$\mathbf{A} = [\vec{w}\ \mathbf{T}\vec{w}\ \mathbf{T}^2\vec{w}\ \cdots\ \mathbf{T}^{(n+1)M-1}\vec{w}] \tag{3.58}$$

$$\mathbf{B} = [\mathbf{T}^{M}\vec{w}\ \mathbf{T}^{M+1}\vec{w}\ \cdots\ \mathbf{T}^{(n+1)M-1}\vec{w}] \tag{3.59}$$

$$\mathbf{C} = [\mathbf{T}^{M-1}\vec{w}\ \mathbf{T}^{M}\vec{w}\ \cdots\ \mathbf{T}^{(n+1)M-2}\vec{w}] \tag{3.60}$$

$$\mathbf{T} = \mathbf{H}_{12}^{-1}\mathbf{H}_{32}\mathbf{H}_{31}^{-1}\mathbf{H}_{21}\mathbf{H}_{23}^{-1}\mathbf{H}_{13} \tag{3.61}$$

$$\vec{w} = [1\ 1\ \cdots\ 1]^T. \tag{3.62}$$

It can be observed that:

$$\mathbf{A} = [\vec{w}\ \mathbf{T}\vec{w}\ \cdots\ \mathbf{T}^{M-1}\vec{w}\ \mathbf{B}] \tag{3.63}$$

$$= [\vec{w}\ \mathbf{T}\vec{w}\ \cdots\ \mathbf{T}^{M-2}\vec{w}\ \mathbf{C}\ \mathbf{T}^{(n+1)M-1}\vec{w}]. \tag{3.64}$$

At receiver 1, the received signals can be written as:

$$\begin{aligned}
\vec{y}_1 &= \mathbf{H}_{11}\mathbf{V}_1\vec{x}_1 + \mathbf{H}_{21}\mathbf{V}_2\vec{x}_2 + \mathbf{H}_{31}\mathbf{V}_3\vec{x}_3 \\
&= \mathbf{H}_{11}\mathbf{V}_1\vec{x}_1 + \mathbf{H}_{21}\mathbf{H}_{23}^{-1}\mathbf{H}_{13}\mathbf{C}\vec{x}_2 + \mathbf{H}_{31}\mathbf{H}_{32}^{-1}\mathbf{H}_{12}\mathbf{B}\vec{x}_3 \\
&= \mathbf{H}_{11}\mathbf{V}_1\vec{x}_1 + \mathbf{H}_{21}\mathbf{H}_{23}^{-1}\mathbf{H}_{13}\mathbf{C}\vec{x}_2 + \mathbf{H}_{31}\mathbf{H}_{32}^{-1}\mathbf{H}_{12}\mathbf{T}\mathbf{C}\vec{x}_3 \\
&= \mathbf{H}_{11}\mathbf{V}_1\vec{x}_1 + \mathbf{H}_{21}\mathbf{H}_{23}^{-1}\mathbf{H}_{13}\mathbf{C}\vec{x}_2 + \mathbf{H}_{21}\mathbf{H}_{23}^{-1}\mathbf{H}_{13}\mathbf{C}\vec{x}_3 \\
&= \mathbf{H}_{11}\mathbf{V}_1\vec{x}_1 + \mathbf{H}_{21}\mathbf{H}_{23}^{-1}\mathbf{H}_{13}\mathbf{C}(\vec{x}_2 + \vec{x}_3) \\
&= (\mathbf{H}_{11}\mathbf{V}_1\ \mathbf{H}_{21}\mathbf{V}_2) \cdot \begin{pmatrix} \vec{x}_1 \\ \\ \vec{x}_2 + \vec{x}_3 \end{pmatrix}. \qquad (3.65)
\end{aligned}$$

For signals at receiver 2, we have:

$$
\begin{aligned}
\vec{y}_2 &= \mathbf{H}_{12}\mathbf{V}_1\vec{x}_1 + \mathbf{H}_{22}\mathbf{V}_2\vec{x}_2 + \mathbf{H}_{32}\mathbf{V}_3\vec{x}_3 \\
&= \mathbf{H}_{12}(\vec{w}\ \mathbf{T}\vec{w}\ \cdots\ \mathbf{T}^{M-1}\vec{w}\ \mathbf{B})\vec{x}_1 + \mathbf{H}_{22}\mathbf{V}_2\vec{x}_2 + \mathbf{H}_{12}\mathbf{B}\vec{x}_3 \\
&= \mathbf{H}_{12}(\vec{w}\ \mathbf{T}\vec{w}\ \cdots\ \mathbf{T}^{M-1}\vec{w}) \begin{pmatrix} x_1^{(1)} \\ \vdots \\ x_1^{(M)} \end{pmatrix} \\
&+ \mathbf{H}_{12}\mathbf{B} \begin{pmatrix} x_1^{(M+1)} \\ \vdots \\ x_1^{((n+1)M)} \end{pmatrix} + \mathbf{H}_{22}\mathbf{V}_2\vec{x}_2 + \mathbf{H}_{12}\mathbf{B}\vec{x}_3 \\
&= (\mathbf{H}_{22}\mathbf{V}_2\ \mathbf{H}_{12}(\vec{w}\ \mathbf{T}\vec{w}\ \cdots\ \mathbf{T}^{M-1}\vec{w})\ \mathbf{H}_{12}\mathbf{B}) \cdot \\
&\quad \begin{pmatrix} \vec{x}_2 \\ x_1^{(1)} \\ \vdots \\ x_1^{(M)} \\ x_1^{(M+1)} + x_3^{(1)} \\ \vdots \\ x_1^{((n+1)M)} + x_3^{(nM)} \end{pmatrix}.
\end{aligned}
\tag{3.66}
$$

And similarly for signals at receiver 3, we have:

$$
\begin{aligned}
\vec{y}_3 &= \mathbf{H}_{13}\mathbf{V}_1\vec{x}_1 + \mathbf{H}_{23}\mathbf{V}_2\vec{x}_2 + \mathbf{H}_{33}\mathbf{V}_3\vec{x}_3 \\
&= \mathbf{H}_{13}(\vec{w}\ \mathbf{T}\vec{w}\ \cdots\ \mathbf{T}^{M-2}\vec{w}\ \mathbf{C}\ \mathbf{T}^{(n+1)M-1}\vec{w})\vec{x}_1 \\
&+ \mathbf{H}_{13}\mathbf{C}\vec{x}_2 + \mathbf{H}_{33}\mathbf{V}_3\vec{x}_3 \\
&= \mathbf{H}_{13}(\vec{w}\ \mathbf{T}\vec{w}\ \cdots\ \mathbf{T}^{M-2}\vec{w}) \begin{pmatrix} x_1^{(1)} \\ \vdots \\ x_1^{(M-1)} \end{pmatrix} + \mathbf{H}_{33}\mathbf{V}_3\vec{x}_3 \\
&+ \mathbf{H}_{13}\mathbf{C} \begin{pmatrix} x_1^{(M)} \\ \vdots \\ x_1^{((n+1)M-1)} \end{pmatrix} + \mathbf{H}_{13}\mathbf{C}\vec{x}_2 \\
&+ \mathbf{H}_{13}\mathbf{T}^{(n+1)M-1}\vec{w}x_1^{(n+1)M} \\
&= \begin{pmatrix} \mathbf{H}_{33}\mathbf{V}_3 \\ \mathbf{H}_{13}\mathbf{C} \\ \mathbf{H}_{13}(\vec{w}\ \mathbf{T}\vec{w}\ \cdots\ \mathbf{T}^{M-2}\vec{w}) \\ \mathbf{H}_{13}\mathbf{T}^{((n+1)M-1)}\vec{w} \end{pmatrix}^T \cdot \\
&\quad \begin{pmatrix} \vec{x}_3 \\ x_1^{(M)} + x_2^{(1)} \\ \vdots \\ x_1^{((n+1)M-1)} + x_2^{(nM)} \\ x_1^{(1)} \\ \vdots \\ x_1^{(M-1)} \\ x_1^{((n+1)M)} \end{pmatrix}.
\end{aligned} \tag{3.67}
$$

From (3.65)–(3.67), we can see that the desired signals are all free from interferences.

We can also calculate the probability of system outage when multiple antennas are deployed. So we need to find the probability of $\Pr\left\{t_{(1)} \leq \frac{t_{((2n+1)M)}}{\gamma}\right\}$. With similar arguments, the joint PDF of $t_{(1)}$ and $t_{((2n+1)M)}$ can be found as:

$$\begin{aligned}
&f_{t_{(1)}t_{((2n+1)M)}}(x,y) \\
=&\lim_{\Delta x\to 0,\Delta y\to 0} P(x \leq t_{(1)} \leq x+\Delta x, \\
&y \leq t_{((2n+1)M)} \leq y+\Delta y)/(\Delta x \Delta y) \\
=&\binom{(2n+1)M}{0,1,(2n+1)M-2,1,0} p_1^0 p_2^1 p_3^{(2n+1)M-2} p_4^1 p_5^0. \qquad (3.68)
\end{aligned}$$

If t_i is approximated as a Uniform distributed variable in the range of $(0,1)$, the probability $\Pr\left\{t_{(1)} \leq \frac{t_{((2n+1)M)}}{\gamma}\right\}$ can be found as follows.

$$\Pr\left\{t_{(1)} \leq \frac{t_{((2n+1)M)}}{\gamma}\right\} = (2nM+M-1)\cdot \qquad (3.69)$$

$$(2nM+M)\int_0^1 \int_0^{\frac{y}{\gamma}} (y-x)^{2nM+M-2} dxdy \qquad (3.70)$$

$$= 1-\left(1-\frac{1}{\gamma}\right)^{(2n+1)M-1} \qquad (3.71)$$

$$\geq 1-\left(1-10^{-\frac{a}{2(n+1)M-2}}\right)^{(2n+1)M-1}, \qquad (3.72)$$

If t_i is approximated as a Rayleigh distributed variable, there is no closed-form solution for probability $\Pr\left\{t_{(1)} \leq \frac{t_{((2n+1)M)}}{\gamma}\right\}$. The joint PDF of $t_{(1)}$ and $t_{((2n+1)M)}$ can be derived as:

$$\begin{aligned}
f_{t_{(1)}t_{((2n+1)M)}}(x,y) &= ((2n+1)M)((2n+1)M-1)\frac{xy}{\sigma^4}\cdot \\
\exp\left(-\frac{x^2+y^2}{2\sigma^2}\right)&\left[\exp\left(-\frac{x^2}{2\sigma^2}\right)-\exp\left(-\frac{y^2}{2\sigma^2}\right)\right]^{(2n+1)M-2} \qquad (3.73)
\end{aligned}$$

Figs. 3.3 and 3.4 illustrate the probabilities of system outage for Uniform and Rayleigh distributions when $a=3$, respectively. We can see that for $n=1$ and $M=2$, the probabilities are

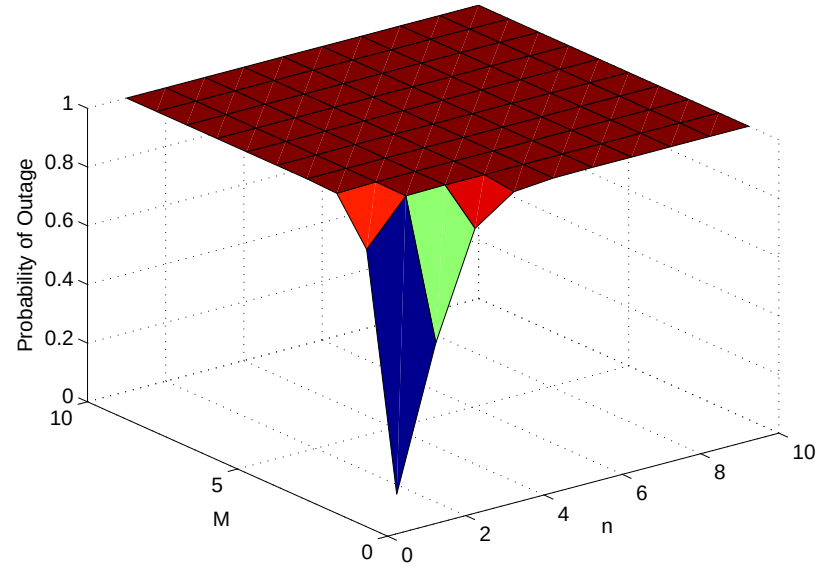

Figure 3.3: Probability of System Outage with multiple antennas for Uniform distribution.

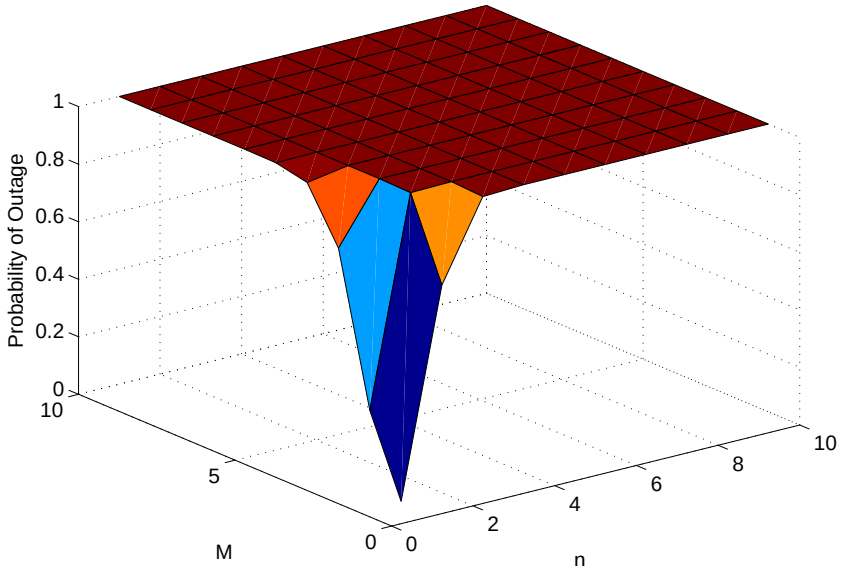

Figure 3.4: Probability of System Outage with multiple antennas for Rayleigh distribution.

0.8505 and 0.2758. For $n = 1$ and $M = 3$, the probabilities are 0.9962 and 0.7937. For $n = 2$ and $M = 2$, the probabilities are 0.9981 and 0.9971.

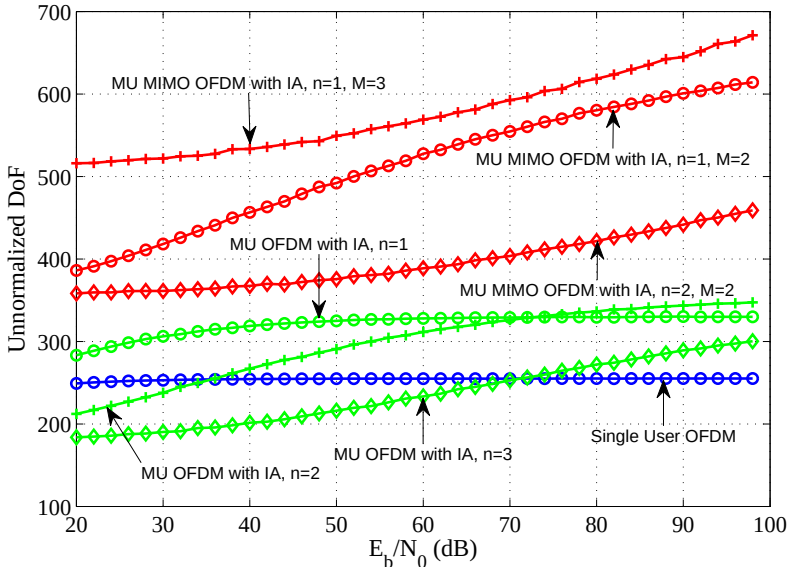

Figure 3.5: System throughput comparison when the channel variance is large.

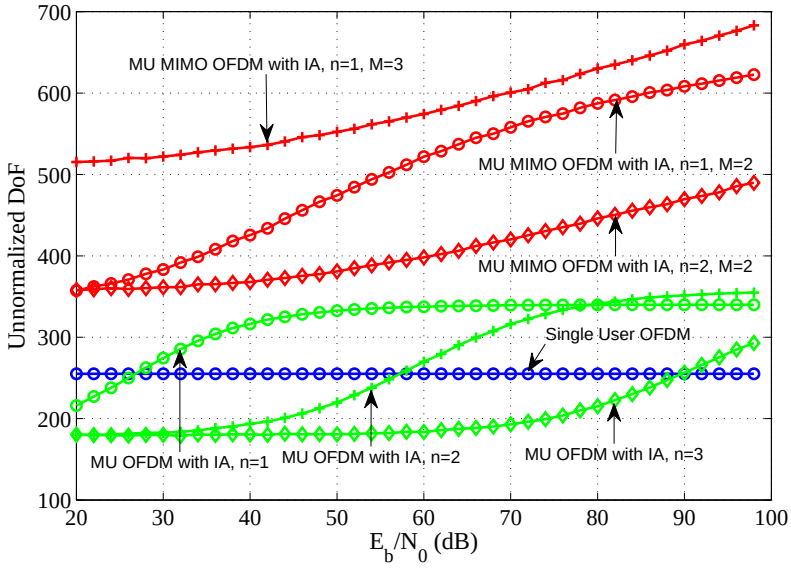

Figure 3.6: System throughput comparison when the channel variance is small.

3.5 Simulation

Simulations are conducted to evaluate the performance of the proposed schemes and verify the benefits brought about by incorporating interference alignment in multi-user OFDM systems. We consider the case of 3 users. The number of subcarriers is 255. Each transmitter precodes over $(2n+1)M$ subcarriers. Block fading channels are used in the simulations, where channel gains

are piece-wise constants for the duration of each time slot drawn from a certain distribution. BPSK is used as the modulation scheme. So we transmit 1 bit on each subcarrier and we measure how many bits are successfully decoded at the receivers. In this way, we are essentially calculating the number of interference-free channels in the system (we call it *unnormalized DoF* hereafter).

Fig. 3.5 and Fig. 3.6 illustrate the performances of different schemes when the channel is drawn from an uniform distribution on $[0, 1]$ and $[0.9, 1]$, respectively. Comparing these two figures, we can see that when the channel variance is small, higher system throughput can be achieved. This conforms to our discussions about the precoding matrix in Section 3.3.3. It can also be observed that the trends and comparative relationships are similar in Fig. 5 and Fig. 6.

We can see from Fig. 3.6 that when $n = 1$, multiuser OFDM with interference alignment can achieve an unnormalized DoF of 339.98. Compared to the highest throughput of single user OFDM of 255, the DoF has been improved by a factor of approximately 1.33 by incorporating interference alignment. When $n = 2$, we can see from both figures that the throughput of multiuser OFDM with interference alignment has degraded when the SNR is in the range $[0, 78]$ dB. That verifies our theorem that under certain power constraint, we can only precode over 3 subcarriers. Same conclusions also hold for $n = 3$ of multiuser OFDM with interference alignment, which exhibits poorer performance in the SNR range of $[20, 100]$ dB.

For the case of multiuser MIMO OFDM with interference alignment, when $n = 1$ with small channel variance, the highest unnormalized DoF is 622.7, which is 2.44 times of the unnormalized DoF of the single user OFDM system. The reason why it is slightly less than 2.66 is also due to the big differences among the elements of the precoding matrices. For $n = 2$ and $M = 2$, we can see that the performance is worse than that of $n = 1$ and $M = 2$. When the devices are equipped with 3 antennas, we let $n = 1$ and precode over 3 subcarriers. The highest unnormalized DoFs are 671.2 and 683.208 for large and small channel variance cases, respectively, which are 2.63 and 2.68 times of that of the single user OFDM system. However, the maximum gain is suppose to be 4 times the single user OFDM system. The performance degradation is also due to big difference among the elements of the precoding matrices.

3.6 Conclusions

In this chapter, we investigated the problem of how to exploiting interference in OFDM systems. We provided an analysis and developed effective schemes on incorporating interference alignment with multi-user (MIMO) OFDM to enhance system throughput. With an integer programming formulation, we derived the maximum efficiency for multi-user (MIMO) OFDM/interference alignment systems, and showed how to achieve the maximum efficiency under practical constraints. The performance of the proposed schemes were validated with simulations.

Chapter 4

Stackelberg Game for Cognitive Radio Networks with MIMO and Distributed Interference Alignment

4.1 Introduction

In the past decade, MIMO has evolved from a theoretic concept to a technology that can be widely used in practice [23]. It is desirable to exploit MIMO for enhanced primary and secondary transmissions.

Another physical layer technology called *interference alignment*, is a significant breakthrough that exploits interference in interference limited wireless networks [19]. Traditionally, if interference is small, it is simply treated as background noise; if interference is large, it can be decoded first and then removed from the received signal (i.e., interference cancellation); if interference is comparable to the desired signal, we usually try to avoid this case by orthogonalizing the channels. Unlike traditional approaches, interference alignment casts interference to half of the received signal space to achieve a normalized Degree of Freedom (DoF) of $K/2$, where K is the number of interfering users. Since an interference-free channel only has a normalized DoF of 1, substantial system throughput gain can be achieved with interference alignment when K is large. For interference alignment, a strong requirement is the availability of global channel state information (CSI) at every node. To relax this requirement, distributed interference alignment is investigated and an iterative algorithm is proposed in [41] to achieve interference alignment with local CSI.

In this chapter, we investigate how to incorporate these two advanced physical layer technologies, i.e., MIMO and distributed interference alignment, in CR networks. The CR network consists of a primary user and multiple secondary users, each with N antennas. Time is divided into equal length time slots with a normalized length. The primary user has some data to sent and requires

a certain non-zero data rate in each time slot. It also leases spectrum to secondary users for more revenue. Secondary users pay the primary user for data transmission in the time slot.

A key observation is that the licensed users usually have finite packages to send. After a period of high data rate transmission, they might be interested in leasing the spectrum to the unlicensed users if they can be reimbursed. On the other hand, the unlicensed users desire the opportunities for data transmission if the costs are acceptable. Therefore, in the proposed cooperative spectrum leasing scheme, the primary user divides the time slot into three phases: (i) in Phase I, only the primary user transmits with MIMO; (ii) in Phase II, the primary user and a selected set of secondary users transmit simultaneously using distributed interference alignment; (iii) in Phase III, only selected secondary users transmit with distributed interference alignment. The primary user decides the division of the three phases, selects the set of secondary users for spectrum leasing, and collects a revenue from the selected secondary users proportional to their transmit powers (or, data rates).

We find such a cooperative spectrum leasing framework fits well with the Stackelberg game theory [42]. In the formulated Stackelberg game, the primary user is the *leader* and the secondary users are *followers*. The leader decides the division of a time slot into three phases and selection of followers, aiming to balance its own data transmission and revenue collection by leasing spectrum. Once the leader decisions are made, a follower can choose a transmit power (and the corresponding data rate) based on how much it is willing to pay. We define the *Stackelberg Equilibrium* where neither the primary user nor any secondary user could gain by unilateral change of strategy. We present a rigorous analysis with the *backward induction* method [42] and derive the unique Stackelberg Equilibrium for the cooperative spectrum leasing game.

We find the most desirable scenario for secondary users is to have only Phase III in the time slot with only 3 players. The strategy for the primary user depends on the number of secondary users. With more than $2N-2$ secondary users, exactly $2N-2$ secondary users will be selected, each having *one* interference free channel, and there will be only Phase II in the time slot. With fewer than $2N-2$ secondary users, *all* secondary users will be selected and there will be only

Phases II and III in the time slot. Therefore, spectrum leasing is always helpful for increasing the utilities of both the primary and secondary users. In the simulation study, we first compare the proposed scheme with a scheme without spectrum leasing to demonstrate the benefits of spectrum leasing. We then compare the proposed scheme with the cooperative scheme presented in [47] to demonstrate the efficacy of distributed interference alignment. Significant performance gains are achieved by the proposed scheme in these simulations.

The remainder of this chapter is organized as follows. In Section 4.2, we present the preliminaries and system model. We define the Stackelberg game in Section 4.3 and derive the unique Stackelberg equilibrium in Section 4.4. Simulation results are presented in Section 4.5 and related work is reviewed in Section 4.6. Section 4.7 concludes this chapter.

4.2 Preliminaries and System Model

4.2.1 MIMO and Distributed Interference Alignment

This chapter is closely related to MIMO and distributed interference alignment. We brief review the preliminaries in this section. More details can be found in [23, 41]. For recently development of MIMO techniques, readers are referred to [55] [56] [57].

MIMO Capacity Basics

With the advance of antenna technology, it is now feasible to equip wireless devices with multiple antennas. In general, three types of performance gains can be achieved with MIMO, namely, *diversity gain*, *multiplexing gain*, and *antenna gain*. In this chapter, we focus on multiplexing gain, namely, DoF. We assume that all transmitters and receivers have the same number of antennas.

For a MIMO system with $N \geq 2$ antennas, assume that the CSI $\mathbf{H}$ is known at the transmitter. Since the MIMO channel can be decomposed into d parallel channels, the channel capacity is given

by [46]

$$C = \max_{p_i : \sum_i p_i \leq P} \sum_{i=1}^{d} \log\left(1 + \frac{\sigma_i^2 p_i}{N_0}\right), \tag{4.1}$$

where P denotes the total transmitter power limit, p_i is the power allocated to the i-th parallel channel, $\sigma_i^2 = \lambda_i$ and λ_i is the i-th largest eigenvalue of matrix $\mathbf{HH}^H$. Note that bandwidth is normalized throughout this chapter.

In the high SNR region, equal power allocation is shown to be sub-optimal, but is easier for mathematical modeling than water-filling. When the transmit power is P/d for each parallel channel, the total capacity is

$$\begin{aligned} C &\approx \sum_{i=1}^{d} \log\left(1 + \frac{P\sigma_i^2}{dN_0}\right) \\ &\approx \sum_{i=1}^{d} \log\left(\frac{P\sigma_i^2}{dN_0}\right) \\ &= d\log(SNR) + \sum_{i=1}^{d} \log\left(\frac{\sigma_i^2}{d}\right) \end{aligned} \tag{4.2}$$

The second item in (4.2) is negligible when the SNR is high. We thus ignore this term in the following discussion. Thus, wireless channel is assumed to be perfect throughout this chapter.

Distributed Interference Alignment

The basic idea of interference alignment is to cast the interference to no more than half of the received signal space, and leave the other half clean and recognizable. If there are K users, totally $K/2$ normalized DoF could be achieved. The system throughput can be greatly enhanced when K is large. For $K = 0$ and 1, there is no interference; for $K = 2$, the normalized DoF is 1, which is trivial. Therefore, we only consider the case where the number of interfering nodes K satisfies $K \geq 3$. It is worth noting that, to align interference perfectly, global CSI is required at

every participating node. To overcome this challenge, an iterative distributed interference alignment algorithm was proposed in [41], which only requires local CSI at each interfering node. By utilizing the reciprocity of wireless networks, it works as follows.

Firstly, compute the interference covariance at each receiver as:

$$\mathbf{Q}_k = \sum_{j=1, j\neq k}^{K} \frac{P_j}{d_j} \mathbf{H}_{jk} \mathbf{V}_j \mathbf{V}_j^H \mathbf{H}_{jk}^H, \tag{4.3}$$

where P_j is the total transmitting power of user j, $\mathbf{V}_j$ is the *precoding matrix* at transmitter j, $\mathbf{H}_{jk}$ is the channel gain from transmitter j to receiver k.

Minimizing the interference leakage at each receiver, the *interference cancellation matrix* $\mathbf{U}_k$ is given as:

$$\vec{u}_{k_i} = \nu_i[\mathbf{Q}_k], i = 1, \ldots, d, \tag{4.4}$$

where $\vec{u}_{k_i}$ is the i-th column of $\mathbf{U}_k$, and $\nu_i[\mathbf{Q}_k]$ is the i-th smallest eigenvalue's corresponding eigenvector.

Then reverse the direction of communication and let $\overleftarrow{\mathbf{V}}_k = \mathbf{U}_k$. The interference at the reverse link's receiver is:

$$\overleftarrow{\mathbf{Q}}_k = \sum_{j=1, j\neq k}^{K} \frac{\overleftarrow{P_j}}{d_j} \overleftarrow{\mathbf{H}}_{jk} \overleftarrow{\mathbf{V}}_j \overleftarrow{\mathbf{V}}_j^H \overleftarrow{\mathbf{H}}_{jk}^H. \tag{4.5}$$

Minimizing the interference leakage at each receiver of the reverse link, the interference cancellation matrix is given as:

$$\overleftarrow{\vec{u}}_{k_i} = \nu_i[\overleftarrow{\mathbf{Q}}_k], i = 1, \ldots, d. \tag{4.6}$$

Then reverse the direction again, and let $\mathbf{V}_k = \overleftarrow{\mathbf{U}}_k$. These steps are repeated until convergence is achieved.

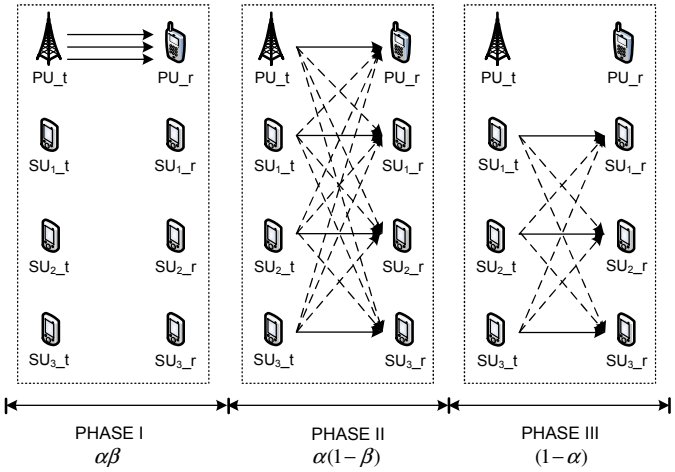

Figure 4.1: The three-phase operation of the MIMO CR network with distributed IA.

The general feasibility condition for interference alignment is given by

$$\mathbf{U}_k^H \mathbf{H}_{jk} \mathbf{V}_j = 0, \text{ for } j \neq k \tag{4.7}$$

$$\text{rank}(\mathbf{U}_k^H \mathbf{H}_{kk} \mathbf{V}_k) = d_k, \text{ for all } k. \tag{4.8}$$

In [20], a system is called to be proper if it satisfies the following condition:

$$d \leq \frac{2N}{K+1}. \tag{4.9}$$

Since distributed interference alignment should also satisfy the conditions given in (4.7) and (4.8), to simplify the discussion, we consider a proper system to be feasible for distributed interference alignment for simplicity.

4.2.2 System Model and Assumptions

The MIMO CR network is illustrated in Fig. 4.1. There are one primary user and K_T secondary users sharing the licensed spectrum, each with N antennas. We consider a time-slotted system, where each time slot is normalized to 1 unit in length and is divided into three phases, with lengths $\alpha\beta$, $\alpha(1-\beta)$, and $(1-\alpha)$, respectively, for fractions $0 \leq \alpha \leq 1$ and $0 \leq \beta \leq 1$.

In Phase I, the primary user transmits its packets at the highest rate using MIMO, and the secondary users remain silent. The DoF for the primary user is $d_I = N$. The achievable rate of the primary user in Phase I is:

$$R_P^I = d_I \log(SNR), \tag{4.10}$$

where SNR is assumed to be constant during a time slot.

We assume that the primary user always has a finite amount of packets to send in each time slot. After a period of high data rate transmission (with length $\alpha\beta$), the primary user has the incentive to lease the spectrum to secondary users to increase its utility, by collecting revenue from selected secondary users (but with a lower data rate for itself). In Phase II, the primary user and $K \in [0, K_T]$ selected secondary users transmit simultaneously using *distributed interference alignment*, with a DoF of $d_{II} = \lfloor \frac{2N}{K+2} \rfloor$. A selected secondary user makes payments that is proportional to its transmit power (i.e., its data rate), and the primary user collects payments from all selected secondary users. The achievable rate of the primary user in Phase II is

$$R_P^{II} = d_{II} \log(SNR). \tag{4.11}$$

The achievable rate of secondary user S_i in Phase II is

$$R_{S_i}^{II} = d_{II} \log(SNR_i), \tag{4.12}$$

where $SNR_i = P_i/N_0$ is the SNR for each selected secondary user, which is assumed to be constant in a time slot.

In Phase III, the primary user stops its transmission and leases the spectrum to selected secondary users, which transmit using distributed interference alignment with $d_{III} = \left\lfloor \frac{2N}{K+1} \right\rfloor$. In Phase

III, the achievable rate of secondary user S_i is

$$R_{S_i}^{III} = d_{III} \log(SNR_i). \tag{4.13}$$

As in [54], we assume a common control channel for the primary user and secondary users to exchange precoding and interference cancellation matrices, the weight factor information, and the fractions α and β. Channel estimation is completed before data transmissions. Note that the DoFs are integers.

4.3 Stackelberg Game Formulation

In the MIMO CR network, the primary user decides the division of a time slot into three phases and selection of secondary users, while balancing its own data transmission and revenue collection by leasing spectrum. Once the decisions are made by the primary user, a secondary user can choose a transmit power (and the corresponding data rate) based on how much it is willing to pay. Such interactions fit perfectly with the Stackelberg game model [42].

4.3.1 Stackelberg Game Formulation

In this section, we formulate a Stackelberg game for the MIMO CR network with distributed interference alignment. The primary user is the *leader* and the secondary users are *followers*. The *strategy* of the primary user is given by

$$S_P = \{\alpha, \beta, K | 0 \leq \alpha \leq 1, 0 \leq \beta \leq 1, 3 \leq K \leq K_T\}, \tag{4.14}$$

where K_T is the total number of secondary user in system.

The secondary user strategy is to find a transmit power P_i, as

$$S_{S_i} = \{P_i | 0 \leq P_i \leq P_{max}\}, \ \ \forall\, i. \tag{4.15}$$

Here we assume that $P_{max} \geq 2w_S N/C_0$, where C_0 is unit price for secondary user transmit power (see (4.16)) and w_S is the weight factor for secondary user utility (see (4.17)).

The primary user transmits its data in Phases I and II, and collects revenue in Phases II and III. The *utility* of the primary user is the sum of data transmitted and revenue collected, as

$$U_P = w_P f_P(R_P) + \sum_{k=1}^{K} C_0 P_i, \tag{4.16}$$

where $R_P = \alpha\beta R_P^I + \alpha(1-\beta)R_P^{II}$ is the amount of primary user data transmitted, w_P is a weight factor, C_0 is the unit price for secondary user power, and $f_P(x)$ is the satisfaction function of the primary user. Since the primary user always has some data to send, it requires a minimum data rate. Naturally we choose $f_P(x) = \ln(x)$, $x \geq 0$. The negative value for very small x serves as a penalty that forces the primary user to achieve a minimum data rate. From the shape of $f_P(x)$, we know that at the beginning stage, the primary user is enthusiastic about data transmission. After a period of transmission, even a great increase in the data transmission can only result in a small increase in the satisfaction.

By defining $f_P(x) = \ln(x)$, we actually also assume that the primary user always has some packages to send. Since if the primary user has no package to send, it will provide all the time and spectrum to the secondary users and merely collect revenues. In this way, the primary user is in fact working as a network service provider not a service user. This case is not allowed. By adjusting the parameter w_P, the primary users is actually putting different weights on the data transmission and the revenues it will collect. This is also related to the content type that the primary user is transmitting. If the primary user is transmitting high resolution video, it may assign w_P a huge number, say 10^8. That is, the primary user currently values the data transmission much more than the revenues collected. To maximize U_P, the primary user simply sets $\alpha = 1$, $\beta = 1$. If the primary user is surfing the internet and is tolerant of the delays, it may assign w_P a small number, say 0.01. Revenue is more helpful to maximize the U_P at this scenario. That means the revenue collected becomes more important to the primary user now.

Therefore, since the primary user is rational and selfish, it aims to maximize U_P by controlling the lengths of the three phases and selecting secondary users to participate in the game. By adjusting weight w_P, the primary users can trade off between data transmission and revenue collection.

Selected secondary users transmit their data during Phases II and III and make a one-time payment to the primary user. The utility of the secondary user is given by

$$U_{S_i} = w_S f_S(R_{S_i}) - C_0 P_i. \tag{4.17}$$

where $R_{S_i} = \alpha(1-\beta)R_{S_i}^{II} + (1-\alpha)R_{S_i}^{III}$, $f_S(x)$ is the satisfaction function of the secondary user and the w_S is the weight factor. As in [47], to simplify notation, we assume identical w_S for all the secondary users. It could be easily extended to heterogeneous cases. Since the essence of cognitive radio is to opportunistically exploit the spectrum, we choose $f_S(x) = x$, indicating that the secondary users operate in the *best efforts* manner. By assigning a big number to w_S, the secondary users care more about the data transmission. On the contrary, if a small number is assigned to w_S, the secondary users is more concerned about the payment. Thus, the weight w_S allows a secondary user to trade off between data transmission and payment.

Therefore we define a Stackelberg game, with players, their roles, strategies ((4.14) and (4.15)), and utilities ((4.16) and (4.17)) specified. We provide a thorough analysis of the game with respect to the existence and uniqueness of the *Stackelberg Equilibrium* and optimal strategies in Section 4.4.

4.3.2 Discussion

From the secondary users' point of view, it wants to transmit more data while keeping the costs as low as possible. If there are fewer players, the DoF can be increased. Since the DoF is a pre-log factor (see (4.12) and (4.13)), transmit more power when the DoF is high is definitely a better choice. At the same time, since the primary user will not participate in the Phase III, with

one less player, the DoF could be further increased. Since once the one-time payment is made, the secondary users can transmit during Phase II and Phase III, the longer the Phase II or Phase III, the better the secondary users will feel. To sum up, with the unit price fixed, the secondary users favor fewer players and longer duration of Phase II or Phase III, preferably Phase III.

Since the primary user is the leader, it has the advantages of making trade-off between data transmission and revenue collecting. In Phase I, the transmission rate is high. More primary user data could be transmitted if Phase I is long. In Phase II, the primary user could collect revenue while transmitting data, although at a lower data rate. With more secondary users selected, more players are paying the primary user, which is helpful to maximize its utility. However, if too many secondary users are selected, The DoF could even be 0 with too many players. Under this situation, there's no revenue since no one could transmit and thus no one would pay. Therefore, K should be carefully decided. In summary, the primary user's strategy should consider the trade-off between data transmission and revenue collection. Since in Phase II, the primary user can transmit while collecting revenue, and the choices of α. β, and K are dependent, the primary user decision is highly complicated.

4.4 Performance Analysis and Solution Strategy

In this section, we analyze the formulated Stackelberg game to find a strategy set, called the equilibrium, for the primary user and secondary users such that no one could gain by unilateral change of strategy.

Let $\vec{P}^*$ be the vector of secondary user powers and $\vec{P}^*_{-i} = \vec{P}^* \backslash P_i$. We first define *Stackelberg Equilibrium* as follows.

Definition 1. *(Stackelberg Equilibrium) A strategy set* $\{\alpha^*, \beta^*, K^*, \vec{P}^*\}$ *is a Stackelberg Equilibrium of the game defined in Section 4.3 if the following conditions are satisfied:*

1. $U_P(\alpha^*, \beta^*, K^*, \vec{P}^*) \geq U_P(\alpha, \beta, K, \vec{P}^*)$*, for all* $\alpha \in [0, 1]$*,* $\beta \in [0, 1]$*, and* $K \in [0, K_T]$.

2. $U_{S_i}(P_i^*, \vec{P}_{-i}^*, \alpha^*, \beta^*, K^*) \geq U_{S_i}(P_i, \vec{P}_{-i}^*, \alpha^*, \beta^*, K^*)$, *for all* $\alpha \in [0,1]$, $\beta \in [0,1]$, $K \in [0, K_T]$ *and* $i \in [1, K]$.

Using the *backward induction* method [42], we prove the uniqueness of the Stackelberg Equilibrium, and derive the unique Stackelberg Equilibrium (and the optimal strategy) for the game defined in Section 4.3 in the remainder of this section.

4.4.1 Secondary User Utility Maximization

From (4.17), the utility of the secondary user is given by:

$$\begin{aligned} U_{S_i}(P_i) &= w_S f_S(R_{S_i}) - C_0 P_i \\ &= w_S[\alpha(1-\beta) d_{II} \log(P_i/N_0) + (1-\alpha) \times \\ &\quad d_{III} \log(P_i/N_0)] - C_0 P_i. \end{aligned} \tag{4.18}$$

To maximize the utility, the secondary user solves the following maximization problem.

$$\max_{0 \leq P_i \leq P_{max}} U_{S_i}(P_i) \tag{4.19}$$

For given α and β, the $U_{S_i}(P_i)$ is a concave function of P_i. Setting $\frac{dU_{S_i}}{dP_i} = 0$, we derive the unique maximizer of (4.19), as

$$P_i^* = \frac{w_S \alpha(1-\beta) d_{II} + w_S(1-\alpha) d_{III}}{C_0}. \tag{4.20}$$

Since $0 \leq \alpha \leq 1$, $0 \leq \beta \leq 1$ and $d_{II} \leq d_{III} \leq 2N$, we have

$$P_i^* \leq w_S d_{III}/C_0 \leq 2 w_S N/C_0 \leq P_{max}, \tag{4.21}$$

indicating that the P_i^* given in (4.20) is a feasible solution. It follows that the maximum utility of the secondary user is

$$U_{S_i}^* = Y \log\left(Y/[2C_0N_0]\right),\ i \in [1, K], \tag{4.22}$$

where $Y = w_S[\alpha(d_{II} - d_{III}) - \alpha\beta d_{II} + d_{III}]$.

Since $U_{S_i}^*$ is a monotone increasing function of Y, and $d_{II} \leq d_{III}$, it can be verified that $U_{S_i}^*$ is a monotone decreasing function of α and β. Since $\alpha(1-\beta) \geq 0$ and $(1-\alpha) \geq 0$, $U_{S_i}^*$ is a monotone increasing function of d_{II} and d_{III}. From a secondary user's perspective, the best scenario is $\alpha = 0$, $\beta = 0$, and $K = 3$, i.e., the entire time slot is Phase III with the minimum number of followers. The selected secondary users enjoy the highest data rate. The primary user can only collect revenue from the three secondary users. This is consistent with our conjectures in Section 4.3.2. However, that is the best case for the secondary users. From later discussions, we can see that the primary user, who tries to maximize his utility, may in part but will not completely set the parameters according to the secondary users' wills.

4.4.2 Primary User Utility Maximization

Given the optimal strategies of all the secondary users, we substitute $f_P(R_P)$ and P_i^* into (4.16). It follows that

$$\begin{aligned} U_P(\alpha, \beta, K) = w_P \ln[\alpha\beta R_P^I + \alpha(1-\beta)R_P^{II}] + \\ Kw_S[\alpha(1-\beta)d_{II} + (1-\alpha)d_{III}]. \end{aligned} \tag{4.23}$$

The primary user solves the following problem to maximize its utility.

$$\max_{0\leq\alpha\leq1, 0\leq\beta\leq1, 3\leq K\leq K_T} U_P(\alpha, \beta, K, \vec{P}^*). \tag{4.24}$$

Maximization of the primary user utility is more complicated. We examine the problem for different parameter ranges and derive the local maximizer in each range. The global optimum is found by comparing the local maximizers. This is similar to finding the maximum element in a matrix: we first find the largest element in each column; then we compare these elements from different columns to find the largest one in the matrix. Without loss of generality, we assume $w_P = w_S$ [1]. The analysis can be easily extended to the case $w_P \neq w_S$.

Case I When $K_T \geq (2N-1)$

When $3 \leq K \leq (2N-1)$ First, let's consider $K \in [3, 2N-1]$. U_P can be rewritten as follows.

$$\begin{aligned} U_P = w_P \ln \left\{ \log(SNR) \left[\alpha\beta N + \alpha(1-\beta) \left\lfloor \frac{2N}{K+2} \right\rfloor \right] \right\} \\ + K w_S \left[\alpha(1-\beta) \left\lfloor \frac{2N}{K+2} \right\rfloor + (1-\alpha) \left\lfloor \frac{2N}{K+1} \right\rfloor \right]. \end{aligned} \tag{4.25}$$

Note that K and β are dependent variables. If $\beta = 1$, there is no Phase II. We next consider $\beta = 1$ and $\beta \in [0, 1)$.

Case (a): $\beta = 1$ We denote the utility of the primary user as U_P^0 in this case, which is given by

$$\begin{aligned} U_P^0 &= w_P \ln(\alpha N \log(SNR)) + K w_S (1-\alpha) \left\lfloor \frac{2N}{K+1} \right\rfloor \\ &\leq w_P \ln(\alpha N \log(SNR)) + w_S (1-\alpha) \frac{2N}{1+\frac{1}{K}} \\ &\leq w_P \ln(\alpha N \log(SNR)) + w_S (1-\alpha)(2N-1). \end{aligned} \tag{4.26}$$

The two equalities hold true when $K = 2N-1$. We then have the following optimization problem.

$$\max_{0 \leq \alpha \leq 1} U_P^0(\alpha, 1, 2N-1), \tag{4.27}$$

[1] There are some special case of w_P and w_S. For instance, $w_P = \infty$. Under this condition, to maximize the utility, the primary user will not lease the spectrum to the secondary users, which is trivial. We focus on the generic case that $w_P = w_S$ in this chapter.

where $U_P^0(\alpha, 1, 2N-1) = w_P \ln(\alpha N \log(SNR)) + w_S(2N-1)(1-\alpha)$. Since U_P^0 is concave with respect to α, problem (4.27) can be solved with convex programming [45]. U_P^0 achieves its maximum when $\alpha = \frac{1}{2N-1}$, and its maximum is given by

$$U_P^{*0}\left(\frac{1}{2N-1}, 1, 2N-1\right) = w_P \ln\left(\frac{N}{2N-1}\log(SNR)\right) + w_S(2N-2). \tag{4.28}$$

Case (b): $\beta \in [0,1)$ Relaxing K to a continuous variable and ignoring the floor functions, we have

$$\frac{\partial U_P}{\partial K} = w_P \left\{ -\frac{2(1-\beta)}{(K+2)^2\beta + 2(K+2)(1-\beta)} + \frac{4N\alpha(1-\beta)}{(K+2)^2} + \frac{2N(1-\alpha)}{(K+1)^2} \right\}.$$

The first item is irrelevant to α, while the last two items are linear in α. If for both $\alpha = 0$ and $\alpha = 1$, $\frac{\partial U_P}{\partial K} \geq 0$ holds true for any β, then for any $0 \leq \alpha \leq 1$ and $0 \leq \beta < 1$, $\frac{\partial U_P}{\partial K} \geq 0$.

We prove this conjecture as follows. When $\alpha = 0$,we have:

$$\begin{aligned} \frac{\partial U_P}{\partial K} &= \frac{2Nw_P}{(K+1)^2} - \left(\frac{w_P}{K+2}\right)\left(\frac{2(1-\beta)}{\beta K+2}\right) \\ &\geq \frac{2Nw_P}{(K+1)^2} - \frac{w_P}{K+2} \geq w_P\left[\frac{1}{K+1} - \frac{1}{K+2}\right] \geq 0. \end{aligned}$$

The first inequality is because $\beta \geq 0$, such that $\frac{2(1-\beta)}{\beta K+2} \leq 1$. The second inequality is due to the fact that $2N \geq (K+1)$.

When $\alpha = 1$, we have

$$\begin{aligned} \frac{\partial U_P}{\partial K} &= w_P \frac{(1-\beta)}{(K+2)^2}\left[4N - (K+2)\frac{2}{\beta K+2}\right] \\ &\geq w_P \frac{(1-\beta)}{(K+2)^2}[4N - (K+2)] \;\geq\; 0. \end{aligned}$$

The first inequality is due to $\beta \geq 0$, such that $\frac{2}{\beta K+2} \leq 1$. The second inequality is due to the fact that $2N \geq (K+1)$.

Therefore, if we treat K as a continuous variable and ignore the floor functions, U_P is a monotone increasing function of K. To maximize U_P, we should have $K = 2N-1$. Now consider K as an integer and take the floor functions into account. We show we should have $K = 2N-2$ in this case.

If $K = 2N-1$, denote the utility of primary user in this case as U_P^1. Since $\lfloor \frac{2N}{K+2} \rfloor = 0$ and $\lfloor \frac{2N}{K+1} \rfloor = 1$, we have:

$$U_P^1 = w_P \ln(\alpha\beta N \log(SNR)) + w_S(2N-1)(1-\alpha). \tag{4.29}$$

It can be verified that U_P^1 is an increasing function of β for $\beta \in [0,1)$. Thus, we have $U_P^1 < U_P^0$. It follows that

$$U_P^{*1} < U_P^{*0}. \tag{4.30}$$

Given (4.30), we no longer need to examine the maximization of U_P^1; $K = 2N-1$ can be discarded for $\beta \in [0,1)$. As a matter of fact, we could see from later discussion that $\max_{\alpha,\beta} U_P(\alpha,\beta,2N-1) < \max_{\alpha,\beta} U_P(\alpha,\beta,2N-2)$.

Since $K = 2N-1$ is excluded, we only need to consider $K \leq 2N-2$. Rewrite (4.25) as

$$\begin{aligned} U_P = w_P \ln\left(N\beta + (1-\beta)\left\lfloor \frac{2N}{K+2} \right\rfloor\right) + \\ Kw_S\left[\alpha(1-\beta)\left\lfloor \frac{2N}{K+2} \right\rfloor + (1-\alpha)\left\lfloor \frac{2N}{K+1} \right\rfloor\right] \\ + w_P \ln(\alpha \log(SNR)). \end{aligned} \tag{4.31}$$

Define $f_1(K) = \ln(N\beta + (1-\beta)\lfloor \frac{2N}{K+2} \rfloor)$ and $f_2(K) = K[\alpha(1-\beta)\lfloor \frac{2N}{K+2} \rfloor + (1-\alpha)\lfloor \frac{2N}{K+1} \rfloor]$. We have the following Lemma for $f_2(K)$.

Lemma 2. $\arg max_{K\in[3,2N-2]} f_2(K) = 2N-2$.

Proof. For the first item in $f_2(K)$, we have:

$$K\left\lfloor\frac{2N}{K+2}\right\rfloor \leq K\frac{2N}{K+2} \leq 2N - \frac{4N}{K+2} \leq 2N-2.$$

The equalities hold true only for $K = 2N-2$. For the second item in $f_2(K)$, if there is no constraint on K, $K\lfloor\frac{2N}{K+1}\rfloor = 0$ for $K > 2N-1$. For $K \leq 2N-1$, we have

$$K\left\lfloor\frac{2N}{K+1}\right\rfloor \leq K\frac{2N}{K+1} \leq 2N - \frac{2N}{K+1} \leq 2N-1.$$

The equalities hold true only for $K = 2N-1$. When the constraint $K \leq 2N-2$ is enforced, if $K = 2N-2$, $K\lfloor\frac{2N}{K+1}\rfloor = 2N-2$. Since $K\lfloor\frac{2N}{K+1}\rfloor$ can only be integers, and $2N-2$ is only 1 less than $2N-1$, $2N-2$ is the largest number we can have for $K\lfloor\frac{2N}{K+1}\rfloor$ when $K \leq 2N-2$. Since both $K\lfloor\frac{2N}{K+2}\rfloor$ and $K\lfloor\frac{2N}{K+1}\rfloor$ are maximized at $K = 2N-2$, $f_2(K)$ attains its maximum at $K = 2N-2$. □

Lemma 3. *For* $K' \in (N-2, 2N-2)$, $U_P(\alpha,\beta,K') < U_P(\alpha,\beta,2N-2)$.

Proof. For $K' \in (N-2, 2N-2)$, we always have $\lfloor\frac{2N}{K'+2}\rfloor = 1$. When $K = 2N-2$, $\lfloor\frac{2N}{K+2}\rfloor = 1$. Thus, $f_1(K') = f_1(2N-2)$. On the other hand, $K'\lfloor\frac{2N}{K'+2}\rfloor < (2N-2)\lfloor\frac{2N}{(2N-2)+2}\rfloor$. For $K' \in (N-2, 2N-2)$, it can be verified that $K'\lfloor\frac{2N}{K'+1}\rfloor \leq (2N-2)\lfloor\frac{2N}{(2N-2)+1}\rfloor$ for $N \geq 2$. We thus have $f_2(K') < f_2(2N-2)$. Summing up $f_1(K)$ and $f_2(K)$, we have $U_P(\alpha,\beta,K') < U_P(\alpha,\beta,2N-2)$. □

The insight from Lemma 3 is that, if $2N$ is not divisible by $K+2$, this K value is not useful for the optimization and can be safely discarded. We have the following corollary.

Corollary 1. *Assume* $2N$ *is divisible by* $(K_1+2), (K_2+2), \ldots, (K_n+2)$, *and* $K_1 > K_2 > \ldots > K_n$, *for any* $K'' \in (K_2, K_1), \ldots, \overbrace{K''\cdots'}^{n} \in (K_n, K_{n-1})$, *we have:*

$$U_P(\alpha,\beta,\overbrace{K''\cdots'}^{i}) < U_P(\alpha,\beta,K_{i-1}),\ \forall\, i = 2,\ldots,n. \tag{4.32}$$

According to Corollary 1, to find the value of K that maximizes U_P, we only need to consider the K values such that $2N$ is divisible by $K+2$.

Lemma 4. *If $K_0 = N-2$ is feasible, it follows that $U_P(\alpha,\beta,2N-2) > U_P(\alpha,\beta,N-2)$.*

Proof. $K_0 = N-2$ is feasible if $K_0 \geq 3$. It follows that $N \geq 5$ in this case. Therefore, we have

$$\left\lfloor \frac{2N}{K_0+1} \right\rfloor = \left\lfloor \frac{2N}{N-1} \right\rfloor = 2 + \left\lfloor \frac{2}{N-1} \right\rfloor = 2.$$

It follows that

$$\begin{aligned} & U_P(2N-2) - U_P(N-2) \\ = \; & w_P \left[\ln\left(\frac{N\beta + (1-\beta)}{N\beta + 2(1-\beta)} \right) + 2(1-\alpha\beta) \right] \\ \geq \; & w_P \left[\ln\left(\frac{N\beta + (1-\beta)}{N\beta + 2(1-\beta)} \right) + 2(1-\beta) \right]. \end{aligned}$$

The inequality is because $U_P(2N-2) - U_P(N-2)$ is a monotone decreasing function of α. For $\beta = 0$, $U_P(2N-2) - U_P(N-2) = w_P[2 - \ln(2)] > 0$. For $\beta \in (0,1)$, define $f_3(N) = \ln(\frac{N\beta+(1-\beta)}{N\beta+2(1-\beta)})$, and treat N as a continuous variable. We have

$$\frac{\partial f_3(N)}{\partial N} = \frac{\beta}{N\beta + (1-\beta)} - \frac{\beta}{N\beta + 2(1-\beta)} > 0,$$

which indicates that $f_3(N)$ is a strictly monotone increasing function of N. Since currently $N \geq 5$, we have $f_3(N) > f_3(1) = -\ln(2-\beta)$. That is:

$$U_P(2N-2) - U_P(N-2) > w_P[-\ln(2-\beta) + 2(1-\beta)].$$

Define $f_4(\beta) = -\ln(2-\beta) + 2(1-\beta)$. Since $\frac{\partial^2 f_4}{\partial \beta^2} = \frac{1}{(2-\beta)^2} > 0$, $f_4(\beta)$ is a convex function. The domain $\{\beta | \beta \in (0,1)\}$ is also a convex set. Suppose β can be equal to 0 and 1. Solving the

following problem,

$$\min_{0\leq\beta\leq 1} -\ln(2-\beta)+2(1-\beta),$$

we have $\min_{\beta\in[0,1]} f_4(\beta)=0$, and the minimum is achieved at $\beta=1$. We conclude that $f_4(\beta)>0$ for $\beta\in(0,1)$.

It follows that $U_P(\alpha,\beta,2N-2)-U_P(\alpha,\beta,N-2)\geq w_P[f_3(N)+2(1-\beta)]>w_P[f_3(1)+2(1-\beta)]>0$. The proof is completed. □

Lemma 5. *Consider $K_1, K_2, \ldots, K_n$, such that $2N$ is divisible by $K_1+2, K_2+2, \ldots,$ and K_n+2, and if $\frac{2N}{K_1+2}=3$, $\frac{2N}{K_2+2}=4, \ldots \frac{2N}{K_n+2}=N$, it follows that $U_P(\alpha,\beta,2N-2)>U_P(\alpha,\beta,K_i)$, $i=1,2,\cdots,n$.*

Proof. For K_1, we have:

$$\begin{aligned}
& U_P(N-2)-U_P(K_1)\\
= \;& w_P\left[\ln\left(\frac{N\beta+2(1-\beta)}{N\beta+3(1-\beta)}\right)+2(1-\alpha\beta)\right]\\
\geq \;& w_P\left[\ln\left(\frac{N\beta+2(1-\beta)}{N\beta+3(1-\beta)}\right)+2(1-\beta)\right]\\
> \;& w_P\left[\ln\left(\frac{N\beta+(1-\beta)}{N\beta+2(1-\beta)}\right)+2(1-\beta)\right]>0.
\end{aligned}$$

The first inequality is due to the fact that $U_P(N-2)-U_P(K_1)$ is a monotone decreasing function of α. The second inequality is due to $\ln(\frac{N\beta+2(1-\beta)}{N\beta+3(1-\beta)})>\ln(\frac{N\beta+(1-\beta)}{N\beta+2(1-\beta)})$ for $\beta\in[0,1)$, and the last inequality is proved in Lemma 4. Thus, we have:

$$U_P(2N-2)>U_P(N-2)>U_P(K_1).$$

For K_2, we have:

$$\begin{aligned} & U_P(K_1) - U_P(K_2) \\ = \; & w_P \left[\ln \left(\frac{N\beta + 3(1-\beta)}{N\beta + 4(1-\beta)} \right) + 2(1-\alpha\beta) \right] \\ \geq \; & w_P \left[\ln \left(\frac{N\beta + 3(1-\beta)}{N\beta + 4(1-\beta)} \right) + 2(1-\beta) \right] \\ > \; & w_P \left[\ln \left(\frac{N\beta + 2(1-\beta)}{N\beta + 3(1-\beta)} \right) + 2(1-\beta) \right] > 0. \end{aligned}$$

Repeat the above for $K_3, \cdots, K_n$. The proof is completed. □

Theorem 4.1. *When $K_T \geq 2N-1$, $3 \leq K \leq 2N-1$ and $0 \leq \beta < 1$, U_P is maximized when $K = 2N-2$.*

Proof. We have shown in Lemma 4 that, if K_0 exists, $U_P(2N-2) > U_P(K_0)$. We have also shown in Lemma 5 that, if $K_i,\ i = 1, \ldots, n$ exists, $U_P(2N-2) > U_P(K_i)$. Also considering Corollary 1, $K = 2N-2$ is the maximizer. □

Substitute $K = 2N-2$ into (4.31), we have:

$$\begin{aligned} U_P(2N-2) \; = \; & w_P\{\ln[(\alpha \log(SNR))(N\beta + (1-\beta))]\} \\ & + w_S(2N-2)(1-\alpha\beta). \end{aligned}$$

We next divide the range of α into three ranges and examine each of them in the following.

Case (a): $\alpha \in [0, \frac{1}{2N}]$ Denoting the utility of the primary user in this case as U_P^2, we have

$$\begin{aligned} \frac{\partial U_P^2}{\partial \beta} \; = \; & w_P \frac{N-1}{N\beta + (1-\beta)} - w_S(2N-2)\alpha \\ \geq \; & w_P \left[\frac{N-1}{(N-1)\beta + 1} - \frac{N-1}{N} \right] \\ > \; & w_P \left[\frac{N-1}{(N-1)+1} - \frac{N-1}{N} \right] = 0. \end{aligned}$$

The first inequality is because $\frac{\partial U_P^2}{\partial \beta}$ is a monotone decreasing function of α, and the second inequality is due to $\beta < 1$. So U_P is a monotone increasing function of β. For $\alpha \in [0, \frac{1}{2N}]$, we have $U_P^2 < w_P \ln[N\alpha \log(SNR)] + w_S(2N-2)(1-\alpha) < U_P^0 \leq U_P^{*0}$. This case can be safely discarded.

Case (b): $\alpha \in [\frac{1}{2}, 1]$ Denoting the utility of the primary user in this case as U_P^3, we have

$$\begin{aligned} \frac{\partial U_P^3}{\partial \beta} &= w_P \frac{N-1}{N\beta + (1-\beta)} - w_S(2N-2)\alpha \\ &\leq w_P \left[\frac{N-1}{(N-1)\beta + 1} - (N-1) \right] \leq 0. \end{aligned}$$

The first inequality is because $\frac{\partial U_P^3}{\partial \beta}$ is a monotone decreasing function of α, and the second inequality is due to $\beta \geq 0$. So U_P is a non-increasing function of β. Letting $\beta = 0$, we have the following maximization problem.

$$\max_{\frac{1}{2} \leq \alpha \leq 1} U_P^3 = w_P \ln(\alpha \log(SNR)) + w_S(2N-2). \tag{4.33}$$

Since U_P^3 is now an monotone increasing function of α, letting $\alpha = 1$, we have

$$U_P^{*3}(1, 0, 2N-2) = w_P \ln(\log(SNR)) + w_S(2N-2). \tag{4.34}$$

For $N \geq 2$, we have $U_P^{*3} - U_P^{*0} = w_P \ln(\frac{2N-1}{N}) > 0$. Recall that $U_P^{*1} < U_P^{*0}$, as stated previously. It follows that $U_P^{*1} < U_P^{*3}$. The case of $K = 2N-1$ can also be safely discarded.

Case (c): $\alpha \in (\frac{1}{2N}, \frac{1}{2})$ Denote the utility of the primary user in this case as U_P^4. U_P^4 is a concave function of β. Letting $\frac{\partial U_P^4}{\partial \beta} = 0$, we have $\hat{\beta} = (\frac{1}{2\alpha} - 1)\frac{1}{N-1}$. Since $\alpha > \frac{1}{2N}$, $\hat{\beta} < 1$. Since $\alpha < \frac{1}{2}$, $\hat{\beta} > 0$. So $\hat{\beta} = (\frac{1}{2\alpha} - 1)\frac{1}{N-1}$ is feasible. Substitute $\hat{\beta}$ into U_P^4, we have

$$U_P^4 = w_P \ln\left(\frac{1}{2}\log(SNR)\right) + w_S(2N + 2\alpha - 3).$$

Since U_P^4 is a monotone increasing function of α, $U_P^{*4} < w_P \ln(\frac{1}{2}\log(SNR)) + w_S(2N-2) < U_P^{*0} < U_P^{*3}$. Therefore, we have the following lemma.

Lemma 6. *For $K_T \geq 2N-1$ and $K \leq 2N-1$, U_P achieves its maximum when $\alpha = 1,\ \beta = 0,\ K = 2N-2$, and the maximum value is given by (4.34).*

When $K > (2N-1)$ For $K > 2N-1$, we always have $\lfloor \frac{2N}{K+2} \rfloor$=0 and $\lfloor \frac{2N}{K+1} \rfloor = 0$. Denote the utility of the primary user in this case as U_P^5, we have

$$U_P^5 = w_P \ln(N\alpha\beta \log(SNR)).$$

Obviously, U_P^5 is a monotone increasing function of α and β. So the maximum is achieved when $\alpha = 1$ and $\beta = 1$.

$$U_P^{*5} = w_P \ln(N \log(SNR)). \tag{4.35}$$

Note that under this condition, there is no Phases II and III. There is no spectrum leasing and the transmission rates of all the secondary users are 0.

Comparing U_P^{*5} with U_P^{*3}, we have

$$\begin{aligned} U_P^{*3} - U_P^{*5} &= -w_P \ln(N) + w_S(2N-2) \\ &> w_P[(2N-2) - N] \ \geq \ 0. \end{aligned} \tag{4.36}$$

The first inequality is due to $\ln(x) < x$ for $x > 0$ and the second inequality is due to $N \geq 2$. Therefore $U_P^{*3} > U_P^{*5}$. The implication of (4.36) is that leasing spectrum to secondary users is helpful to maximize the utility of the primary user [2]

Compared with Lemma 6, we summarize the above analysis as a Lemma as follows.

[2]One may note that if $w_P >> w_S$, the inequality does not hold. However, as we noted before, we focus on the generic case where $w_P = w_S$.

Lemma 7. *For $K_T \geq 2N-1$, U_P achieves its maximum when $\alpha = 1,\ \beta = 0,\ K = 2N-2$, and the maximum of U_P is given in (4.34).*

Case II When $K_T = (2N-2)$

It can be readily concluded that the conclusion given in Section 4.4.2 still holds. So we finally have the following theorem.

Theorem 4.2. *When $K_T \geq 2N-2$, U_P is maximized when $\alpha = 1,\ \beta = 0,\ K = 2N-2$, and the maximum of U_P is given in (4.34).*

Note that when $K = 2N-2$, $d_{II} = 1$, $d_{III} = 1$. Theorem 4.2 indicates that, when there are plenty of secondary users, to maximize the primary user's utility, we should select $2N-2$ out of them so that each of the selected secondary user can have exactly *one* interference free channel. Since $\alpha = 1$ and $\beta = 0$, there is no Phase I and Phase III. To maximize the primary user utility, there's no need for the primary user to use MIMO transmission alone. Transmitting data with distributed interference alignment while collecting revenue from spectrum leasing is the best strategy for the primary user.

Case III When $3 \leq K_T \leq (2N-3)$

In this section, we consider the case when $3 \leq K_T \leq 2N-3$. So the number of antennas must satisfy $2N-3 \geq 3$, which indicates $N \geq 3$.

For simplicity, we assume that $2N$ is divisible by both K_T+2 and K_T+1. That is $\lfloor \frac{2N}{K_T+2} \rfloor = \frac{2N}{K_T+2}$ and $\lfloor \frac{2N}{K_T+1} \rfloor = \frac{2N}{K_T+1}$. Using similar arguments as in Section 4.4.2, to maximize U_P, we should let $K = K_T$.

Given the strategies of all the secondary users, the primary user tries to maximize its own utility by solving the following problem.

$$\max_{0 \leq \alpha \leq 1,\ 0 \leq \beta \leq 1} U_P(\alpha, \beta). \tag{4.37}$$

Plug in K_T and P_i^*, we have

$$\begin{aligned} U_P(\alpha,\beta) &= w_P \ln[\alpha\beta R_P^I + \alpha(1-\beta)R_P^{II}] + \\ &\quad K_T w_S[\alpha(1-\beta)d_{II} + (1-\alpha)d_{III}] \\ &= w_P \ln\{\alpha[\beta(R_P^I - R_P^{II}) + R_P^{II}]\} + \\ &\quad K_T w_S\{\alpha[(1-\beta)d_{II} - d_{III}] + d_{III}\}. \end{aligned} \tag{4.38}$$

We also assume that $w_P = w_S$. To find the maximum, we divide α axis into three adjacent intervals: $[0, \frac{1}{2N}]$, $[\frac{1}{2N}, \frac{K_T+2}{4N}]$ and $[\frac{K_T+2}{4N}, 1]$. Note that for $K_T \geq 3$, $\frac{1}{2N} < \frac{K_T+2}{4N}$.

Case (a): $0 \leq \alpha \leq \frac{1}{2N}$ Denote the utility of the primary user as U_P^6, we have

$$\begin{aligned} \frac{\partial U_P^6}{\partial \beta} &= w_P \frac{R_P^I - R_P^{II}}{\beta R_P^I + (1-\beta)R_P^{II}} - K_T w_S \alpha d_{II} \\ &= w_P[\frac{d_I - d_{II}}{\beta d_I + (1-\beta)d_{II}} - K_T \alpha d_{II}] \\ &\geq w_P[\frac{d_I - d_{II}}{d_I} - K_T \alpha d_{II}] \\ &= w_P[\frac{N - \frac{2N}{K_T+2}}{N} - K_T \alpha \frac{2N}{K_T+2}] \\ &= w_P[\frac{K_T}{K_T+2} - K_T \alpha \frac{2N}{K_T+2}] \geq 0. \end{aligned} \tag{4.39}$$

where the first inequality is due to $\max_{\beta\in[0,1]} \beta d_I + (1-\beta)d_{II} = d_I$, and the second inequality is due to $\alpha \leq \frac{1}{2N}$.

So for $0 \leq \alpha \leq \frac{1}{2N}$, $U_P(\alpha,\beta)$ is a monotone increasing function of β. That is $U_P(\alpha,\beta) \leq U_P(\alpha,1)$. To maximize the utility, the primary user solves the following problem.

$$\max_{0\leq\alpha\leq\frac{1}{2N}} \quad U_P^6(\alpha,1) = w_P \ln(\alpha R_P^I) + K_T w_S(1-\alpha)d_{III}. \tag{4.40}$$

Using convex programming, it can be found that U_P achieves its maximum when $\alpha = \frac{1}{2N}$. And the maximum value is:

$$\begin{aligned} U_P^{*6}(\frac{1}{2N}, 1) &= w_P \ln(\frac{R_P^I}{2N}) + K_T w_S(\frac{2N-1}{2N}) d_{III} \\ &= w_P \ln(\frac{\log(SNR)}{2}) + K_T w_S \frac{2N-1}{K_T+1}. \end{aligned} \tag{4.41}$$

Case (b): $\frac{K_T+2}{4N} \leq \alpha \leq 1$ Denote the utility of the primary user as U_P^7, we have

$$\begin{aligned} \frac{\partial U_P^7}{\partial \beta} &= w_P[\frac{d_I - d_{II}}{\beta d_I + (1-\beta) d_{II}} - K_T \alpha d_{II}] \\ &\leq w_P[\frac{d_I - d_{II}}{d_{II}} - K_T \alpha d_{II}] \\ &= w_P[\frac{K_T}{2} - K_T \alpha \frac{2N}{K_T+2}] \leq 0. \end{aligned} \tag{4.42}$$

where the first inequality is due to $\min_{\beta \in [0,1]} \beta d_I + (1-\beta) d_{II} = d_{II}$, and the last inequality is due to $\alpha \geq \frac{K_T+2}{4N}$.

Thus, for $\frac{K_T+2}{4N} \leq \alpha \leq 1$, $U_P^7(\alpha, \beta)$ is a monotone decreasing function of β, which indicates $U_P^7(\alpha, \beta) \leq U_P^7(\alpha, 0)$. To maximize the utility, the primary user solves the following problem.

$$\begin{aligned} \max_{\frac{K_T+2}{4N} \leq \alpha \leq 1} \quad & U_P(\alpha, 0) = w_P ln(\alpha R_P^{II}) + \\ & K_T w_S[\alpha d_{II} + (1-\alpha) d_{III}]. \end{aligned} \tag{4.43}$$

Using convex programming, it can be found that U_P achieves its maximum when

$$\alpha = \frac{(K_T+1)(K_T+2)}{2NK_T}. \tag{4.44}$$

Notice that, since we assume that $2N$ is divisible by both K_T+1 and K_T+2, $\frac{(K_T+1)(K_T+2)}{2N} \leq 1$. That is $\alpha = \frac{(K_T+1)(K_T+2)}{2NK_T} < 1$. On the other hand, $\frac{(K_T+1)(K_T+2)}{2NK_T} > \frac{K_T+2}{4N}$, so $\frac{(K_T+1)(K_T+2)}{2NK_T}$ is a

feasible point. The maximum value is given by:

$$\begin{aligned} & U_P^{*7}(\frac{(K_T+1)(K_T+2)}{2NK_T}, 0) \\ = \; & w_P \ln[\log(SNR)\frac{K_T+1}{K_T}] + K_T w_S(\frac{2N}{K_T+1} - \frac{1}{K_T}). \end{aligned} \tag{4.45}$$

Case (c): $\frac{1}{2N} \leq \alpha \leq \frac{K_T+2}{4N}$ Denote the utility of the primary user as U_P^8. For any fixed α, U_P^8 is a concave function with respect to β. We could maximize U_P^8 by firstly maximizing it with respect to β then with respect to α. We have:

$$\frac{\partial U_P^8}{\partial \beta} = w_P \frac{R_I - R_{II}}{\beta R_I + (1-\beta)R_{II}} - K_T w_S \alpha d_{II} \tag{4.46}$$

Set $\frac{\partial U_P^8}{\partial \beta} = 0$ results in:

$$\beta = \frac{1}{K_T \alpha d_{II}} - \frac{d_{II}}{d_I - d_{II}} \tag{4.47}$$

Since $\alpha \geq \frac{1}{2N}$, $\beta \leq \frac{1}{K_T \frac{2N}{K_T+2}\frac{1}{2N}} - \frac{\frac{2N}{K_T+2}}{N - \frac{2N}{K_T+2}} = 1$; $\alpha \leq \frac{K_T+2}{4N}$, $\beta \geq \frac{1}{K_T \frac{2N}{K_T+2}\frac{K_T+2}{4N}} - \frac{2}{K_T} = 0$. So the value of β given by (4.47) is a feasible point. Under this condition, we have:

$$\begin{aligned} U_P^8 &= w_P ln(\frac{w_P(R_P^I - R_P^{II})}{K_T w_S d_{II}}) + K_T w_S\{d_{III} - \frac{w_P}{K_T w_S} \\ &\quad + \alpha[(1 + \frac{R_{II}}{R_I - R_{II}})d_{II} - d_{III}]\} \\ &= w_P \ln(\frac{\log(SNR)}{2}) + w_P \alpha \frac{2N}{(K_T+1)} - w_P \\ &\quad + K_T w_P d_{III}. \end{aligned} \tag{4.48}$$

which is monotone increasing function of α. When $\alpha = \frac{K_T+2}{4N}$, the maximum is attained. Plug the value of α into (4.47), we have $\beta = 0$. So the maximum value is given by:

$$\begin{aligned} & U_P^{*8}(\frac{K_T+2}{4N}, 0) \\ = \; & w_P \ln(\frac{log(SNR)}{2}) + w_P \frac{K_T+2}{2(K_T+1)} \\ & -w_P + K_T w_P d_{III} \\ = \; & w_P \ln(\frac{\log(SNR)}{2}) + w_P \frac{K_T(4N-1)}{2(K_T+1)}. \end{aligned} \tag{4.49}$$

It can be readily concluded that $U_P^{*6} < U_P^{*8}$, we only need to compare U_P^{*7} with U_P^{*8}, then we could find the maximum value of U_P. We have:

$$\begin{aligned} U_P^{*7} - U_P^{*8} &= w_P[\ln(2\frac{K_T+1}{K_T}) - \frac{K_T+2}{2(K_T+1)}] \\ &= w_P[\ln(2+\frac{2}{K_T}) - \frac{1}{2} - \frac{1}{2(K_T+1)}]. \end{aligned} \tag{4.50}$$

Denote $f_5(K_T) = \ln(2\frac{K_T+1}{K_T}) - \frac{K_T+2}{2(K_T+1)}$. Consider K_T as a continuous variable, we have:

$$\frac{\partial f_5}{\partial K_T} = \frac{-(K_T+2)}{2K_T(K_T+1)^2} < 0. \tag{4.51}$$

So $f_5(K_T)$ is a monotone decreasing function of K_T, which means $f_5(K_T) > f_5(+\infty)$. Therefore, we have:

$$\begin{aligned} U_P^{*7} - U_P^{*8} &= w_P[\ln(2+\frac{2}{K_T}) - \frac{1}{2} - \frac{1}{2(K_T+1)}] \\ &> w_P[\ln(2) - \frac{1}{2}] = 0.193 > 0. \end{aligned} \tag{4.52}$$

Since $U_P^{*7} > U_P^{*6}$ and $U_P^{*7} > U_P^{*8}$, we readily have the following theorem.

Theorem 4.3. *For $K_T \leq 2N-3$, U_P achieves its maximum when $\alpha = \frac{(K_T+1)(K_T+2)}{2NK_T}$, $\beta = 0$, $K = K_T$, and the maximum of U_P is given by (4.45).*

It would be still interesting to compare the U_P^{*7} with U_P^{*5} for which there is no spectrum leasing. We have:

$$\begin{aligned}
& U_P^{*7} - U_P^{*5} \\
= \; & w_P \ln[\log(SNR)\frac{K_T+1}{K_T}] + K_T w_S(\frac{2N}{K_T+1} - \frac{1}{K_T}) \\
& -w_P \ln(N\log(SNR)) \\
= \; & w_P[\ln(\frac{K_T+1}{K_T}) + 2N\frac{K_T}{K_T+1} - 1 - \ln(N)] \\
> \; & w_P[2N\frac{K_T}{K_T+1} - 1 - \ln(N)] \\
\geq \; & w_P[\frac{3}{2}N - 1 - \ln(N)] \\
> \; & w_P[\frac{1}{2}N - 1] \\
> \; & 0, \qquad (4.53)
\end{aligned}$$

where the first inequality is due to $\ln(1+x) > 0$ for $x > 0$, the second inequality is because $\frac{K_T}{K_T+1}$ is an monotone increasing function of K_T, the thrid inequality is due to $\ln(x) < x$ for $x > 0$, and the last inequality is due to $N \geq 3$.

This indicates that even with an insufficient number of secondary users, leasing spectrum to the secondary users is still beneficial for the primary user to increase its utility.

4.4.3 The Unique Stackelberg Equilibrium

We now summarize the analysis in Sections 4.4.1 and 4.4.2. The unique Stackelberg Equilibrium of the game defined in Section 4.3 is given in the following theorem.

Theorem 4.4. *The unique Stackelberg Equilibrium is given by:*

$$(\alpha^*, \beta^*, K^*) = \begin{cases} (1, 0, 2N-2), & \text{if } K_T \geq 2N-2 \\ \left(\frac{(K_T+1)(K_T+2)}{2NK_T}, 0, K_T\right), & \text{if } 3 \leq K_T \leq 2N-3 \end{cases} \tag{4.54}$$

$$P_i^* = [w_S \alpha^*(1-\beta^*)d_{II} + w_S(1-\alpha^*)d_{III}]/C_0, \ \forall\, i. \tag{4.55}$$

Since we can rewrite (4.55) as $P_i^* = w_S[\alpha(d_{II} - d_{III}) - \alpha\beta d_{II} + d_{III}]/C_0$ and $d_{II} \geq d_{III}$, P_i^* is a monotone decreasing function of α and β. On the other hand, P_i^* is a monotone increasing function of d_{II} and d_{III}, indicating that P_i^* is a monotone decreasing function of K. The secondary users will adjust their transmitter power in light of α, β and K. The best scenario for them is $\alpha = 0$, $\beta = 0$ and $K = 3$, for which there is only Phase III with the fewest players.

Knowing the optimal strategies of the secondary users, the primary user will set $\alpha = 1$, $\beta = 0$, and $K = 2N - 2$ when there are a sufficient number of secondary users. Each selected secondary user has exactly *one* interference free channel, and there is only Phase II in the time slot. In this case, the primary user can collect as much revenue as possible while keeping a relatively low-rate data transmission. The secondary users' claim is satisfied in part. If there are not as many secondary users as needed, the primary user will set the parameters carefully according to (4.54). Under this condition, the primary user selects *all* the secondary users, discards Phase I, and makes a trade-off between Phase II and Phase III according to how many secondary users are there in the system.

4.5 Simulation Study

Simulations are conducted to validate the performance of the proposed scheme. We first compare the proposed scheme with a scheme without spectrum leasing to demonstrate the benefits of spectrum leasing. We then compare the proposed scheme with the cooperative scheme presented in [47] to demonstrate the efficacy of distributed interference alignment.

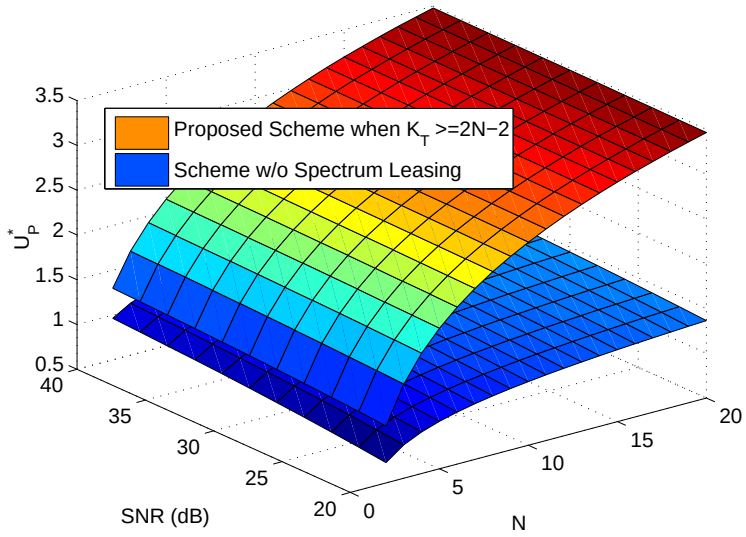

Figure 4.2: Utility of the primary user in Log scale.

4.5.1 With or Without Spectrum Leasing

We first consider the case when there is a sufficient number of secondary users, i.e., $K_T \geq 2N - 2$, since in many real-world applications there are usually more secondary users than the number of antennas at each node. In Fig. 4.2, we plot the primary user utility U_P^* versus the number of antennas N and SNR. In the simulation, the weight factors are $w_P = w_S = 0.8$. The noise spectral density is $N_0 = 0.1$. The unit price is $C_0 = 0.001$. Note that the maximum utility of the primary user without spectrum leasing is given in (4.35). It can be seen from Fig. 4.2 that there is a huge gap between the proposed scheme and the scheme without spectrum leasing. Note that the utility increase due to SNR is less obvious than that due to N, since the impact of SNR is diminished by the logarithms functions in (4.10) and (4.11). This clearly indicates that under the same setting, leasing spectrum to secondary users can greatly improve the primary user utility. Also note that, from (4.36), the utility of the proposed scheme is strictly larger than that of no spectrum leasing, for any feasible values of w_P, N and SNR.

In Fig. 4.3, we examine the impact of weight w_P on the primary user utility U_P^*. We plot the results with or without spectrum leasing, and for $N = 2$, 4, and 6. It can be seen that when w_P is increased, the gap between the proposed scheme and the scheme without spectrum leasing becomes

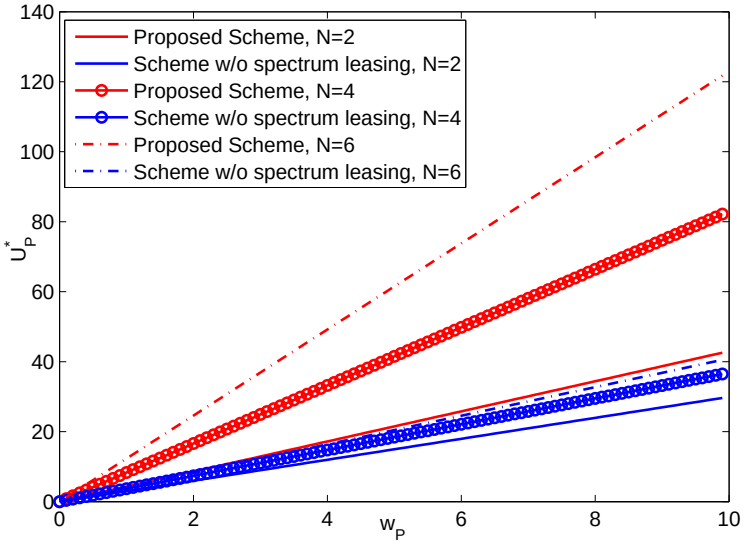

Figure 4.3: Utility of the primary user when $K_T \geq 2N - 2$.

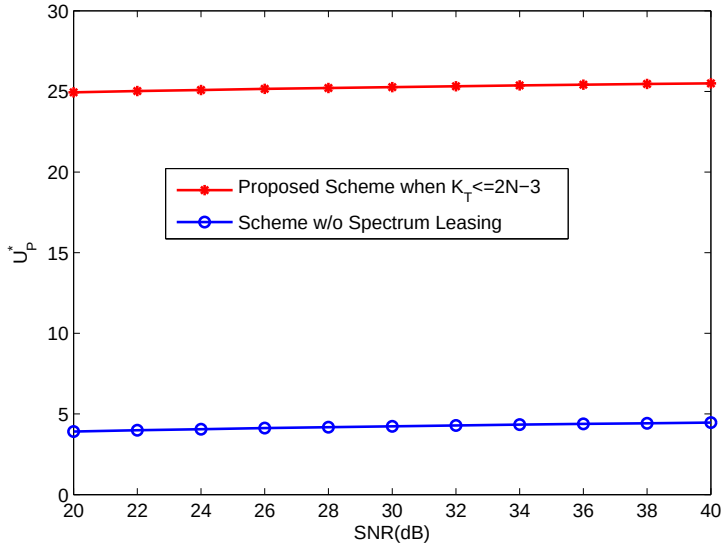

Figure 4.4: Utility of the primary user when $K_T \leq 2N - 3$.

larger. Although with increased w_P, the primary user emphasizes more on data transmission, the revenue is still increased at a higher speed with spectrum leasing. The gap also becomes larger when the number of antennas for each node is increased. This is also because the revenue increases faster with spectrum leasing than the no leasing scheme as N is increased.

We then consider the case of an insufficient number of secondary users. In the simulation, there are $K_T = 3$ secondary users. The number of antennas is $N = 20$. We plot the primary

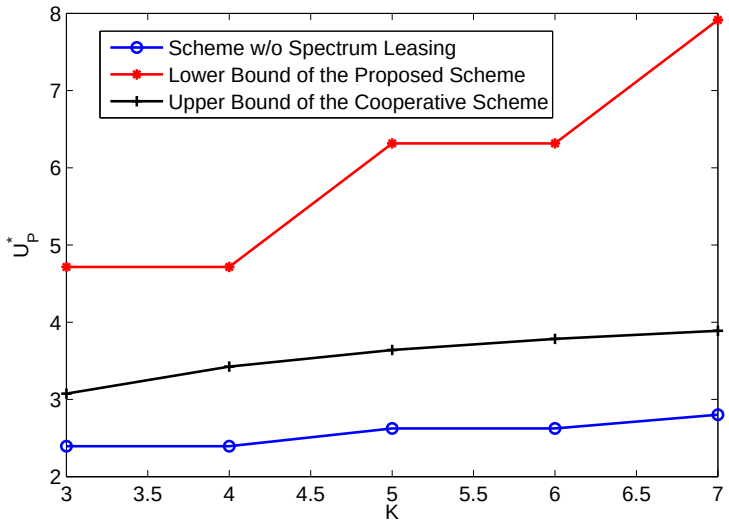

Figure 4.5: Comparison of the proposed scheme with the cooperative scheme.

user utility for the proposed scheme and the no-spectrum-leasing scheme in Fig. 4.4. We find that there's also a big gain achieved by the proposed scheme. This is consistent with our previous discussions. In this case, the primary user should still lease its spectrum to secondary users to maximize it own utility.

4.5.2 With or Without Distributed Interference Alignment

Next, we compare our proposed scheme with cooperative scheme in [47]. To make fair comparisons, replace the satisfaction function $f_P(R_P) = \frac{1}{1+e^{-a(R_P-R_0)}}$ in [47] with $f_P(R_P) = \ln(R_P)$. We firstly derive a upper bound of the utility of the primary user (denoted as U_P^9) in [47] using our notation. Then we compare our proposed scheme with the derived upper bound.

$$U_P^9 = w_P \ln(R_P) + \frac{w_S(1-\alpha)(K-1)}{\sum_i(\frac{1}{R_{S_i}})}. \tag{4.56}$$

where $R_P = \min\{\alpha\beta R_{PS}, \alpha(1-\beta)R_{SP}\}$, $R_{PS} = \log(1 + \frac{\min_i |h_{PS,i}|^2 P}{N_0})$, $R_{SP} = \log(1 + \frac{|h_P|^2 P}{N_0} + \sum_i \frac{\min_i |h_{SP,i}|^2 P}{N_0})$, $R_{S_i} = \log(1 + \frac{|h_{S_i}|^2 P}{N_0})$, and all the h are channel states. Since

$$\begin{aligned} R_P &= \min\{\alpha\beta R_{PS}, \alpha(1-\beta)R_{SP}\} \\ &\leq \alpha \frac{R_{PS}R_{SP}}{R_{PS}+R_{SP}} \\ &< \alpha R_{PS} = \alpha \log(1 + \frac{\min_i |h_{PS,i}|^2 P}{N_0}) \\ &\leq \alpha \log(1 + \frac{P}{N_0}). \end{aligned} \tag{4.57}$$

and

$$R_{S_i} \leq \log(1 + \frac{P}{N_0}), \tag{4.58}$$

So we have:

$$\begin{aligned} U_P^9 &= w_P \ln(R_P) + \frac{w_S(1-\alpha)(K-1)}{\sum_i (\frac{1}{R_{S_i}})} \\ &< w_P \ln[\alpha \log(1+SNR)] + \\ &\quad \frac{w_S(1-\alpha)(K-1)}{K} \log(1+SNR). \end{aligned} \tag{4.59}$$

Denote $f_6(\alpha) = \ln[\alpha \log(1+SNR)] + \frac{(1-\alpha)(K-1)}{K} \log(1+SNR)$. For $SNR \geq 3$, $f_6(\alpha)$ is maximized at $\hat{\alpha} = \frac{K}{(K-1)\log(1+SNR)}$. Since we consider high SNR region, the condition of $SNR \geq 3$ is easily satisfied. Plug in $\hat{\alpha}$, we have:

$$U_P^9 < w_P \ln(\frac{K}{K-1}) + w_S[\frac{K-1}{K} \log(1+SNR) - 1], \tag{4.60}$$

that means the utility of the cooperative scheme is upper bounded by $w_P \ln(\frac{K}{K-1}) + w_S[\frac{K-1}{K} \log(1+SNR) - 1]$.

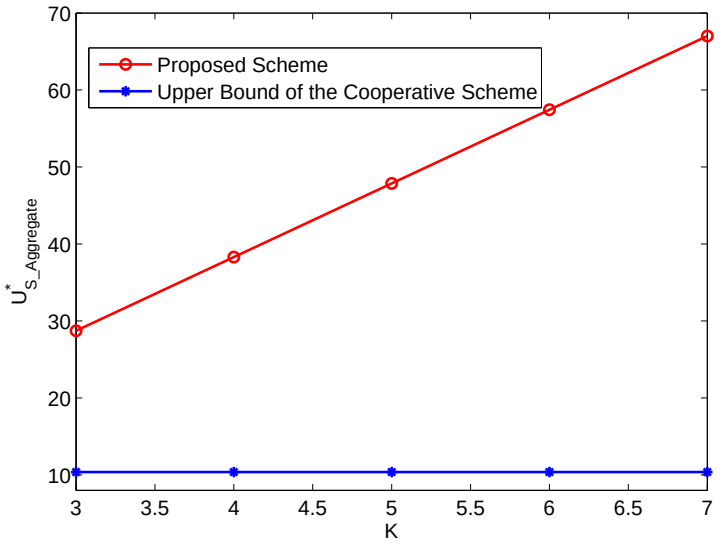

Figure 4.6: Aggregated SU utility comparison of the proposed scheme with the cooperative scheme.

In Fig. 4.5, we plot the simulation results for the proposed scheme, the cooperative scheme, and the no-spectrum-leasing scheme. Since in [47], all the primary user and the secondary users are equipped with single antenna, to make fair comparison, we choose K, number of secondary users selected as the variable in the simulation. In the simulations, since the number of antennas must satisfy $\lfloor \frac{2N}{K+2} \rfloor \geq 1$, as the number of K varies, we set $N = \lceil \frac{K+2}{2} \rceil$. So we are actually comparing the lower bound of our proposed scheme with the upper bound of the cooperative scheme. It can be seen from Fig. 4.5 that both spectrum leasing schemes outperform the no-spectrum-leasing scheme. Furthermore, the proposed scheme outperforms the cooperative scheme with considerable gains. Such gains justify the efficacy of distributed interference alignment, which greatly enhance the overall system capacity.

Finally, we compare our proposed scheme with the cooperative scheme in [47] in terms of aggregate secondary user utility and average secondary users utility. We firstly derive an upper bound of the secondary users' utility in [47], then compare it to the secondary users' utility in our proposed scheme with the identical number of selected secondary users and identical transmission power. Note that, under the scenario of no spectrum leasing, the secondary users utility is always 0. Thus, we do not include it in the comparison.

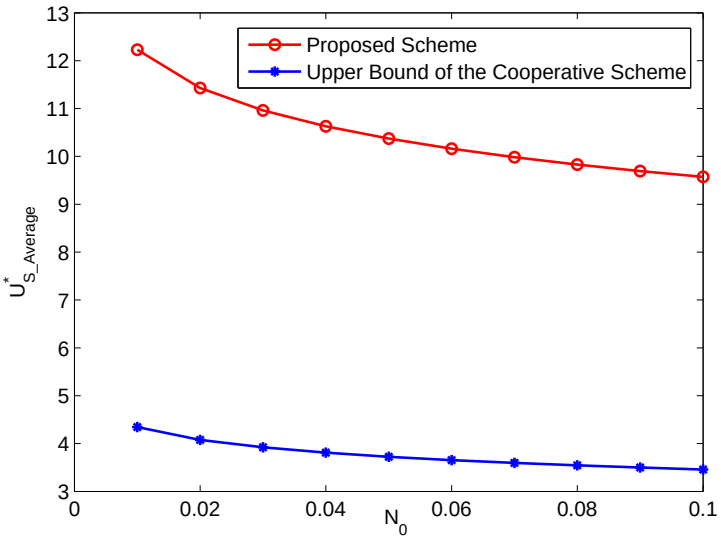

Figure 4.7: Average SU utility comparison of the proposed scheme with the cooperative scheme.

From Theorem 4.4, we obtain the maximum utility for each secondary user as:

$$U^*_{S\_Average\_1} = w_S log(\frac{w_S}{2C_0N_0}), \tag{4.61}$$

and the aggregate maximum utility for all the secondary user as:

$$U^*_{S\_Aggregate\_1} = Kw_S log(\frac{w_S}{2C_0N_0}), \tag{4.62}$$

The utility for each secondary user in [47] is given by:

$$\max_{c_i} u_i(c_i) = \max_{c_i}\{\frac{w_S(1-\alpha)c_iR_i}{\sum_j c_j} - c_i\}, \tag{4.63}$$

where $R_i = \log(1+\frac{|h_{S_i}|^2P_S}{N_0})$. Since we assume perfect channel and consider high SNR, $R_i \approx R = \log(\frac{P_S}{N_0})$.

The maximum is achieved at:

$$c_i^* = w_S(1-\alpha)(K-1)[\sum_j \frac{1}{R_j} - \frac{K-1}{R_i}]/(\sum_j \frac{1}{R_j})^2. \tag{4.64}$$

Denote $X_i = (K-1)[\sum_j \frac{1}{R_j} - \frac{K-1}{R_i}]/(\sum_j \frac{1}{R_j})^2$, we have $c_i^* = w_S(1-\alpha)X_i$. The maximum aggregate secondary user utility denoted as $U^*_{S\_Aggregate\_2}$ is derived as follows.

$$\begin{aligned}
U^*_{S_Aggregate_2} &= \sum_i u_i(c_i^*) \\
&= w_S(1-\alpha)\left[\frac{\sum_i X_i R_i}{X_i} - \sum_i X_i\right] \\
&\leq w_S\left[\frac{\sum_i X_i R_i}{X_i} - \sum_i X_i\right] \\
&< w_S \frac{\sum_i X_i R_i}{X_i} \\
&\approx w_S R = w_S \log(\frac{P_S}{N_0}),
\end{aligned} \tag{4.65}$$

where the first inequality is due to $0 \leq \alpha \leq 1$ and second inequality is due to $X_i > 0$.

Using P_i^* from Theorem 4.4, we have:

$$U^*_{S\_Aggregate\_2} = w_S log(\frac{w_S}{C_0 N_0}), \tag{4.66}$$

and

$$U^*_{S\_Average\_2} = \frac{w_S}{K} log(\frac{w_S}{C_0 N_0}) \leq \frac{w_S}{3} log(\frac{w_S}{C_0 N_0}), \tag{4.67}$$

where the inequality is due to $K \geq 3$.

It can be readily seen from Fig. 4.6 and Fig. 4.7 that, the proposed scheme outperform the cooperative scheme, no matter from the perspective of each secondary user or the whole group of secondary user.

4.6 Related Work

This chapter is closely related to the research on CR networks. For a general survey of CRs, interested readers are referred to [2]. In a CR network, the primary user is either aware or unaware of the existence of the secondary users. This chapter falls into the first category. The primary user is not only aware of the existence of the secondary user, but also knows the impact of the rules on the secondary user behavior. Most of the previous work, such as [47, 49–51, 54], only considered the single antenna case, while we consider multiple antennas and exploit multiplexing gain in this chapter.

This chapter is also related to the research on interference alignment. In [19], the authors introduced the interference alignment technique. The significance of their work is that, by adopting interference alignment, the system is no longer interference limited. With symbol extension, the system could achieve a normalized DoF of $K/2$. Another important issue, the feasibility condition, was investigated in [20] for structureless generic wireless channels. For wireless channels with a structure, such as diagonal channels, our recent chapter [48] investigated the application of interference alignment in multi-user OFDM networks. To address the concern on the global CSI requirement, a distributed interference alignment algorithm was proposed in [41], which only requires local CSI. In [33], interference alignment and cancellation were integrated to achieve enhance the throughput of MIMO Wi-Fi networks. In [32], Li et al. proposed a general algorithm for the multi-hop mesh networks. This work was motivated by these interesting papers. However, many of the related work mainly focused on physical layer issues. This chapter considers how to adopt distributed interference alignment in a MIMO CR network with a novel Stackelberg game based approach.

Recent work [52] and [53] considered incorporating IA in cognitive radio networks. However, they do not take the fact that the primary user has finite packages to send into consideration. This chapter mainly considers how to use interference alignment in the network and has taken the finite demand of primary users into consideration.

4.7 Conclusions

In this chapter, we investigated the behaviors of the primary user and secondary users in a MIMO CR network. We proposed a three-phase cooperative spectrum leasing scheme with distributed interference alignment. The system was modeled as a Stackelberg game. With backward induction, we derived the unique Stackelberg equilibrium. Through rigorous analysis, we found the best strategies for the primary user and secondary users under a broad range of conditions and parameters, and discussed practical implications. We also found that leasing spectrum to secondary users is always helpful for enhancing the primary user utility. Simulation results demonstrated that the proposed scheme outperformed a no-spectrum-leasing scheme and a cooperative scheme from prior work.

Chapter 5

User Grouping for Massive MIMO in FDD Systems: New Design Methods and Analysis

5.1 Introduction

Last decades have witnessed ever-increasing demand for higher data rates. To cater for this demand, many advanced physical layer techniques have been developed, e.g., multiple input multiple output with orthogonal frequency division multiplexing (MIMO-OFDM). However, with linear throughput improvement but the exponential growth on the data traffic, the gap between the demand and supply has widen more and more. To solve the issue, the next technology we could resort to is massive MIMO, (or called large-scale MIMO, full-dimension MIMO, hyper MIMO, we will use these terms interchangeably hereafter) which significantly increases the system throughput by employing a large number of transmit antennas at the base station. As an emerging and promising technology, besides the throughput enhancement, large-scale MIMO also enjoys advantages of low-power, robust transmissions, simplified transceiver, and simple multiple-access layer [58, 59]. Recently, lab demo systems have demonstrated the benefits of the massive MIMO systems [60,61].

In general, equipped with more transmit antennas, more degrees of freedom the massive MIMO system could provide, resulting in better reliability or higher throughput. So we expect the massive MIMO system to boost up the system throughput tremendously by simultaneously serving many users. However, due to the difficulties of acquiring channel state information at the transmitter side (CSIT), it is challenging to simultaneously support a large number of users [59]. Most of the existing works on large scale MIMO systems consider time-division-duplexing (TDD) mode [62–64], since by exploiting the channel reciprocity in the TDD system, the downlink channel can be estimated from the uplink training. However, the frequency-division-duplexing (FDD) system does not have such privilege. Pilot based channel estimation and uplink channel feedback are required, which consumes lots of spectrum resources.

According to [65], there are much more FDD LTE licenses (≥ 300) than TDD (≤ 40) ones worldwide. With so many FDD deployments worldwide, it is of great significance to investigate the large-scale MIMO design for FDD systems. Recently, a two-stage precoding scheme has been proposed in [66] to reduce pilot resources and the channel state information (CSI) feedback in FDD systems. Firstly, the users in service are put into groups with each group of users having similar second-order channel statistics, i.e., transmit correlation. The same pre-beamforming, or the first-stage precoding, is then used for each group of users semi-statically. Then, with reduced dimensions on the effective channel, simple channel feedback can be realized and the second-stage dynamic precoding can be applied. Therefore, one important issue for such system design is user grouping. In [67], a K-means clustering using chordal distance as the clustering metric is introduced for the user grouping. In this chapter, instead of chordal distance, we propose three similarity measures as the grouping metric, namely, *weighted likelihood similarity measure*, *subspace projection based similarity measure*, and *Fubini-Study based similarity measure*. We also propose two clustering methods i.e. *hierarchical clustering* method and *K-medoids clustering* method, for user grouping. Through theoretical analysis and simulations, we show that the weighted likelihood similarity measure and hierarchical clustering could achieve higher throughput.

Given user grouping, another important issue is user scheduling, i.e., selecting users for transmission based on instantaneous channel condition. We propose a dynamic user scheduling method and derive a lower bound for its performance. If there are only a few active users, some groups may barely have users while some other groups are overloaded. Therefore, we also consider the load balancing problem and present an effective algorithm to solve it.

The remainder of this chapter is organized as follows. In Section 5.2, related works are discussed. In Section 5.3, we present the system model and some preliminaries. We discuss the user grouping and user scheduling problem in Section 5.4 and Section 5.5, respectively. The scheme for user grouping considering group load balancing is presented in Section 5.6. Simulation studies are presented in Section 5.7. And Section 5.8 concludes this chapter.

5.2 Related Works

As aforementioned, most of the existing works on massive MIMO focus on TDD systems. Although TDD has the advantage of exploiting the channel reciprocity, pilot contamination remains the biggest problem for TDD systems [58] [59] [62].

For FDD systems, the system bottleneck lies in the cost of acquiring CSIT. Broadly speaking there are two types of transmission modes: open-loop and close loop, representing the system without and with feedback, respectively. This chapter falls into the latter category.

Assuming that the base station and the users share a common set of training signals beforehand, both open-loop and close-loop training frameworks are proposed in [69]. In the open-loop mode, the base station transmits the training signal in a round-robin manner, so that the receivers could estimate current channel using spatial or temporal correlations and previous channel estimations. In the close-loop mode, users select the best training signal based on previously received signals and send back the index of these training signals to the base station. During the next phase, the base station sends the training signals according to the feedback of previous phases.

In [70] the feedback rate has been taken into consideration. Since for fixed feedback rate per antenna, channel quantization grew exponentially with the number of transmit antennas, a noncoherent trellis-coded quantization is proposed with complexity growing linearly with the number of antennas.

Pilot pattern design for channel estimation is considered in [71]. Presuming wireless channel to be a stationary Gauss-Markov random process, pilot pattern is then designed based on Kalman filtering, spatial and temporal channel correlations. It is shown that the proposed scheme has low complexity but better performance, especially for the one-ring channel model.

A codebook design method is presented in [72] with limited or extremely low feedback, which could be considered as a open-loop approach. The compressive sensing technique is proposed in [73] to reduce the training and feedback overhead for CSIT acquisition. Due to the hidden joint sparsity structure of massive MIMO system, a distributed compressive CSIT estimation scheme is proposed. The advantage of the proposed scheme is that compressed measurements are taken

locally at users, while CSIT recovery is performed at the base station jointly. The proposed scheme has been shown to outperform five other algorithms in terms of normalized mean absolute error for CSIT recovery and have close performance to a so-called genie-aided scheme.

Similar to [66,67], Chen and Lau [74] decomposed the overall precoder into an outer precoder and inner precoder, where outer precoder suppresses the inter-cell or inter-cluster interference and inner precoder is used for intra-cluster multiplexing. The contribution of [74] is that it reduces the complexity of calculating outer precoder from $\mathcal{O}(M^3)$ to $\mathcal{O}(M^2)$, and it is an online algorithm which is suitable for time-varying channels.

We safely conclude that those papers have not considered the user grouping and scheduling problems in massive MIMO systems. Based on the framework of [67], our recent work in [68] proposes an improved K-means clustering scheme and a dynamic user selection scheme. Another problem considered in [68] is the load balancing problem, which is also addressed in [75]. However, the system considered in [75] is in the TDD mode.

In summary, the contribution of this chapter on massive MIMO in FDD systems over [67, 68] lies in three aspects: new user grouping schemes with new grouping metric, new user scheduling schemes, and efficient load balancing design.

5.3 System Model and Preliminaries

We consider a downlink system with M antennas at base station (BS) and single antenna at each user terminal (UT). The transmit antennas can have different geometries, e.g., being placed along one axis to form uniform linear array (ULA), along a circle to form uniform circular array (UCA), or in two or three dimensions. Denote y_k as the received signal at user k, $k = 1, \ldots, K$. The signals received by all UTs $\mathbf{y}$ can be written as

$$\mathbf{y} = \mathbf{H}^H \mathbf{V}\mathbf{d} + \mathbf{z}, \tag{5.1}$$

where $(\cdot)^H$ denotes the Hermitian of a matrix; $\mathbf{H}$, of dimension $M \times K$, is the actual channel between the BS and the users; $\mathbf{V}$ is the precoding matrix of dimension $M \times S$; $\mathbf{d}$ is the data vector of dimension S; and $\mathbf{z}$ is the zero mean circulant symmetric complex Gaussian noise vector. Note that throughout this chapter, we use bold upper (lower) case letter to denote a matrix (vector), and normal letter to denote a scalar.

Based on the two-stage precoding approach in [66], the precoding is formed as a multiplication of two precoding matrices, i.e., $\mathbf{V} = \mathbf{BP}$. The first part $\mathbf{B}$ of dimension $M \times b$ is pre-beamforming matrix, which is designed based on the second order channel statistics, or particularly, the transmit spatial correlation. The same pre-beamforming matrix is semi-statically applied to the users with the same or similar transmit correlation, which forms a user group. Therefore, pre-beamforming matrix is designed to suppress the interferences among the groups. We can see that the effective transmit size after the pre-beamforming is b, which is determined by dominant eigenmodes of the average transmit correlation of user groups. The second part $\mathbf{P}$ of dimension $b \times S$, is designed to suppress the interferences within each group with dynamical channel condition. To find $\mathbf{P}$, we can just apply conventional zero-forcing beamforming (ZFBF) or regularized zero-forcing beamforming (RZFBF). Note that we have $S \leq b$ as the second-stage precoding is supposed to suppress the interference within the group.

Denote $\tilde{\mathbf{H}} = \mathbf{B}^H\mathbf{H}$ as the effective channel after pre-beamforming. The signal model in (5.1) can be rewritten as

$$\mathbf{y} = \mathbf{H}^H\mathbf{BPd} + \mathbf{z} = \tilde{\mathbf{H}}^H\mathbf{Pd} + \mathbf{z}. \tag{5.2}$$

We adopt the one-ring channel model in [66, 68], in which θ is the azimuth angle of the user location, s is the distance between the BS and the user, r is the radius of the scattering ring, and Δ is the angle spread, which can be approximated as

$$\Delta \approx \arctan(r/s). \tag{5.3}$$

Denote $\mathbf{R}$ as the channel covariance matrix of the transmitter with the (m,p)-th entry given by

$$[\mathbf{R}]_{m,p} = \frac{1}{2\Delta}\int_{-\Delta}^{\Delta} e^{j\mathbf{k}^T(\alpha+\theta)(\mathbf{u}_m-\mathbf{u}_p)}d\alpha, \tag{5.4}$$

where $\mathbf{k}(\alpha) = -\frac{2\pi}{\lambda}(\cos(\alpha),\sin(\alpha))^T$ is the vector for a planar wave impinging with Angle of Arrival (AoA) α, λ is the carrier wavelength, $\mathbf{u}_m$ and $\mathbf{u}_p$ are the position vectors of antenna m, p, and $(\cdot)^T$ denotes the transpose operation. It can be verified that $\mathbf{R}$ is a normal matrix. With eigen-decomposition, we have

$$\mathbf{R} = \mathbf{U}\mathbf{\Lambda}\mathbf{U}^H, \tag{5.5}$$

where $\mathbf{U}$ is a unitary matrix comprising eigenvectors of $\mathbf{R}$ and $\mathbf{\Lambda}$ is a diagonal matrix with eigenvalues of $\mathbf{R}$ as the diagonal entries. Furthermore, the actual channel is generated using the following model

$$\mathbf{h} = \mathbf{U}\mathbf{\Lambda}^{\frac{1}{2}}\mathbf{w}, \tag{5.6}$$

where $\mathbf{w}$ is a vector of complex random variables and $\mathbf{w} \sim \mathcal{CN}(\mathbf{0},\mathbf{I})$.

Denote G as the number of groups. We then have $\mathbf{H}_g = [\mathbf{h}_{g_1},\ldots,\mathbf{h}_{g_{K_g}}]$, $\mathbf{H} = [\mathbf{H}_1,\ldots,\mathbf{H}_G]$, $\mathbf{B} = [\mathbf{B}_1,\ldots,\mathbf{B}_G]$, and $\tilde{\mathbf{H}}_g = \mathbf{B}_g^H\mathbf{H}_g$. The signal vector received by the g-th group of users is then given by

$$\mathbf{y}_g = \tilde{\mathbf{H}}_g^H\mathbf{P}_g\mathbf{d}_g + \sum_{g'\neq g}\mathbf{H}_g^H\mathbf{B}_{g'}\mathbf{P}_{g'}\mathbf{d}_{g'} + \mathbf{z}_g, g = 1,\ldots,G. \tag{5.7}$$

From (5.7) we can see that the design of $\mathbf{B}_g$ is to achieve

$$\mathbf{H}_g^H\mathbf{B}_{g'} \approx 0, \forall g' \neq g. \tag{5.8}$$

Generally speaking, there are three different approaches of obtaining $\mathbf{B}_g$, namely *Eigen-beamforming*, *Approximate Block Diagonalization (BD)* and *DFT Matrix Approximation*.

1) *Eigen-beamforming*: If the locations of all group members in a group are close, we assume they have similar transmit correlations. We can design $\mathbf{B}_g$ as

$$\mathbf{B}_g = \mathbf{V}_g, \tag{5.9}$$

where $\mathbf{V}_g$ is the unitary matrix after eigen-decomposing $\mathbf{R}_g$, which is the average of the transmit correlation matrices of users within the group g and can be viewed as the group center.

2) *Approximate Block Diagonalization (BD)*: Firstly, find the group center for all groups $\{\mathbf{R}_g\}$. Then we form

$$\mathbf{\Xi}_g = [\mathbf{V}_1, \ldots, \mathbf{V}_{g-1}, \mathbf{V}_{g+1}, \ldots, \mathbf{V}_G]. \tag{5.10}$$

Perform Singular Value Decompostion (SVD) to $\mathbf{\Xi}_g$ to obtain $[\mathbf{E}_g^{(1)},\ \mathbf{E}_g^{(0)}]$, such that Span$(\mathbf{E}_g^{(0)}) =$ Span$^{\perp}(\{\mathbf{V}_{g'} : g' \neq g\})$. Find

$$\hat{\mathbf{R}}_g = (\mathbf{E}_g^{(0)})^H \mathbf{U}_g \mathbf{\Lambda}_g \mathbf{U}_g^H \mathbf{E}_g^{(0)}. \tag{5.11}$$

And perform SVD to $\hat{\mathbf{R}}_g$, such that

$$\hat{\mathbf{R}}_g = \mathbf{G}_g \mathbf{\Phi}_g \mathbf{G}_g^H. \tag{5.12}$$

Let $\mathbf{G}_g = [\mathbf{G}_g^{(1)}, \mathbf{G}_g^{(0)}]$, where $\mathbf{G}_g^{(1)}$ contains b_g dominant eigenmodes of $\hat{\mathbf{R}}_g$. Finally, $\mathbf{B}_g$ can be obtained as

$$\mathbf{B}_g = \mathbf{E}_g^{(0)} \mathbf{G}_g^{(1)}. \tag{5.13}$$

3) *DFT Matrix Approximation*: For large scale MIMO systems with ULA antennas, we have

$$\lim_{M \to \infty} \frac{1}{M} \left\| \mathbf{U}\mathbf{U}^H - \mathbf{F}_S \mathbf{F}_S^H \right\|^2 = 0, \tag{5.14}$$

where $\mathbf{F}_S$ is a submatrix of unitary DFT matrix whose (a, b)-th entry is given by $[\mathbf{F}]_{a,b} = \frac{e^{-j2\pi ab/M}}{\sqrt{M}}$. Thus, we can select certain columns of a DFT matrix to approximate the prebeamforming matrix.

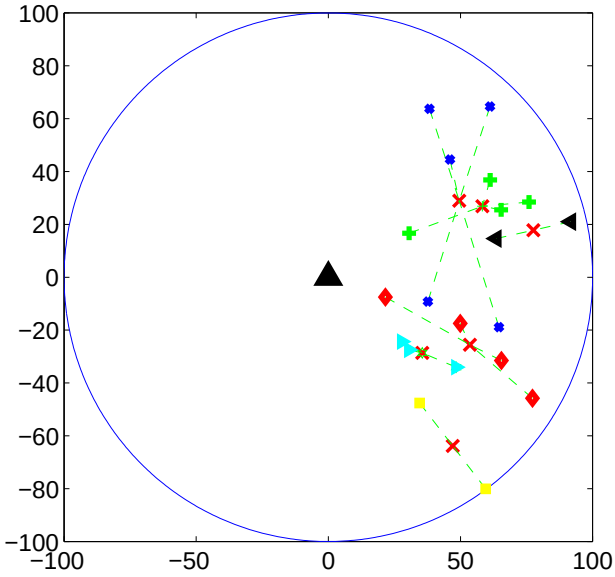

Figure 5.1: User grouping Scenario.

For the second stage precoding, we apply conventional zero-forcing beamforming (ZFBF) or regularized zero-forcing beamforming (RZFBF). The precoding matrix is given by

$$\mathbf{P}_g = \tilde{\mathbf{H}}(\tilde{\mathbf{H}}^H\tilde{\mathbf{H}} + S_g\alpha\mathbf{I}_{S_g})^{-1}, \tag{5.15}$$

where α can be set as $\alpha = 0$ for ZFBF or $\alpha = \frac{\sum_g S_g}{p\sum_g b_g}$ for RZFBF, S_g is number of data streams in the g-th group and p is the total transmit power of the BS.

5.4 User Grouping in Massive MIMO System

In order to suppress the inter-group interferences, the prebeamforming matrix $\mathbf{B}_g$ for group g shall be carefully designed based on all the group centers $\mathbf{R}_g, g = 1, \ldots, G$. Note that the group center can be obtained by averaging the subspace of all the group members or assigning one of the group members to be the group center. User grouping also has impacts on the user scheduling, since for each prebeamforming group, only the users within its group can be scheduled. Therefore it is important to design an effective user grouping method.

The idea of user grouping is illustrated in Fig. 5.1. The big triangle in the middle represents the massive MIMO base station. Other markers except the red-cross represent users. Users from different groups are differentiated by different markers and colors. The red cross is the virtual group center. The dashed lines indicate the connections between users and group centers.

For user grouping, we first need to obtain the similarities (or distances) among the users and groups, and then group users based on a certain metric. Each user grouping scheme consists of two parts, the similarity measure and clustering method. In this section, we first review the K-means clustering method and the chordal distance as similarity measure presented in [67, 68]. Then we propose new clustering methods and similarity measures as the grouping metric.

Most of the clustering schemes in the literature only handle matrix dataset, i.e., the whole dataset is a matrix. However, for our case here, each data entry is a matrix. The whole dataset is comprised of a large number of matrices. Thus, one of our contributions is to form efficient low-complexity grouping methods for datasets with many matrices. Also note that different clustering methods and similarity measures can be combined in various ways.

5.4.1 K-means User Grouping and Chordal Distance

In [67], a K-means clustering algorithm for user grouping is presented. The similarity measure of the K-means clustering algorithm to group users is the chordal distance between the eigenvectors $\mathbf{U}_k$ of user's channel correlation $\mathbf{R}_k$ and that of the group center $\mathbf{R}_g$, given as

$$d_c(\mathbf{U}_k, \mathbf{V}_g) = \left\| \mathbf{U}_k \mathbf{U}_k^H - \mathbf{V}_g \mathbf{V}_g^H \right\|_F^2, \tag{5.16}$$

where $\mathbf{U}_k$ is the matrix of the eigen vectors of $\mathbf{R}_k$, i.e., $\mathbf{R}_k = \mathbf{U}_k \mathbf{\Lambda}_k \mathbf{U}_k^H$. User grouping is then formed via an iterative process. In each iteration, each user is assigned to the group with minimum distance. Then the group center is updated using unitary matrix of users associated to the group as

$$\mathbf{V}_g = \Upsilon\Big\{ \frac{1}{|\mathcal{S}_g|} \sum_{k \in \mathcal{S}_g} \mathbf{U}_k \mathbf{U}_k^H \Big\}. \tag{5.17}$$

Note that $\Upsilon(\cdot)$ denotes the unitary matrix after eigen decomposition, $\mathcal{S}_g$ denotes the user set of group g, $|\mathcal{S}_g|$ denotes the size of group g.

5.4.2 Weighted Likelihood Similarity Measure

Instead of chordal distance, we propose a weighted likelihood function as the similarity measure between a user and a group, which is defined as

$$L(\mathbf{R}_k, \mathbf{V}_g) \triangleq \left\| (\mathbf{U}_k \mathbf{\Lambda}_k^{\frac{1}{2}})^H \mathbf{V}_g \right\|_F^2. \tag{5.18}$$

We can see that the proposed likelihood metric uses the projection of the eigenspaces of the users to that of the group centers, so that users can be readily separated into different groups. For instance, if user k is very close to group center g, or $\mathbf{U}_k \approx \mathbf{V}_g$, then $\mathbf{U}_k^H \mathbf{V}_g$ would result in a large value due to the property of unitary matrix. If $\mathbf{U}_k$ is much different from $\mathbf{V}_g$, then $\mathbf{U}_k^H \mathbf{V}_g$ would produce a very small value due to the orthogonality of unitary matrices. The weighted likelihood also takes into account the weights of different eigenmodes so that the user's group is mainly determined by the dominant eigenmodes.

Given $L(\mathbf{R}_k, \mathbf{V}_g)$ for each user and each group, we assign each user to the group with maximum likelihood and update group center by

$$\mathbf{V}_g = \Upsilon\Big\{ \frac{1}{|S_g|} \sum_{k \in S_g} \mathbf{R}_k \Big\}. \tag{5.19}$$

Notice that the updates of the group center and the total likelihood L_{tot} also consider the weights of eigenmodes in the proposed algorithm. The reason is that if a group has only one user, the group center should be the user itself. So considering the weight of different eigenmodes should help to enhance the system throughput.

With the weighted likelihood similarity measure, we now propose an improved K-means clustering algorithm, which is described in Algorithm 1. Note that in Algorithm 1, $\mathbf{U}_{\pi(g)}$ is the

Algorithm 1: Improved K-means Clustering Algorithm with Weighted Likelihood Similarity Measure

Set $n = 0$, $L_{tot}^{(0)} = 1$; Randomly choose G different indices (denoted as $\pi(g), \forall g$) from the set $\{1, \ldots, K\}$ and set $\mathbf{V}_g^{(n)} = \mathbf{U}_{\pi(g)}, \forall g$;
$n = 1$, $L_{tot}^{(n)} = 0$;
while $\left| L_{tot}^{(n)} - L_{tot}^{(n-1)} \right| > \epsilon L_{tot}^{(n-1)}$ **do**
    Let $\mathcal{S}_g^{(n)} = \emptyset$, $g = 1, \cdots, G$;
    for $k = 1, \ldots, K$ **do**
        for $g = 1, \ldots, G$ **do**
            Compute $L(\mathbf{R}_k, \mathbf{V}_g^{(n-1)}) = \left\| (\mathbf{U}_k \mathbf{\Lambda}_k^{\frac{1}{2}})^H \mathbf{V}_g^{(n-1)} \right\|_F^2$
        end
        Find $g_k^* = \arg\max_{g'} L(\mathbf{R}_k, \mathbf{V}_{g'}^{(n-1)})$ and let $\mathcal{S}_{g_k^*}^{(n)} = \mathcal{S}_{g_k^*}^{(n)} \cup \{k\}$;
    end
    for $g = 1, \ldots, G$ **do**
        $\mathbf{V}_g^{(n)} = \Upsilon \left\{ \frac{1}{\left| \mathcal{S}_g^{(n)} \right|} \sum_{k \in \mathcal{S}_g^{(n)}} \mathbf{R}_k \right\}$;
    end
    Compute $L_{tot}^{(n)} = \sum_{g=1}^{G} \sum_{k \in \mathcal{S}_g^{(n)}} L(\mathbf{R}_k, \mathbf{V}_g^{(n)})$
    $n = n + 1$;
end
Assign $\mathbf{V}_g = \mathbf{V}_g^{(n)}$ and $\mathcal{S}_g = \mathcal{S}_g^{(n)}$.

unitary matrix of the user with index $\pi(g)$ and ϵ is a small number to control the convergence of the algorithm.

5.4.3 Subspace Projection Based Similarity Measure

We now present another similarity measure, which is based on subspace projection, given by

$$\mathcal{P}(\mathbf{U}_k, \mathbf{V}_g) = \left\| \mathbf{V}_g \mathbf{V}_g^H \mathbf{U}_k - \mathbf{U}_k \right\|_F^2 . \tag{5.20}$$

We can see from the above equation that we measure the similarity between user k and group g by firstly projecting user k to group g, then calculating the distance between user k and its projection on group g. If user k is the group center or in close proximity to the group center, $\mathcal{P}(\mathbf{U}_k, \mathbf{V}_g)$ would be zero.

5.4.4 Fubini Study Based Similarity Measure

One last similarity measure we consider is Fubini-Study (FS) Based Similarity Measure. The classic FS distance is given by

$$\mathcal{F}_S(\mathbf{U}_k, \mathbf{V}_g) = \arccos \left| \det \left(\mathbf{U}_k^H \mathbf{V}_g \right) \right|. \tag{5.21}$$

We can see that if user k is close to the group center g, then $\mathcal{F}(\mathbf{U}_k, \mathbf{V}_g)$ would be close to 0. Otherwise, $\mathcal{F}(\mathbf{U}_k, \mathbf{V}_g)$ would be larger if the user is farther from the group center. The FS distance can then be another choice of the similarity measure for the user grouping.

5.4.5 Hierarchical User Grouping

We now propose a new user grouping scheme employing the agglomerative hierarchical clustering method. Different from the K-means method, which essentially looks at all possible combinations of users and groups, the agglomerative hierarchical clustering method starts with each individual user forming a user group, then proceeds by a series of successive mergers based on certain criteria. Eventually, all users can form one single group. We can terminate the iterations when the desired number of groups is reached.

An example of agglomerative hierarchical clustering method is illustrated in Fig. 5.2. Initially, there are 20 users and thus 20 groups. The distance between any two users (or two initial groups) is calculated. At the first iteration, we find that the distance between user 2 and 9 is the smallest. So user 2 and 9 are merged to a group as shown in Fig. 5.2. At the second iteration, the distance between user 4 and 15 is found to be the smallest. So user 4 and 15 are merged as group. We iterate such group merging process until the desired number of groups is reached.

One may notice in the example above, at one intermediate step, group comprised of user 1 and 20 is found to be close to the group comprised of user 2, 9 and 19. So one important issue in hierarchical clustering is how to define the similarity measure or distance between existing groups and newly defined groups (or called linkage methods). Typical linkage methods include: single

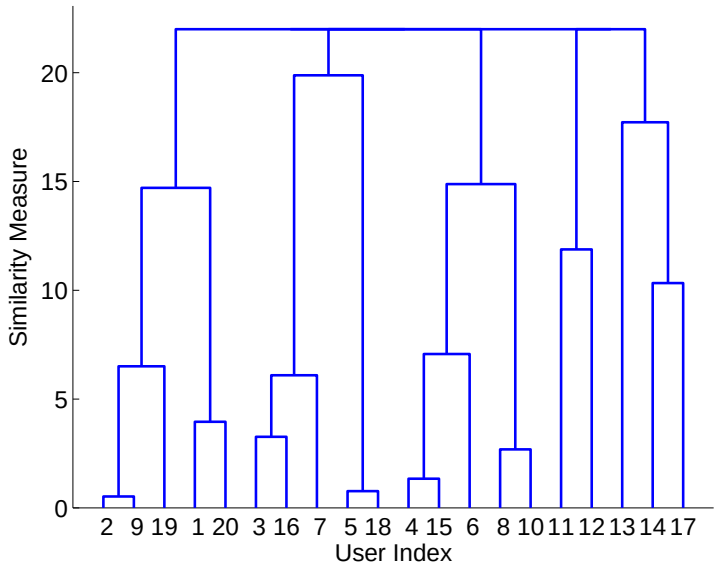

Figure 5.2: Hierarchical clustering illustration.

linkage, complete linkage, average linkage, ward linkage, median linkage, and weighted average linkage, which are explained as follows.

Since we only merge two groups at each step, we give the definition of linkage methods in an inductive manner. Suppose we have merged group v_i and v_j to get a new group $(v_i v_j) \triangleq v_i \bigcup v_j$. Now we need to define the distance between the remaining groups and the new group $(v_i v_j)$. Let group v_q be one of the remaining groups. The distance between $(v_i v_j)$ and v_q given by single linkage method is

$$d_{(v_i v_j),v_q} \triangleq \min\left\{d_{v_i,v_q}, d_{v_j,v_q}\right\}. \tag{5.22}$$

That means the distance between group $(v_i v_j)$ and v_q is the minimum of the two distances d_{v_i,v_q} and d_{v_j,v_q}, where distance d_{v_i,v_q} and d_{v_j,v_q} have been previously calculated in the same way.

Complete linkage defines the distance between $(v_i v_j)$ and v_q as the maximum of the two distances d_{v_i,v_q} and d_{v_j,v_q}, given by

$$d_{(v_i v_j),v_q} \triangleq \max\left\{d_{v_i,v_q}, d_{v_j,v_q}\right\}. \tag{5.23}$$

Algorithm 2: Hierarchical Clustering Algorithm

Set the value G. Start from the initial user set $\mathcal{U} = \{1, 2, \ldots, K\}$. Each user forms a group, i.e., $v_q = \{q\}$, $q = 1, \cdots, K$.
for $k = 1, \ldots, K$ **do**
  for $k' = 1, \ldots, K$ **do**
    Calculate pair-wise similarity between users (or groups) using (5.16) or (5.18).
  end
end
while *The number of groups is greater than* G **do**
  Search for and merge the groups with maximal similarity.
  Calculate the pair-wise distance between user (or group) and updated group using one of the linkage methods (5.22)-(5.27).
end

Average linkage defines the distance between $(v_i v_j)$ and v_q as the average of all the pair-wise distances, given by

$$d_{v_i v_j, v_q} = \frac{|v_i|\, d_{v_i, v_q} + |v_j|\, d_{v_j, v_q}}{|(v_i v_j)|}. \tag{5.24}$$

Ward linkage defines the distance between $(v_i v_j)$ and v_q as

$$d_{(v_i v_j), v_q} \triangleq \frac{(|v_i| + |v_q|) d_{v_i, v_q} + (|v_j| + |v_q|) d_{v_j, v_q} - |v_q|\, d_{v_i, v_j}}{|v_i| + |v_j| + |v_q|}. \tag{5.25}$$

Median linkage defines the distance between $(v_i v_j)$ and v_q as

$$d_{(v_i v_j), v_q} \triangleq \frac{1}{2} d_{v_i, v_q} + \frac{1}{2} d_{v_j, v_q} - \frac{1}{4} d_{v_i, v_j}. \tag{5.26}$$

Weighted average linkage defines the distance between $(v_i v_j)$ and v_q as:

$$d_{(v_i v_j), v_q} \triangleq \frac{1}{2} d_{v_i, v_q} + \frac{1}{2} d_{v_j, v_q}. \tag{5.27}$$

Given these definitions, we propose our hierarchical clustering algorithm shown in Algorithm 2.

Next we present the complexity analysis for K-means clustering and hierarchical clustering methods. Note that the framework of K-means is essentially similar to Algorithm 1.

Denote the complexity of computing similarities for all user-group (or group-group) pairs as $C_{s-kmean}$ for K-means clustering and C_{s-hier} for hierarchical clustering; searching for the maximal similarity pair and pairing them up as $C_{m-kmean}$ for K-means clustering and C_{m-hier} for hierarchical clustering; and updating grouping center as $C_{u-kmean}$ for K-means clustering and C_{u-hier} for hierarchical clustering.

Proposition 1. *The complexity of K-means clustering is $\mathcal{O}(G^K C_{s-kmean})$. More specifically, it is $\mathcal{O}(KG\times(2M^3+M^2))$ for K-means clustering with chordal distance and $\mathcal{O}(KG\times[(r^*)^3+(Mr^*)^2])$ for K-means clustering with weighted likelihood similarity measure, where r^* is effective rank for $\mathbf{R}_k$, i.e. number of columns for $\mathbf{U}_k$.*

Proof. Each iteration of K-means algorithm can be divided into 3 consecutive steps:

1. Calculating $K \times G$ similarities;
2. Searching for the maximum similarity for each user;
3. Updating group center for each group.

So during each iteration of K-means algorithm, it takes the total of $\{C_{s-kmean}, C_{m-kmean}, C_{u-kmean}\}$ computations, where the one with the highest order determines the complexity of the whole algorithm. The complexity of the first step depends on the choice of similarity measure. For (5.16), the complexity is $\mathcal{O}(KG \times (2M^3 + M^2))$; while for (5.18), the complexity is $\mathcal{O}(KG \times [(r^*)^3 + (Mr^*)^2])$. The second step involves selecting maximum element from a size G array for each user. So the complexity is $\mathcal{O}(KG)$. The complexity of the third step also depends on the specific scheme. For (5.17), it requires $\Theta(KM^3)$ computations. For (5.19), it only needs $\Theta(KM^2)$ computations. Thus, the one with the highest complexity order is $C_{s-kmean}$ for each iteration.

Since there are K users and G groups, in the worst case, it could take G^K iterations for the algorithm to converge. Therefore, for the worst case analysis, the computational complexity of K-means clustering algorithm is $G^K\mathcal{O}(C_{s-kmean})$.

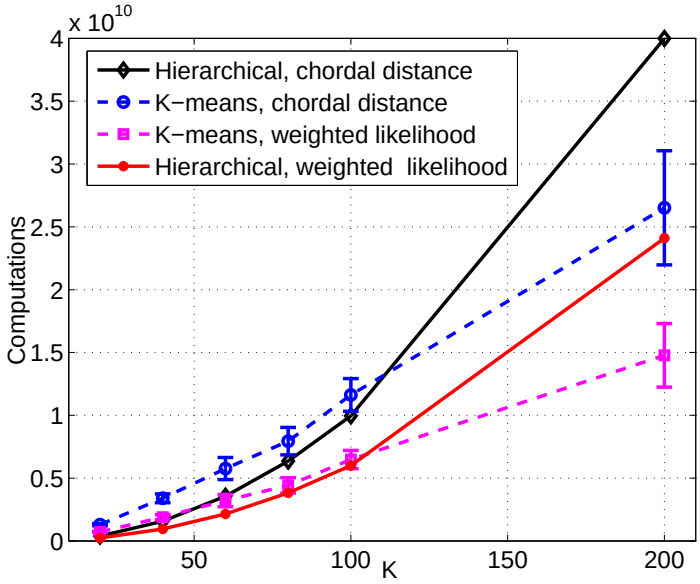

Figure 5.3: Complexity comparison.

□

For Algorithm 2 we have the following proposition.

Proposition 2. *The complexity of hierarchical clustering is* $\mathcal{O}(C_{s-hier})$. *More specifically, it is* $\mathcal{O}(\frac{K(K-1)}{2}(2M^3+M^2))$ *for hierarchical clustering with chordal distance and* $\mathcal{O}(\frac{K(K-1)}{2}[(r^*)^3+(Mr^*)^2])$ *for hierarchical clustering with weighted likelihood similarity measure.*

Proof. Algorithm 2 firstly calculates $K(K-1)/2$ similarities, resulting in the complexity of $\mathcal{O}(\frac{K(K-1)}{2}(2M^3+M^2))$ or $\mathcal{O}(\frac{K(K-1)}{2}[(r^*)^3+(Mr^*)^2])$.

The 'while' loop at step 7 will be executed $(K-G-1)$ times. The total cost for step 8 is $K+(K-1)+\ldots+2=(K+2)(K-1)/2$, and for step 9 the worse-case total cost is $(K-2)+(K-3)+\ldots+1+0=(K-2)(K-1)/2$. Note that in step 9, there are additional constant costs $\mathcal{O}(1)$ for linkage updating. For instance, for weighted average the constant is 2 (one addition and one division). Constant is dropped for big $\mathcal{O}$ complexity analysis.

Therefore, the complexity of Algorithm 2 is dominated by $\mathcal{O}(C_{s-hier})$. □

Table 5.1 is a summary of the complexity comparison. We can see that complexity relationships depend on the number of users K, the number of antennas M, the effective rank r^*, and

Table 5.1: Complexity Comparison of Clustering Schemes

	Chordal Distance	*Weighted Likelihood*
K-means	$\mathcal{O}(KG \times (2M^3 + M^2))$	$\mathcal{O}(KG \times [(r^*)^3 + (Mr^*)^2])$
Hierarchical	$\mathcal{O}(\frac{K(K-1)}{2}(2M^3 + M^2))$	$\mathcal{O}(\frac{K(K-1)}{2}[(r^*)^3 + (Mr^*)^2])$

the choice of number of groups G. If K is relatively small and G is relatively large, hierarchical clustering is much more computationally efficient. However, if K is much large and G is small, K-means clustering may be more computationally efficient. Figure 5.3 presents the complexity comparison for an example case. In this simulation, we let $M = 100$, $G = 6$, and $r^* = 11$.

Clearly there are two advantages of hierarchical clustering compared with K-means clustering.

- Hierarchical clustering does not rely on the initial choices of group center. For example, given the users' distributions, K-means clustering may end up with user groups shown in Fig. 5.4. We can see that there are several crossing lines for different groups, which suggests possibly inappropriate user grouping. On the contrary, Fig. 5.5 shows the grouping results obtained by hierarchical clustering, which is clearly a better grouping configuration. This advantage is especially true when the number of users is small.

- According to Propositions 1 and 2, hierarchical clustering is generally more computationally efficient when the number of users is less than or equal to 100.

5.4.6 K-medoids User Grouping

We also consider K-medoids clustering method. K-medoids clustering is similar to K-means clustering. The difference lies in the approach of updating group center. While K-means uses the average of the group members (or called centroids), K-medoids tries every group member (medoids) as the group center and uses the one which has the least within group residue sum of squares (WGRSS). The user grouping algorithm based on the K-medoids clustering method is described in Algorithm 3. Due to exhaustive search of group centers, the computational complexity of K-medoids is lower bounded by the complexity of K-means, and hence comparably high.

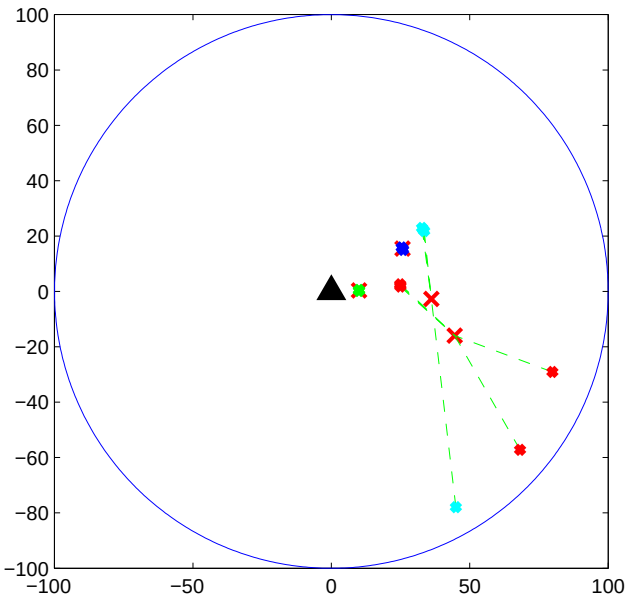

Figure 5.4: User Grouping with K-means Clustering.

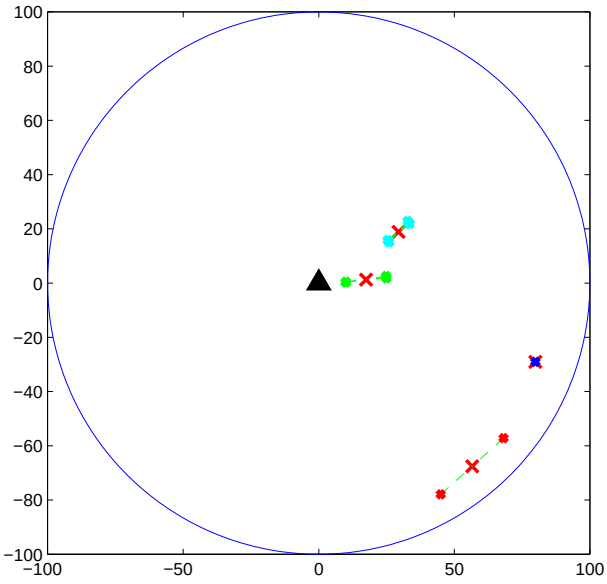

Figure 5.5: User grouping with Hierarchical Clustering.

5.5 User Scheduling in Massive MIMO System

After forming the user groups, we can obtain the prebeamforming matrix $\mathbf{B}_g, \forall g$. At a particular time slot, based on the instantaneous channel conditions of the users, we dynamically schedule a subset of users in each group for the transmissions in this time slot.

Algorithm 3: K-medoids Clustering Algorithm

Set $n = 0$, $L_{tot}^{(0)} = 1$; Randomly choose G different indices (denoted as $\pi(g), \forall g$) from the set $\{1, \ldots, K\}$ and set $\mathbf{V}_g^{(n)} = \mathbf{U}_{\pi(g)}, \forall g$;
$n = 1$, $L_{tot}^{(n)} = 0$;
while $\left| L_{tot}^{(n)} - L_{tot}^{(n-1)} \right| > \epsilon L_{tot}^{(n-1)}$ **do**
    Let $\mathcal{S}_g^{(n)} = \emptyset$, $g = 1, \cdots, G$;
    for $k = 1, \ldots, K$ **do**
        for $g = 1, \ldots, G$ **do**
            Compute similarity measure using (5.16) or (5.18)
        end
        Find $g_k^* = \arg\max_{g'} L(\mathbf{R}_k, \mathbf{V}_{g'}^{(n-1)})$, or $g_k^* = \arg\min_{g'} d_c(\mathbf{U}_k, \mathbf{V}_{g'}^{(n-1)})$ and let $\mathcal{S}_{g_k^*}^{(n)} = \mathcal{S}_{g_k^*}^{(n)} \cup \{k\}$;
    end
    for $g = 1, \ldots, G$ **do**
        for $k \in \mathcal{S}_g^{(n)}$ **do**
            Compute $WGRSS(g)_k^{(n)} = \sum_{k \in \mathcal{S}_g^{(n)}} L(\mathbf{R}_k, \mathbf{R}_{k'})$ or $WGRSS(g)_k^{(n)} = \sum_{k \in \mathcal{S}_g^{(n)}} d_c(\mathbf{U}_k, \mathbf{U}_{k'})$
        end
        Find $k^* = \arg\max_k WGRSS(g)_k^{(n)}$, let $\mathbf{V}_g^{(n)} = \mathbf{U}_k$
    end
    Compute $L_{tot}^{(n)} = \sum_{g=1}^{G} WGRSS(g)_{k^*}^{(n)}$
    $n = n + 1$;
end
Assign $\mathbf{V}_g = \mathbf{V}_g^{(n)}$ and $\mathcal{S}_g = \mathcal{S}_g^{(n)}$.

In [67], a MAX and an ALL user scheduling algorithm are presented. The MAX user scheduling is the scheduling based on only the feedback of beam index with max SINR, while the ALL user scheduling is based on the user's feedback of all beamforming SINRs, i.e., SINR for every beam selection. The SINR can be computed as

$$SINR_{g_k,m} = \frac{\left| h_{g_k}^H b_{g_m} \right|^2}{\frac{1}{\rho} + \sum_{n \neq m} \left| h_{g_k}^H b_{g_n} \right|^2 + \sum_{g' \neq g} \left\| h_{g_k}^H B_{g'} \right\|^2} \tag{5.28}$$

Different from this approach, we propose a dynamic user scheduling algorithm which schedules users in a greedy manner. In particular, at each step, the proposed algorithm only schedules

the user which results in the largest system throughput improvement. The proposed method is summarized in Algorithm 4.

Given the user grouping and scheduling, we can calculate the instantaneous SINR, γ_{g_k}, for user k in group g as

$$\begin{aligned}\gamma_{g_k} &= \frac{\frac{p}{\sum_g S_g}\zeta_g^2 \left|\mathbf{h}_{g_k}^H \mathbf{B}_g \mathbf{P}_g(:, g_k)\right|^2}{1 + I_{in}(g,k) + I_{it}(g,k)}, \\ I_{in}(g,k) &= \frac{p}{\sum_g S_g}\zeta_g^2 \sum_{j \neq k} \left|\mathbf{h}_{g_k}^H \mathbf{B}_g \mathbf{P}_g(:, g_j)\right|^2, \\ I_{it}(g,k) &= \frac{p}{\sum_g S_g} \sum_{g' \neq g} \zeta_{g'}^2 \sum_{j} \left|\mathbf{h}_{g_k}^H \mathbf{B}_{g'} \mathbf{P}_{g'}(:, g_j)\right|^2. \end{aligned} \tag{5.29}$$

where I_{in} denotes the inner group interferences, I_{it} denotes the inter group interferences, $\mathbf{P}_g(:, g_k)$ denotes the submatrix containing all the rows and the g_k-th column of $\mathbf{P}_g$ and ζ_g^2 is the scaling factor for satisfying certain power constraint, which can be obtained as

$$\zeta_g^2 = \frac{S_g}{\text{tr}(\mathbf{P}_g^H \mathbf{B}_g^H \mathbf{B}_g \mathbf{P}_g)}. \tag{5.30}$$

Then the rate for the scheduled user g_k is given by

$$\eta_{g_k} = \log_2(1 + \gamma_{g_k}). \tag{5.31}$$

System throughput r_{ws} is obtained as $r_{ws} = \sum_{g=1}^{G} \sum_{k \in \mathcal{K}_g} \eta_{g_k}$, where $\mathcal{K}_g$ is the scheduled user set in the gth group. Obviously, r_{ws} is a function of $\{\mathcal{K}_g\}$ and precoding for all co-scheduled users, denoted as $r_{ws}(\{\mathcal{K}_g\}, \{\mathbf{B}_g\}, \{\mathbf{P}_{g_k}\})$.

In the following part of this section, we present a lower bound of the proposed greedy algorithm for dynamic user selection.

Lemma 8. *In Algorithm 4, the first user scheduled results in largest rate increase.*

Proof. This is resulted from Step 11 of Algorithm 4 and the fact that the first user scheduled has the largest rate among all users without any interference. For each user scheduled in the subsequent

Algorithm 4: Greedy algorithm for dynamic user selection and beamforming with determined user grouping

User grouping $\{\mathcal{S}_g\}$ is given;
Initially set $\mathcal{U} = \{1, \ldots, K\}$, the weighted sum rate $r_{ws} = 0$ and $\mathcal{K}_g = \emptyset$ for $g = 1, \ldots, G$;
while *Termination conditions ($\sum_g |\mathcal{K}_g| = \sum_g b_g$, $\kappa(k^*, g_{k^*}) = 0$, or $\mathcal{U} = \emptyset$) are not satisfied* **do**
    for $k \in \mathcal{U}$ **do**
        if $|\mathcal{K}_{g_k}| < S_g$ **then**
            Set $\mathcal{K}'_g = \mathcal{K}_g \cup \{k\}$ if $k \in \mathcal{S}_g$, and $\mathcal{K}'_{g'} = \mathcal{K}_{g'}, \forall g' \neq g$;
            Perform ZFBF or RZFBF based on $\{\mathcal{K}'_g\}$ and $\{\mathbf{B}_g\}$;
            Compute the gain $\kappa(k, g) = \max\left\{0, r_{ws}(\{\mathcal{K}'_g\}, \{\mathbf{B}_g\}) - r_{ws}(\{\mathcal{K}_g\}, \{\mathbf{B}_g\})\right\}$;
        end
    end
    Obtain $(k^*, g_{k^*}) = \arg\max_{k \in \mathcal{U}} \kappa(k, g)$;
    if $(k^*, g_{k^*}) > 0$ **then**
        Let $\mathcal{U} \leftarrow \mathcal{U} \backslash k^*$;
        Let $\mathcal{K}_{g_{k^*}} \leftarrow \mathcal{K}_{g_{k^*}} \cup \{k^*\}$;
    end
end

iterations, the resulting user rate is always smaller than the user rate evaluated in the first iteration due to the intra- and inter-group interference from the users already scheduled and power splitting among scheduled users. Therefore the rate increase in all other iterations is smaller that that of the first iteration. □

Denote the achievable rate of the first scheduled user as $\mathcal{Z}_1$, the system sum rate of Algorithm 4 as x, and the system sum rate of the optimal user scheduling as $\mathcal{X}$. We have the following lemma.

Lemma 9. $\mathcal{Z}_1 \leq x \leq |\mathcal{U}|\, \mathcal{Z}_1$.

Proof. $\mathcal{Z}_1 \leq x$ is trivial, since Algorithm 4 would schedule at least one user. Since there are $|\mathcal{U}|$ users, from Lemma 8 we know that the achievable rates of them are all upper bounded by $\mathcal{Z}_1$, $x \leq |\mathcal{U}|\, \mathcal{Z}_1$ thus holds. □

Using similar arguments as the proof of Lemma 8, we can show that the following lemma holds.

Lemma 10. $\mathcal{X} \leq |\mathcal{U}|\, \mathcal{Z}_1$.

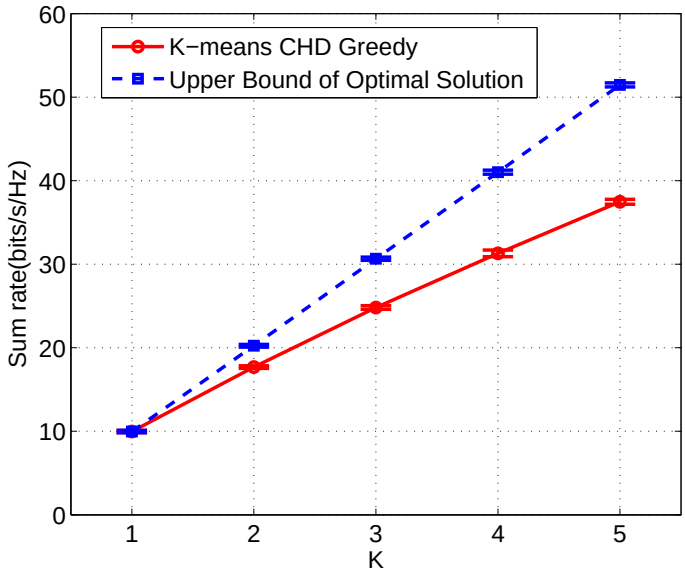

Figure 5.6: Greedy algorithm and the Optimal Scheduling Algorithm's Upper Bound.

From Lemma 9 and Lemma 10 we have $\frac{\mathcal{X}}{|\mathcal{U}|} \leq \mathcal{Z}_1 \leq x \leq |\mathcal{U}|\,\mathcal{Z}_1$. So we have the following Theorem.

Theorem 5.1. *The greedy algorithm for dynamic user selection can achieve an objective value which is at least* $\frac{1}{|\mathcal{U}|}$ *of the optimal user selection solution.*

Lemma 10 and Theorem 5.1 not only give the lower and upper bounds of the greedy algorithm, but also the optimal user scheduling scheme. Fig. 5.6 illustrates this bound of the optimal scheme. For obvious reason, we let $G = 1$ here. We can see that when the number of users is not large, our greedy user scheduling algorithm approaches the upper bound of the optimal user scheduling. Note that as the number of users increases, the bound becomes looser.

5.6 User grouping with joint group load balancing and precoding design

When the number of users is not too large, with the previously discussed grouping approaches, some groups may end up with few users while some others may be overcrowded with users. This situation clearly wastes the precious spectrum resources and affects the user fairness. We now form a user grouping method considering group load balancing and user proportional fairness. The user

grouping with proportional fairness can be summarized as the following optimization problem.

$$\begin{aligned} \max_{x_{kg}} \quad & \mathcal{J} = \sum_{k=1}^{K} \sum_{g=1}^{G} x_{kg} \log(\frac{\overline{\eta}_{g_k}}{\sum_i x_{ig}}) \\ s.t. \quad & \sum_g x_{kg} = 1, \ \forall k \in [1, K], \end{aligned} \tag{5.32}$$

where $\mathcal{J}$ denotes the utility to optimize, $\overline{\eta}_{g_k}$ is the average user throughput, i.e., $\overline{\eta}_{g_k} = \log_2(1+\overline{\gamma}_{g_k})$, $\overline{\gamma}_{g_k}$ is the average SINR when user k is assigned to group g, and x_{kg} is the assignment indicator defined as

$$x_{kg} = \begin{cases} 1, & \text{if user } k \text{ is in group } g, \forall k, g; \\ 0, & \text{otherwise.} \end{cases} \tag{5.33}$$

Given constraint (5.33), we can see that the optimization problem (5.32) is combinatorial in nature. If we apply exhaustive search for this problem, the complexity is $\Theta(G^K)$. That means even for a 100 GHz CPU[1], it needs more than 84 days[2] to solve this optimization problem with just 6 groups and 20 users, which is obviously not an option for nowadays cellular system.

To make the problem tractable, we relax the variable x_{kg} to be a real number in the range of $[0, 1]$. So the optimization problem (5.32) can be rewritten as follows.

$$\begin{aligned} \max_{x_{kg}} \quad & \mathcal{J} = \sum_{k=1}^{K} \sum_{g=1}^{G} x_{kg} \log(\frac{\overline{\eta}_{g_k}}{\sum_i x_{ig}}) \\ s.t. \quad & \sum_g x_{kg} = 1, \ \forall k \in [1, K] \\ & 0 \leq x_{kg} \leq 1, \ \forall k \in [1, K], \ g \in [1, G]. \end{aligned} \tag{5.34}$$

And we have the following Proposition.

[1]Typical base station processor has lower frequency than 100 GHz. For instance, TCI6616from TI can deliver up to 4.8 GHz processing. http://www.ti.com/lit/ml/sprt579/sprt579.pdf

[2]Given that modern processor typically needs about 200 clock cycles to execute one computation step, a CPU of 100 GHz (i.e. 10^{11} clock cycles per second), can carry out 5×10^8 computation steps each second. So it needs $6^{20}/(5 * 10^8)/86400 = 84.6333$ days to solve this problem.

Proposition 3. *Even if we solve the optimization problem by relaxing the constraints, the optimal user associations do not change.*

Proof. Since we relax the variables from binary to real, the solutions to problem (5.34) actually upper bound the problem of (5.32). However we can see from Algorithm 6 that the solutions to problem (5.34) are integers other than fractions. So the solutions to problem (5.32) can be chosen exactly the same as the solutions to problem (5.34). Since the solutions to problem (5.32) cannot result in higher utility than the solutions to problem (5.34), the solutions to problem (5.34) are the solutions to problem (5.32) as well. Thus, even though the constraints are relaxed, the optimal user associations do not change. □

We also have the following Proposition for the optimization.

Proposition 4. *Problem (5.34) is a convex optimization problem.*

Proof. The objective function of problem (5.34) can be represented as $\sum_k \sum_g x_{kg} \log(\overline{\eta}_{g_k}) - \sum_k \sum_g x_{kg} \log(\sum_i x_{ig})$. The first term is affine. The second term is basically two concatenated sums of $x \log(x+a)$, where $0 \leq a \leq (K-1)$. The second derivative of $x \log(x+a)$ is $\frac{1}{x+a} + \frac{a}{(x+a)^2}$, which is positive for $0 \leq a \leq (K-1)$. So $x \log(x+a)$ is a convex function and $-\sum_k \sum_g x_{kg} \log(\sum_i x_{ig})$ is concave due to negative sums. Therefore $\sum_k \sum_g x_{kg} \log(\overline{\eta}_{g_k}) - \sum_k \sum_g x_{kg} \log(\sum_i x_{ig})$ is concave. □

Given Proposition 4, we could apply sophisticated convex optimization techniques to solve problem (5.34). However, we can see that one of the important issues is to obtain the average SINR $\overline{\gamma}_{g_k}$. The challenge is without user grouping and scheduling information, we cannot calculate the exact SINR of each user. Moreover, over different time slots, different users will be scheduled based on the user grouping and the instantaneous channels. Thus, in order to solve (5.32), we need to find a way to approximate average SINR for each user in each group. Here we propose to approximate the average SINR based on following assumptions.

(i) We assume conjugate precoding [76] [77] for the target user.

(ii) There are no intra-group co-scheduled users.

(iii) Identity precoding for inter-group co-scheduled users is assumed.

We can obtain the SINR approximation as

$$\overline{\gamma}_{g_k} = \frac{\frac{p}{\sum_g b_g} \left| tr(\mathbf{B}_g^H \mathbf{R}_{g_k} \mathbf{B}_g) \right|}{1 + \frac{p}{\sum_g b_g} \sum_{g' \neq g} \left| tr(\mathbf{B}_{g'}^H \mathbf{R}_{g_k} \mathbf{B}_{g'}) \right|}. \tag{5.35}$$

Due to the dynamic nature of the user scheduling and the objective of user group assignment itself, it is difficult to obtain the average SINR presuming the multiuser MIMO scheduling. However, as in [78], when we consider the load balancing problem, it is reasonable to consider the single user resource allocation with user average SNR for the targeted cell. Therefore in our case, when we compute the average SINR for a user, we assume in an instantaneous time slot, only the user of interest is scheduled in its group. Moreover, we treat other groups as the virtual neighboring cells and consider the identity precoding matrix for the interfering groups, which is a fairly good approximation for the interference. With these assumptions, we assume the best resource allocation for each user with average interference assumption, which we think is appropriate for studying the user load balancing among groups. Otherwise it would be very difficult to approximate the average intra-group and inter-group interferences.

After obtaining average SINR, similar to [78], the procedures to solve the user grouping optimization problem with load balancing in (5.32) are presented in Algorithm 6.

5.7 Simulation

More numerical simulations are performed to evaluate the proposed schemes. System configurations are provided in Table 5.2. In particular, we consider a 120° sector. For each user drop, the azimuth angle θ_k, angle spread Δ_k and distance s_k for user k are randomly generated within the interval $[\theta_{\min}, \theta_{\max}]$, $[\Delta_{\min}, \Delta_{\max}]$ and $[s_{\min}, s_{\max}]$, respectively. We average over 100 user drops for the whole simulation. In each user drop, we evaluate the performance with 200 channel realizations. We fix the number of groups $G = 6$. For the antenna configuration, we consider the ULA

Algorithm 5: User grouping with joint group load balancing and precoding design algorithm

Perform K-means Clustering Algorithm or Algorithm 1 to obtain user group ID x_{ij}.
while $\mathcal{J}^{*(n-1)} - \mathcal{J}^{*(n-2)} > \epsilon \mathcal{J}^{*(n-2)}$ **do**
  for $g \in G$ **do**
    Find $\mathbf{V}_g^{*(n)}$ using (5.17) or the proposed weighted likelihood (5.19)
  end
  for $g \in G$ **do**
    Find $\mathbf{B}_g$ using approximate BD approach
  end
  for $k = 1, \ldots, K$ **do**
    for $g = 1, \ldots, G$ **do**
      Find γ_{g_k} using (5.35)
    end
  end
  Optimize (5.32) using Algorithm 6 ;
  Update x_{ij} and $\mathcal{J}^{*(n)}$;
end

Algorithm 6: Optimization Algorithm for (5.32)

$n = 0$, $\mu^{(1)} = 0$;
while *the optimization has not converged* **do**
  $n \leftarrow n + 1$;
  for $k = 1, \ldots, K$ **do**
    for $g = 1, \ldots, G$ **do**
      Compute $\overline{\gamma}_{g_k}$ and $\overline{\eta}_{g_k}$;
    end
    Assign user k to group g^* where $g^* = \arg\max_g(\log(\overline{\eta}_{g_k}) - \mu_g^{(n)})$, and let $x_{kg^*}^{(n)} = 1$, $x_{kg}^{(n)} = 0$ for $g \neq g^*$;
  end
  for $g = 1, \ldots, G$ **do**
    Each group chooses a step size $\delta^{(n)}$ and computes $K_g^{(n+1)} = \min\{K, e^{(\mu_g^{(n)}-1)}\}$, $\mu_g^{(n+1)} = \mu_g^{(n)} - \delta^{(n)}(K_g^{(n)} - \sum_k x_{kg}^{(n)})$.
  end
end

case and place 100 antennas along the y-axis with spacing 0.5λ. So from (5.4), the (m, p)-th entry of the covariance matrix is given by

$$[\mathbf{R}]_{m,p} = \frac{1}{2\Delta} \int_{-\Delta}^{\Delta} e^{-j2\pi D(m-p)\sin(\alpha+\theta)} d\alpha. \tag{5.36}$$

Table 5.2: System Configuration in the Simulations

Parameter	*Value*	*Parameter*	*Value*
θ_{min}	$-60°$	M	100
θ_{max}	$60°$	D	0.5
Δ_{min}	$5°$	G	6
Δ_{max}	$15°$	r_g^*	11
s_{min}	20 (m)	ϵ	10^{-3}
s_{max}	100 (m)	p	10, 20 dB

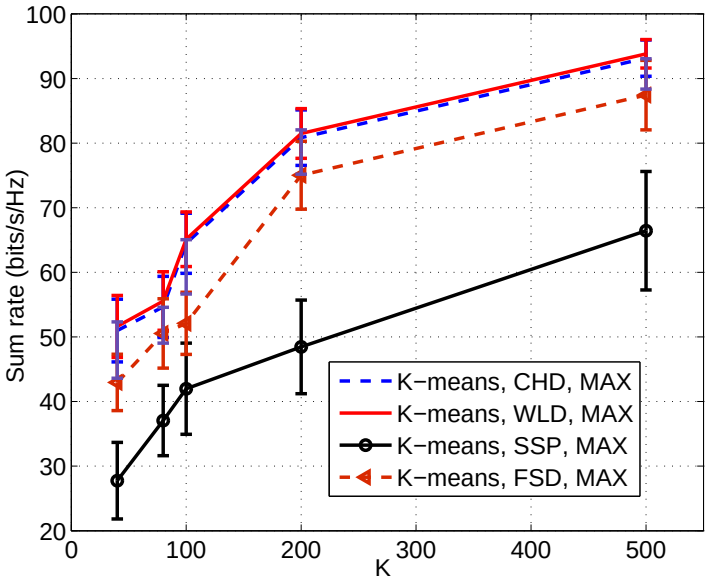

Figure 5.7: Similarity Measure Comparison.

Throughout the simulations, to find the first and second stage precoding matrices, we adopt the approximate BD approach and the regularized ZF precoding approach, respectively.

Fig. 5.7 gives a comparison of the similarity measures. For fair comparison, we use the same clustering method K-means and user scheduling method MAX. Note that CHD stands for chordal distance, which is (5.16); WLD stands for weighted likelihood, which is (5.18); SSP stands for subspace projection, which is (5.20); FSD represents Fubini Study distance, which is (5.21). We can see that WLD has slightly higher throughput than CHD, which verifies the effectiveness of our proposed scheme. However, the sum rates of EFS, FSD and SSP are lower than CHD. We thus abandon them.

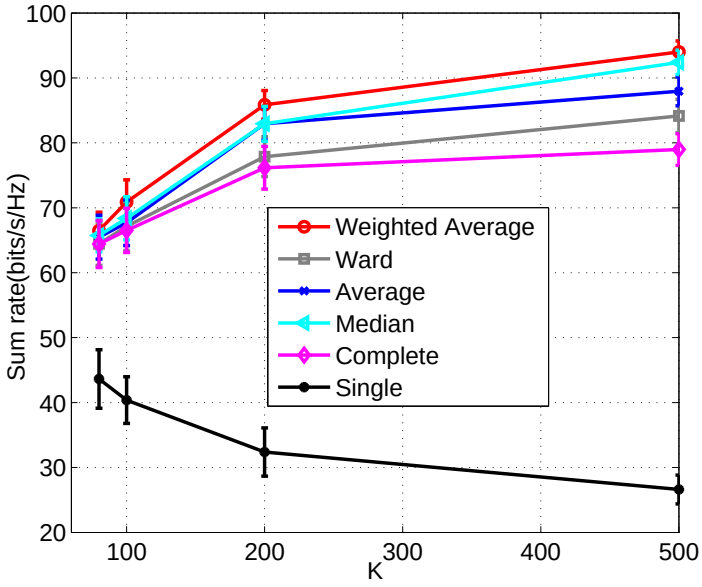

Figure 5.8: Comparison of Linkage Methods for Hierarchical Clustering.

Fig. 5.8 provides a comparison among the linkage methods for hierarchical clustering. For fair comparison, we use agglomerative hierarchical clustering, weighted likelihood similarity measure, and MAX user scheduling for all linkage methods. We can see that as the number of users increases, the sum rate of single linkage gradually drops. This is because that as the number of users increases, the volume of each cluster expands. Using the distance between the nearest points of two clusters to represent the distance between two clusters becomes inaccurate. We can also observe that weighted average linkage has the highest throughput. Carefully looking into the definition of weighted average linkage, we can see that weighted average linkage puts higher weights on the members who join the group late, which are less similar to other group members. For instance, we have group $1-5$. Group 1 and 2 are firstly merged to form group $\langle 1,2\rangle$. Then group $\langle 1,2\rangle$ and group 3 are merged to form group $\langle 12,3\rangle$. Now we need to find the distance between group $\langle 12,3\rangle$ and group 4. In light of (5.27), $d_{\langle 123\rangle,4} = \frac{1}{2}d_{\langle 12\rangle,4}+\frac{1}{2}d_{\langle 3\rangle,4} = \frac{1}{4}d_{\langle 1\rangle,4}+\frac{1}{4}d_{\langle 2\rangle,4}+\frac{1}{2}d_{\langle 3\rangle,4}$. Member 3 joins the group late and is less similar to other group members (that is why it joins the group late). Therefore, by putting higher weights on members who join the group late results in better performance in our scheme. We thus use weighted average linkage method for hierarchical clustering hereafter.

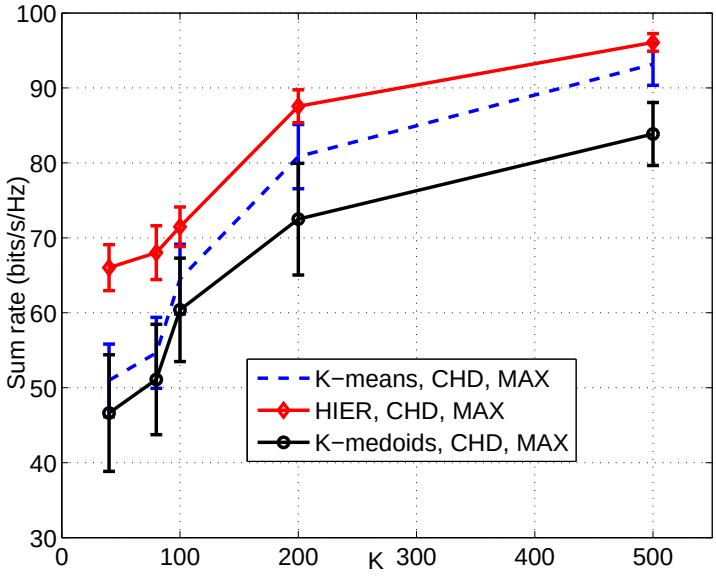

Figure 5.9: Clustering Method Comparison.

Fig. 5.9 presents a comparison among the clustering methods. For fair comparison, we use the same similarity measure CHD in (5.16) and MAX user scheduling. It can be observed that hierarchical clustering has the highest throughput, K-medoids clustering has the lowest throughput and K-means has a throughput lying in between. Due to high computational complexity and inferior performance, we abandon K-medoids clustering. However, the efficacy of agglomerative hierarchical clustering has been demonstrated. Moreover, hierarchical clustering also has the advantage of lower computational complexity, which has been shown in Fig. 5.3.

Fig. 5.10 compares the user scheduling schemes. Also for fair comparison, we use the same K-means clustering and CHD similarity measure. We readily observe that our proposed greedy algorithm has the highest throughput. Although the proposed greedy algorithm is suboptimal, it greatly enhances the system throughput. Note that since MAX has better performance than ALL, we only use MAX for comparison in later discussions.

Fig. 5.11 presents the sum rate comparison of our proposed effective schemes and the one in [67]. We can see that all the proposed schemes outperform the scheme in [67]. In particular, hierarchical clustering greedy user selection with weighted likelihood has the highest system throughput. Hierarchical clustering greedy user selection with chordal distance has slightly lower

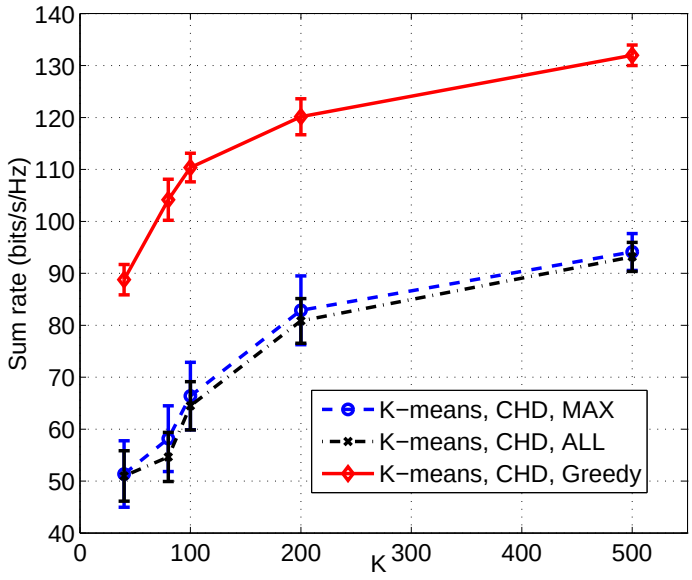

Figure 5.10: Scheduling Methods Comparison.

throughput than the highest one. Hierarchical clustering MAX user scheduling with weighted likelihood and K-means clustering greedy user selection with chordal distance both have higher throughput than the scheme in [67]. We could also observe that greedy user scheduling has greater impact than the user grouping methods on the system throughput. This is because no matter how the grouping is, greedy user scheduling has direct impact on the throughput and could always select the users who benefit the throughput most.

One last observation is that, as the number of users increases, for instance, $K = 500$, the gap between K-means and hierarchical clustering narrows. This is because with that many users, different grouping schemes tend to produce similar user grouping.

For user grouping with load balancing, we set $p = 20$ dB. Fig. 5.12 shows the resulting utility metric of the optimization in (5.32) which is solved by Algorithm 5. Note that negative values of utility are resulted from the $\log$ function of achievable rate over the number of group members. We can see that even the proposed scheme without iteration could greatly enhance the utility with user fairness compared with the scheme without considering load balancing. The proposed iterative load balancing scheme could achieve even higher utility.

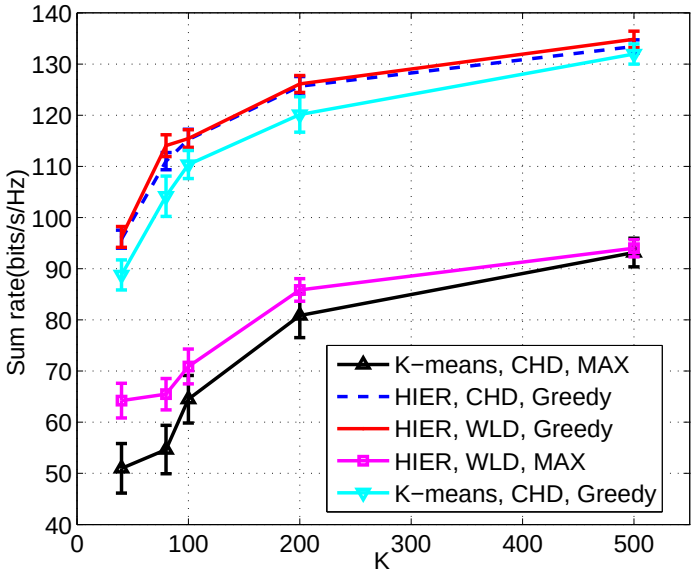

Figure 5.11: System sum rate Vs. number of users when $M = 100$.

Having looked at the utility comparison, we are also interested in the number of users in each group. Note that the average number of users in each group does not make sense, since in each iteration, the number of users in each group is random. Averaging over these random numbers is approximately K/G for every group. So we just look at one particular simulation, which is depicted in Fig. 5.13. Total number of user is $K = 40$. We can see that the number of users is $\{14, 3, 7, 10, 2, 4\}$ for group $1 - 6$ without considering load balancing. However the number of users is $\{11, 6, 7, 5, 4, 7\}$ for the non-iterative load balancing scheme and $\{8, 9, 7, 5, 5, 6\}$ for the load balancing scheme carried out iteratively. So the difference between the most loaded group and the least loaded group is 7 for the proposed non-iterative scheme, only 4 for the proposed iterative scheme, but 12 for the scheme without considering load balancing. Fig. 5.14 depicts the maximum difference of number of users among all groups. The number of groups G is prefixed to be 6. We can see that when $K = 10$, the maximum differences are 2.33, 2.11, and 1.93 for the scheme without load balancing, with load balancing but non-iterative, with load balancing and iterative, respectively. When $K = 40$, the numbers become 9.11, 4.24, and 3.56. When $K = 80$, the maximum differences are 15.62, 8.07, and 5.44. Therefore, the proposed scheme strikes a much better balance as the users are comparatively evenly distributed among all the groups.

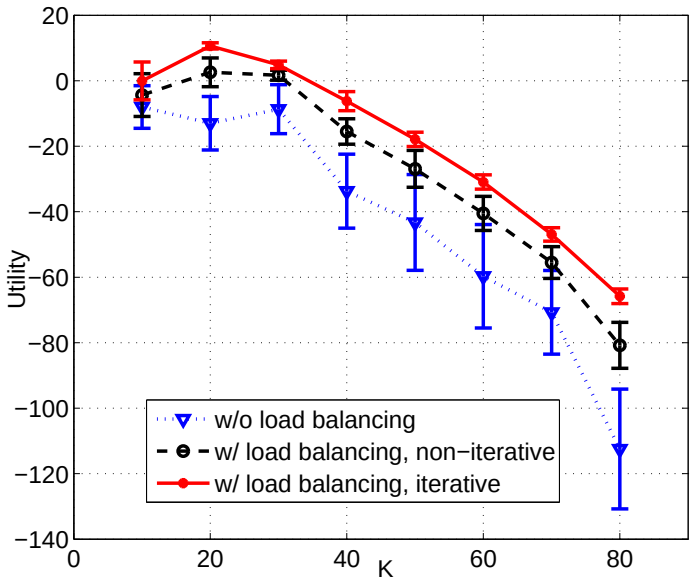

Figure 5.12: User grouping with joint group load balancing and precoding design when $M = 100$.

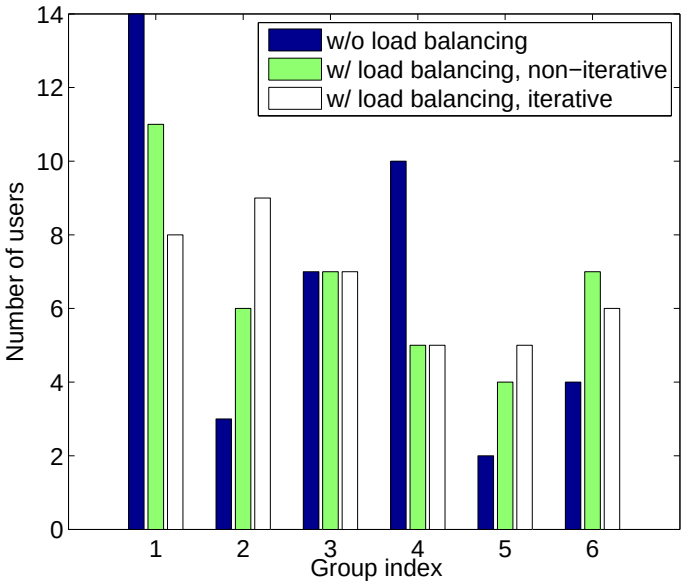

Figure 5.13: Number of group members Vs. Group.

5.8 Conclusions

In this chapter, based on a two-stage precoding framework for massive MIMO systems with FDD duplexing, we have studied the user grouping and scheduling problems. We have proposed weighted likelihood similarity measure, subspace projection based similarity measure, Fubini Study based similarity measure, hierarchical clustering, K-medoids clustering for user grouping.

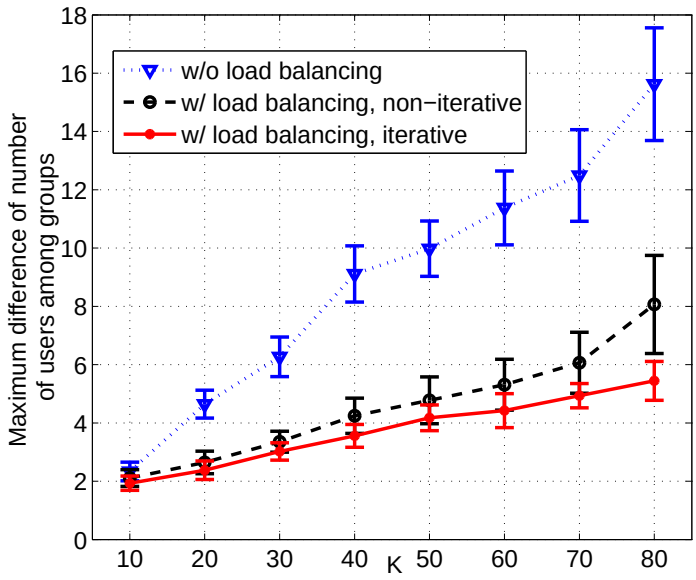

Figure 5.14: Maximum difference of number of users among groups Vs. Number of users.

We have also proposed a dynamic user scheduling scheme. Moreover, to achieve load balancing and user fairness for massive MIMO system with few users, we have proposed a user grouping algorithm considering loading balancing. All the theoretical analysis and simulation studies have demonstrated the efficacy of the proposed schemes.

Chapter 6

User Association in Massive MIMO with Small Cells

6.1 Introduction

MIMO (Multiple Input Multiple Ouput) has evolved from a pure theory to a practical technique over the last two decades, which has greatly enhanced the system capacity due to much more degrees of freedoms provided. However, due to the so-called "smartphone" revolution, wireless users demand higher and higher data rates for rich media applications. There have been tremendous efforts trying to cater for this demand. Based on MIMO and OFDM, LTE-Advanced targets at a peak rate of 1 Gbps, but the average rate is less than 100 Mbps. For the foreseeable future, with more and more video related data traffic [79], these rates can hardly be satisfactory for the data-hungry wireless users. To further boost up the data rate, two technologies have gained most attractions from both industry and academia.

The first one is called massive MIMO (a.k.a. large-scale MIMO, full-dimension MIMO, or hyper MIMO) [58] [59]. The idea of massive MIMO is to equip the base station (BS) with hundreds, thousands or even tens of thousands of antennas, hereby providing unprecedented level of degrees of freedom for wireless users. Demos of massive MIMO can be found in [60] [61].

The second technology is to deploy small cells. The greatest benefits of deploying the small cells is reducing the distance from the end user to the BS. With this benefit, transmission power can be reduced and higher data rate can be achieved.

The trend of merging massive MIMO and small cell technologies to form HetNet (heterogeneous networks) has become more and more bright and clear. Many researchers and standardization organizations have considered them as the core technologies for 5G. [80] views massive MIMO and small cell as two of the "big three" technologies for 5G wireless communication system.

Given these envisioned benefits of massive MIMO and small cells, to combine these two technologies, the first question would be how to associate the users and the BSs, so that the system throughput or user experience can be ultimately enhanced. There are some existing works pushing forward in this direction. [66] [67] [68] [81] considered the problem of user association in massive MIMO system operated in FDD mode. But they didn't take small cells into consideration. For the problem of user association in massive MIMO system operated in TDD mode, it was investigated in [75]. However, it is worth pointing out that fractional user association is allowed in [75]. [82] models the problem of user association in femtocell HetNet using a dynamic matching game and finds the optimal user association. But massive MIMO is not considered in the system model. [83] investigates the problem of cell association with conventional MIMO BS and propose simple bias based selection criterion to approximate more complex selection rules. [84] considers the problem of improving the energy efficiency without sacrificing the QoS(quality of service) of users in massive MIMO and small cell networks.

Different from these works, this chapter considers the user association problems in TDD massive MIMO HetNet considering limited loading capacity of each BS without allowing fractional user association. The main goal of these problems is maximizing system throughput. More specifically, this chapter contains two parts: centralized user association and distributed user association.

For centralized user association, we investigate the problem of rate maximization, rate maximization with proportional fairness, and joint resource allocation and user association. We prove the unimodularity of our problem and leverage the unimodularity to obtain optimal user association to the problem of rate maximization and rate maximization with proportional fairness. We propose a series of primal decomposition and dual decomposition algorithm to solve the joint resource allocation and user association problem and prove the algorithm leads to optimal solution.

For distributed user association, we model the interaction between the service provider who owns the BSs and users as repeated games. We consider all the possible cases: service provider sets the price and users bid for the opportunity of connection. We prove that in either case the repeated game converges and propose algorithms to reach the Nash Equilibrium (NE) of each game.

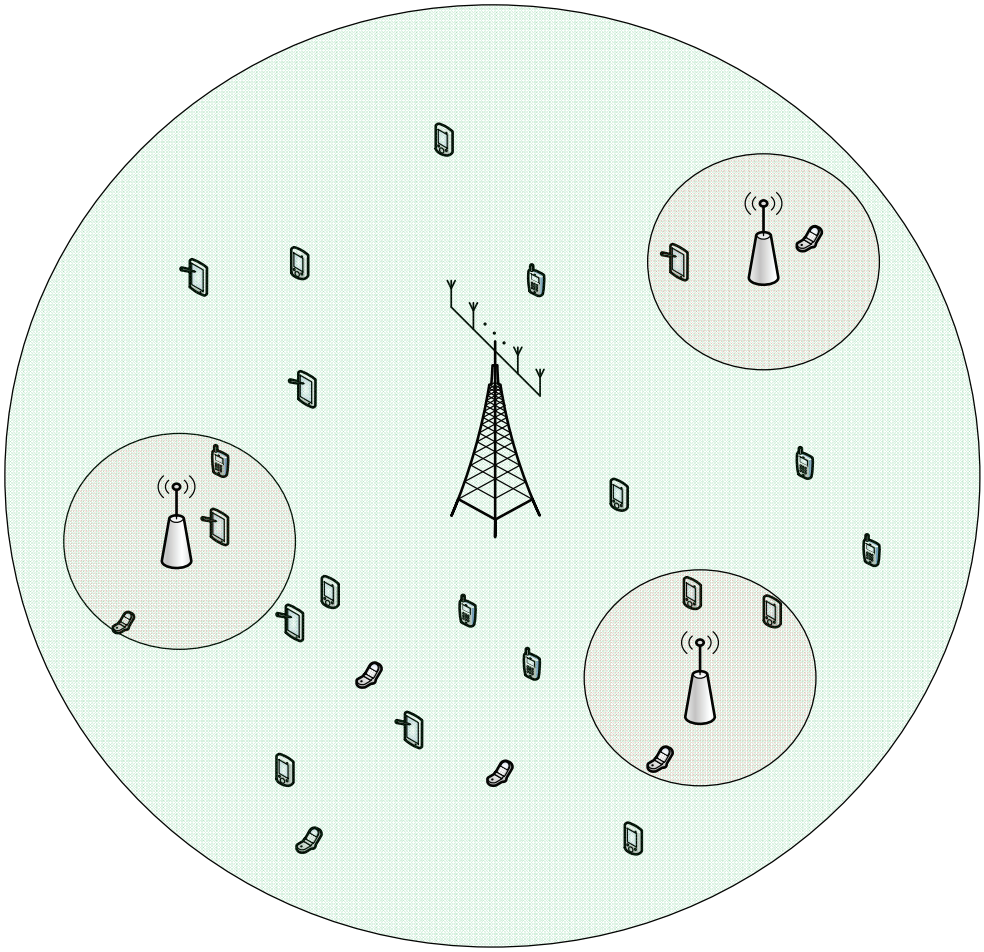

Figure 6.1: Illustration of Massive MIOM System with Small Cells.

The remainder of this chapter is organized as follows. Section 6.2 introduces the system model and preliminaries. Optimal centralized and distributed user association are discussed in Section 6.3 and Section 6.4, respectively. Section 6.5 presents the simulation studies. Conclusion is drawn in Section 6.6.

6.2 System Model and Preliminaries

The system we consider includes a massive MIMO base stations and many picocell base stations (conventional MIMO) as illustrated in Fig. 6.1. As stated in [85], picocells can benefit from inter-cell interference coordination (ICIC). The channel model we consider is given as follows [86].

$$h_{j,k,n} = g_{j,k,n} l_{j,k}, \tag{6.1}$$

where $h_{j,k,n}$ denotes the channel of the n-th antenna of the j-th BS to user k, $g_{j,k,n}$ represents the small scale fading coefficient between the n-th antenna of the j-th BS and user k, and $l_{j,k}$ stands for the large scale fading coefficient between the j-th base station and user k. Concatenating all the channel coefficients from all the antennas of the j-th base station, we obtain $\mathbf{h}_{j,k}$. Thus $\mathbf{h}_{j,k}$ is the channel vector from the j-th BS to user k. Putting the channels from all users along the column, we denote $\mathbf{H}_j = [\mathbf{h}_{j,1}, \mathbf{h}_{j,2}, \ldots, \mathbf{h}_{j,k}]$ as the channel coefficient matrix for signals transmitted from the j-th BS. We further denote y_j as the signals received by the users connecting to the j-th BS, $\mathbf{V}_j$ as the precoding matrix of the j-th BS and $\mathbf{d}_j$ as the data sent from the j-th BS. Then we have:

$$\mathbf{y}_j = \mathbf{H}_j \mathbf{V}_j \mathbf{d}_j + \mathbf{n}_j, \tag{6.2}$$

where $\mathbf{n}_j$ is the zero mean circulant symmetric complex Gaussian noise vector. Note that throughout this chapter, we use boldface upper (lower) case letter to denote a matrix (vector), and normal letter to denote a scalar.

For users connecting to the massive MIMO BS, we could approximate their achievable rate using the following deterministic rate [75].

$$R_{k_j} = \log\left(1 + \frac{M_j - L_j + 1}{L_j} \frac{P_j l_{j,k}}{1 + \sum_{j' \neq j} P_{j'} l_{j',k}}\right), \tag{6.3}$$

where M_j is the number of antenna at the j-th BS, L_j is the prefixed loading parameter of the j-th BS indicating how many users it could serve, and P_j is transmit power from the j-th BS. Note that in (6.3), there is no small scale fading factor. This approximation has been proven to be accurate [75].

For a user k, who may or may not connect to the massive MIMO base station, denoting its achievable rate regarding to the j-th BS as η_{k_j}, we readily have:

$$\eta_{k_j} = x_{k_j} R_{k_j}, \tag{6.4}$$

where

$$x_{k_j} = \begin{cases} 1, & \text{if user } k \text{ connected to BS } j. \\ 0, & \text{otherwise}. \end{cases} \tag{6.5}$$

Denote η_k as the sum rate for user k, then we have:

$$\eta_k = \sum_j \eta_{k_j}, \tag{6.6}$$

For the picocell BS with conventional MIMO, we assume that there are no interferences among the small cell BSs, since transmission powers of these small cell BSs are typically low. The achievable rate of the user connecting to these small cell base stations can be represented as follows.

$$\widetilde{R}_{k_j} = \log\left(1 + \frac{P_j \left|\mathbf{h}_{j,k}^H \mathbf{w}_{j,k}\right|^2}{1 + \sum_{k' \neq k} P_j \left|\mathbf{h}_{j,k}^H \mathbf{w}_{j,k'}\right|^2}\right), \tag{6.7}$$

where $\mathbf{w}_{j,k}$ is the k-th column of the j-th BS's precoding matrix $\mathbf{W}_j$. There are many precoding designs for the conventional MIMO BSs.

$$\mathbf{W}_j = \frac{1}{\sqrt{\varphi}} \mathbf{H}_j^H, \tag{6.8}$$

$$\mathbf{W}_j = \frac{1}{\sqrt{\varphi}} \mathbf{H}_j^H (\mathbf{H}_j^T \mathbf{H}_j^H)^{-1}, \tag{6.9}$$

$$\mathbf{W}_j = \frac{1}{\sqrt{\varphi}} \mathbf{H}_j^H (\mathbf{H}_j^T \mathbf{H}_j^H + \delta \mathbf{I})^{-1}. \tag{6.10}$$

Above equations exhibit the precoding matrices for matched filter (MF) precoding, zero forcing (ZF) precoding and regularized zero forcing (RZF) precoding [86], respectively. Note that here φ is a power normalization factor.

Here we adopt MF precoding, then the signal received by all the users connecting to the j-th BS can be rewritten as follows.

$$\mathbf{y}_j = \begin{pmatrix} h_{j,1}^H h_{j,1} d_1 + h_{j,1}^H h_{j,2} d_2 + \ldots + h_{j,1}^H h_{j,k} d_k \\ h_{j,2}^H h_{j,1} d_1 + h_{j,2}^H h_{j,2} d_2 + \ldots + h_{j,2}^H h_{j,k} d_k \\ \ldots \\ h_{j,k}^H h_{j,1} d_1 + h_{j,k}^H h_{j,2} d_2 + \ldots + h_{j,k}^H h_{j,k} d_k \end{pmatrix}. \tag{6.11}$$

Thus, the achievable rate for user k regarding to a conventional BS j can be obtained as follows.

$$\eta_{k_j} = \log \left(1 + \frac{P_j \left| x_{k_j} h_{j,k}^H h_{j,k} \right|^2}{1 + \sum_{k' \neq k} P_j \left| x_{k'_j} h_{j,k}^H h_{j,k'} \right|^2} \right). \tag{6.12}$$

6.3 Centralized User Association

In this section, we consider the problem of centralized user association. We assume that the BSs have obtained all the channel state information (CSI) via uplink training. We define the utility of each user $\mathcal{U}(\eta_k)$ based on its achievable rate as follows.

$$\mathcal{U}(\eta_k) = \begin{cases} \eta_k, & \text{if } \alpha = 0, \\ \log(\eta_k), & \text{if } \alpha = 1, \\ \frac{\eta_k^{1-\alpha}}{1-\alpha}, & \text{if } \alpha > 0, \alpha \neq 1. \end{cases} \tag{6.13}$$

The implications behind (6.13) are as follows.

1. $\alpha = 0$ yields the maximization of the sum rate (no fairness).

2. $\alpha \to \infty$ yields the maximization of the worst-case rate (max-min fairness).

3. $\alpha = 1$ yields the maximization of the geometric mean rate (proportional fairness).

Our goal is to maximize the system utility by configuring the user-BS association. Typically, we consider the cases when $\alpha = 0$ and $\alpha = 1$. Note that if $\alpha = 1$, we define $\mathcal{U}(\eta_k) = 0$, if $\eta_k = 0$.

6.3.1 Maximizing Sum-rate

We firstly investigate the problem of maximizing the system sum rate, i.e. $\alpha = 0$ in (6.13) and $\mathcal{U}(\eta_k) = \eta_k$. The problem is to maximize $\sum_k \mathcal{U}_k(z)$ given the system configuration and user distribution, which is mathematically formulated as follows.

$$\begin{aligned} \textbf{P1-1:} \max_{x_{k_j}} \quad & \sum_{k=1}^{K} \eta_k \\ \text{s.t.} \quad & \sum_{k} x_{k_j} \leq L_j \leq M_j,\ j = 1, 2, \ldots, J \\ & \sum_{j} x_{k_j} \leq 1,\ k = 1, 2, \ldots, K \\ & \text{Constraints (6.3) (6.4) (6.5) (6.6) (6.12).} \end{aligned} \tag{6.14}$$

Note that the second constraint requires the number of users connecting to a base station to be less than or equal to its prefixed loading parameter. And this parameter should be less than or equal to the number of antennas it equips, since theoretically the BS can provide at most M_j degrees of freedom. But constraint $L_j \leq M_j$ should be satisfied by when configuring the system parameters. So we could drop this constraint out of the optimization problem. The third constraint simply claims that each user can at most connect to one base station.

A key observation is that we could rewrite (6.12) in the following way.

$$\eta_{k_j} = x_{k_j} \log \left(1 + \frac{P_j \left| h_{j,k}^H h_{j,k} \right|^2}{1 + \sum_{k' \neq k} P_j \left| x_{k'_j} h_{j,k}^H h_{j,k'} \right|^2} \right), \tag{6.15}$$

so that we could redefine $\widetilde{R}_{k_j}$ in (6.7) as:

$$\widetilde{R}_{k_j} = \log\left(1 + \frac{P_j \left|h_{j,k}^H h_{j,k}\right|^2}{1 + \sum_{k' \neq k} P_j \left|x_{k'_j} h_{j,k}^H h_{j,k'}\right|^2}\right). \tag{6.16}$$

We can see from (6.16) that $\widetilde{R}_{k_j}$ depends on other users' choices $x_{k'_j}$. Here we use the worst-case approximation. That is we assume that all users within the coverage of BS j (denoted as $\mathcal{G}_j$) will connect to BS j and their channel links are perfect. In this way, (6.16) can be approximated as:

$$\widetilde{R}_{k_j} = \log\left(1 + \frac{P_j \left|h_{j,k}^H h_{j,k}\right|^2}{1 + (|\mathcal{G}_j| - 1)P_j}\right), \tag{6.17}$$

where $|\cdot|$ for a set stands for the cardinality of a set.

Define auxiliary variables c_{k_j} as follows.

$$c_{k_j} = \begin{cases} R_{k_j} \text{ in (6.3)}, & \text{BS } j \text{ being massive mimo BS}; \\ \widetilde{R}_{k_j} \text{ in (6.17)}, & \text{BS } j \text{ being small cell BS}. \end{cases} \tag{6.18}$$

The optimization problem can be reformulated as:

$$\begin{aligned} \textbf{P1-2:} \max_{x_{k_j}} \quad & \sum_{k=1}^{K} \sum_{j=1}^{J} x_{k_j} c_{k_j} \\ \text{s.t.} \quad & \sum_{k} x_{k_j} \leq L_j,\ j = 1, 2, \ldots, J \\ & \sum_{j} x_{k_j} \leq 1,\ k = 1, 2, \ldots, K \\ & \text{Constraints (6.5) (6.18).} \end{aligned} \tag{6.19}$$

For the above optimization problem, since its variable x_{k_j} is binary, it falls into the category of *Multiple Knapsack Problem*, which is one of the Karp's 21 NP-complete problems [87]. At this

point, one may try to use a greedy algorithm to obtain sub-optimal solutions. However, by taking advantage of the coefficients of the constraints, we could obtain the optimal solution.

Let $\mathbf{X}$ be a matrix with entries x_{k_j}, $k = 1, 2, \ldots, K$, $j = 1, 2, \ldots, J$. We could convert $\mathbf{X}$ to a vector $\mathbf{x}$ by concatenating the rows of $\mathbf{X}$ and taking a transpose. For instance, the following matrix

$$\mathbf{X} = \begin{pmatrix} x_{1_1} & x_{2_1} & \ldots & x_{K_1} \\ x_{1_2} & x_{2_2} & \ldots & x_{K_2} \\ \ldots & \ldots & \ldots & \ldots \\ x_{1_J} & x_{2_J} & \ldots & x_{K_J} \end{pmatrix}. \tag{6.20}$$

is reshaped as $\mathbf{x} = [x_{1_1}\ x_{2_1}\ \ldots\ x_{K_1}\ \ldots\ x_{1_J}\ \ldots\ x_{K_J}]^T$. We further simply the notation as $\mathbf{x} = [x_1\ x_2\ \ldots\ x_{K_J}]^T$ and apply the same conversion to the matrix comprising c_{k_j} and obtain vector $\mathbf{c}$. Given these transformation, we rewrite our optimization problem as:

$$\begin{aligned} \textbf{P1-3:} \max_{\mathbf{x}} \quad & \mathbf{c}^T\mathbf{x} \\ \text{s.t.} \quad & \sum_{k=1}^{K} x_{(j-1)K+k} \leq L_j,\ j = 1, 2, \ldots, J \\ & \sum_{j=1}^{J} x_{k+(j-1)K} \leq 1,\ k = 1, 2, \ldots, K \\ & \text{Constraints (6.5) (6.18).} \end{aligned} \tag{6.21}$$

Ignoring constraints (6.5) and (6.18), define $\mathbf{A}$ as the constraint matrix with entries being the coefficients of the first and second constraints. We next introduce an important definition and derive a key lemma.

Definition 2. *A matrix $\mathbf{A}$ is called totally unimodular if the determinant of every square submatrix of $\mathbf{A}$ is either 0, $+1$ or -1.*

Lemma 11. *The constraint matrix $\mathbf{A}$ is totally unimodular.*

Proof. To prove that $\mathbf{A}$ is totally unimodular, we need to check if every square submatrix of $\mathbf{A}$ has determinant either 0, $+1$ or -1. Inspecting the constraints, we find that $\mathbf{A}$ is of the following form.

$$\mathbf{A} = \begin{pmatrix} 1\,1\ldots1 & 0\,0\ldots0 & 0\,0\ldots0 \\ 0\,0\ldots0 & 1\,1\ldots1 & 0\,0\ldots0 \\ \vdots & \vdots & \vdots \\ 0\,0\ldots0 & 0\,0\ldots0 & 1\,1\ldots1 \\ 1\,0\ldots0 & 1\,0\ldots0 & 1\,0\ldots0 \\ 0\,1\ldots0 & 0\,1\ldots0 & 0\,1\ldots0 \\ \ddots & \ddots & \ddots \\ 0\,0\ldots1 & 0\,0\ldots1 & 0\,0\ldots1 \end{pmatrix} \tag{6.22}$$

We could divide $\mathbf{A}$ into blocks in the following form.

$$\mathbf{A} = \begin{pmatrix} \mathbf{A}_1 & \mathbf{A}_2 & \ldots & \mathbf{A}_J \\ \mathbf{B}_1 & \mathbf{B}_2 & \ldots & \mathbf{B}_J \end{pmatrix}, \tag{6.23}$$

where each $\mathbf{A}_j,\ j \in [1, J]$ is a submatrix of $\mathbf{A}$ of size $J \times K$; and each $\mathbf{B}_j,\ j =\in [1, J]$ is an identity matrix of size $K \times K$.

Let $\mathbf{S}_n$ denotes any square submatrix of matrix $\mathbf{A}$ of size n. For any submatrix of $\mathbf{A}$ of size 1, it is trivial to see that the determinant of this submatrix is 0 or $+1$, since all of the entries of the constraint matrix is either 0 or $+1$. So we only need to consider the case where the size of the square submatrix is greater than or equal to 2, i.e. $\mathbf{S}_n$ with $n \geq 2$.

Case 1: $\mathbf{S}_n$ is taken entirely from one of the submatrices $\mathbf{A}_j$ or $\mathbf{B}_j$, $j \in [1,\ J]$.

We can see from the structure of $\mathbf{A}_j$ that at least one row of $\mathbf{A}_j$ is all zero. So if the square submatrix is entirely taken from $\mathbf{A}_j$, the determinant of the submatrix is zero. Since matrix $\mathbf{B}_j, \forall j$ is simply the identity matrix, it is straightforward that the determinant of any square submatrix of $\mathbf{B}_j$ is either 0 or $+1$.

Case 2: $\mathbf{S}_n$ is not entirely taken from any one of the submatrices $\mathbf{A}_j$ or $\mathbf{B}_j$, $j \in 1, \ldots, J$.

In this case, the square submatrix must be taken from $2n$ ($n = 1, \ldots, J$) submatrices of the submatrix set ($\mathbf{A}_j \cup \mathbf{B}_j$, $j \in 1, \ldots, J$). We next proceed with our proof by applying induction method.

For the base case $n = 1$, the square submatrix to be examined is of size 2. Since the entries can only be 0 or $+1$, the determinant of the square submatrix can only be 0, $+1$ or -1.

Now assuming that any square submatrix of size $(n-1)$ has determinant 0, $+1$ or -1, we need to check if the same conclusion holds for any square submatrix of size n.

We first notice that each column of $\mathbf{A}$ has at exactly two $+1$s. Moreover, exactly one of them is in $\mathbf{A}_j$, and another in $\mathbf{B}_j$. Let $q^* = \arg\min_q \sum_i \mathbf{S}_{n_{i,q}}$, where $\mathbf{S}_{n_{i,q}}$ is the i,q-th entry of $\mathbf{S}_n$. That is column q^* has the minimum number of 1s among all the columns of $\mathbf{S}_n$. Let $\zeta_{q^*} = \min_q \sum_i \mathbf{S}_{n_{i,q}}$. ζ_{q^*} can only be 0, 1, or 2.

If $\zeta_{q^*} = 0$, then all the entries of the q^*-th column of $\mathbf{S}_n$ are 0, which results in $det(\mathbf{S}_n) = 0$, where det is short for determinant.

If $\zeta_{q^*} = 1$, then we could calculate $det(\mathbf{S}_n)$ by expanding the q^*-th column and obtain $det(\mathbf{S}_n) = det(\mathbf{S}_{(n-1)})$. Since $det(\mathbf{S}_{(n-1)})$ is 0, 1 or -1 by our induction hypothesis, we conclude $det(\mathbf{S}_n)$ is 0, 1 or -1.

If $\zeta_{q^*} = 2$, we could firstly negate all the entries taken from $\mathbf{B}_j$, and then add all the rows in $\mathbf{B}_j$ to any non-zero row in $\mathbf{A}_j$. After this procedure, if that non-zero row in $\mathbf{A}_j$ is still non-zero, add that row to any other non-zero row in $\mathbf{A}_j$. Repeat this process until we get a zero row in $\mathbf{A}_j$. The reason why this process always give us a all-zero row is that we have equal number of $+1$s in $\mathbf{A}_j$ and $\mathbf{B}_j$. Since any basic row operation does not change the determinant and we finally get a all-zero row, $det(\mathbf{S}_n) = 0$. That completes our induction steps.

To sum up, the determinant of any square submatrix is either 0, $+1$ or -1.

□

Lemma 12. *For a linear programming problem, if its constraint matrix satisfies totally unimodularity, then its has all integral vertex solutions.*

Proof of this lemma is skipped here. Interesting readers are referred to [88].

Lemma 13. *For a linear programming problem, if it has feasible optimal solutions, then at least one of them occurs at a vertex of the polyhedron define by its constraints.*

Proof. Linear programming inequality constraints are half-spaces and equality constraints are hyperplanes. So all these constraints together define a polyhedron. By the maximum principle of convex functions [89], the optimal value can be obtained on the boundaries. Since the vertex is the intersection of several constraints, the optimal solution can be found by checking the vertices. □

Given these lemmas, we have the following theorem.

Theorem 6.1. *The optimal solution of **P1** can be obtained by relaxing the constraint x_{k_j} to be real values between* $[0, 1]$.

Proof.

$$\begin{aligned} \textbf{NP1:} \max_{\mathbf{x}} \quad & \mathbf{c}^T\mathbf{x} \\ \text{s.t.} \quad & \sum_{k=1}^{K} x_{(j-1)K+k} \leq L_j,\ j = 1, 2, \ldots, J \\ & \sum_{j=1}^{J} x_{k+(j-1)K} \leq 1,\ k = 1, 2, \ldots, K \\ & 0 \leq x_k \leq 1,\ k = 1, 2, \ldots, K \\ & \text{Constraints (6.18).} \end{aligned} \tag{6.24}$$

Problem **NP1** is a relaxed of version **P1**. We can see that **NP1** is a linear programming problem. By Lemma 13, we know that at least one optimal solution of **NP1** is the vertex solution. Applying Lemma 11 and Lemma 12 to **NP1**, we know that the vertex solutions are integers. Since the variable x_k is restricted to the range of $[0, 1]$, that means the optimal solutions of **NP1** are binary. Since the optimal value of **P1** is upper bounded by the optimal value of **NP1**, we could attain the optimal value of **P1** by setting variables according to the solution of **NP1**. That means **NP1** and **P1** are equivalent. We could solve **NP1** for **P1**. □

Given the above theorem, we could obtain the optimal solution of **P1** by solving **NP1** using common LP solvers.

6.3.2 Proportional Fairness

In this section, we take proportional fairness among user achievable rates into consideration. Since a user's achievable rate is the sum of rate from all the base stations, the problem can be formulated as follows.

$$\begin{aligned}
\textbf{P2-1:} \max_{x_{k_j}} \quad & \sum_{k=1}^{K} \log(\sum_{j=1}^{J} x_{k_j} c_{k_j}) \\
\text{s.t.} \quad & \sum_{k=1}^{K} x_{k_j} \leq L_j, j = 1, 2, \ldots, J \\
& \sum_{j=1}^{J} x_{k_j} \leq 1, k = 1, 2, \ldots, K \\
& \text{Constraints (6.5) (6.18).}
\end{aligned} \tag{6.25}$$

Problem **P2-1** is a nonlinear integer programming problem, which is generally NP-complete as well. To get a better understanding of the problem **P2-1**, we could investigate its equivalent problem as follows.

$$\begin{aligned}
\textbf{P2-2:} \max_{x_{k_j}} \quad & \prod_{k=1}^{K} (\sum_{j=1}^{J} x_{k_j} c_{k_j}) \\
\text{s.t.} \quad & \sum_{k=1}^{K} x_{k_j} \leq L_j, j = 1, 2, \ldots, J \\
& \sum_{j=1}^{J} x_{k_j} \leq 1, k = 1, 2, \ldots, K \\
& \text{Constraints (6.5) (6.18).}
\end{aligned} \tag{6.26}$$

Problem **P2-2** is a geometric programming problem, with binary variables. The objective function is a posynomial function with J^K terms. Conventionally, to solve geometric programming problem we need to introduce new variables such as $y = \log(x)$ so that geometric programming can be solved via convex programming. However, here x_{k_j} is binary. Since $\log(0) = -\infty$, we could not apply these techniques. Another heuristic scheme is to firstly sort these J^K coefficients, and then find L_j maximal coefficients for each base station. However, even sort these J^K coefficients could be computationally prohibitive for a small area with just 10 base stations and 100 users, since it requires $\mathcal{O}(J^K \log(J^K))$ operations.

A key observation about $\log()$ function is that $\log(\sum_i x_i) \leq \sum_i \log(x_i)$, $\forall x_i \geq 2$. Therefore, practical speaking[1], the optimal value of problem **P2-1** is upper bounded by the optimal value of the following problem.

$$\begin{aligned} \textbf{NP2:} \max_{x_{k_j}} \quad & \sum_{k=1}^{K}\sum_{j=1}^{J} x_{k_j}\log(c_{k_j}) \\ \text{s.t.} \quad & \sum_{k=1}^{K} x_{k_j} \leq L_j, j = 1, 2, \ldots, J \\ & \sum_{j=1}^{J} x_{k_j} \leq 1, k = 1, 2, \ldots, K \\ & \text{Constraints (6.5) (6.18).} \end{aligned} \tag{6.27}$$

However, we have the following proposition.

Proposition 5. *Problem **P2-1** and **NP2** are equivalent.*

Proof. Recall that if $\eta_k = 0$, we define $\mathcal{U}(\eta_k) = \log(\eta_k) = 0$. The second constraint $\sum_{j=1}^{J} x_{k_j} \leq 1$ imposes that each user could only connect to one base station. Consequently, $\sum_j x_{k_j}\log(c_{k_j}) = \log(\sum_j x_{k_j} c_{k_j})$. Furthermore, $\sum_k \sum_j x_{k_j}\log(c_{k_j}) = \sum_k \log(\sum_j x_{k_j} c_{k_j})$. □

[1]Remember that c_{k_j} is the achievable rate of user k connecting to base station j. $c_{k_j} \geq 2$ is generally satisfied in current wireless systems with large bandwidth and high transmission power.

Comparing **NP2** to **P1-2**, we find they are actually equivalent. That means we could obtain the optimal value of **P2-1** by applying the same technique used to solve problem **NP1**. An important conclusion stated in Corollary 2 readily follows.

Corollary 2. *Sum rate maximization in Section 6.3.1 also achieves proportional fairness.*

Next we derive an upper bound of the optimal value of problem **P2-1**.

Proposition 6. *The optimal value of problem **P2-1** is upper bounded by* $UB_1 = \sum_{k=1}^{K} \max_j \log_2(c_{k_j})$.

Proof. Denote $m = \max\{\ln(c_{k_1}), \ln(c_{k_2}), \ldots, \ln(c_{k_J})\}$, we derive:

$$\begin{aligned} \log_2(\sum_{j=1}^{J} x_{k_j} c_{k_j}) &\leq \log_2(\sum_{j=1}^{J} \frac{e^m}{e^m} e^{\ln(c_{k_j})}) \\ &= \log_2(e^m) + \log_2(\sum_{j=1}^{J} e^{\ln(c_{k_j})-m}) \\ &\leq m\log_2(e) + \log_2(J) \end{aligned} \tag{6.28}$$

Note that first inequality is because $x_{k_j} \leq 1$. The second inequality above is due to the fact that m is the largest one among all the $x_{k_j} c_{k_j}$ and $e^{\ln(x_{k_j} c_{k_j})-m} \leq 1$.

On the other hand, by utilizing the constraint $\sum_{j=1}^{J} x_{k_j} \leq 1$, we have:

$$\log_2(\sum_{j=1}^{J} x_{k_j} c_{k_j}) \leq \log_2(e^m) \tag{6.29}$$

Since (6.29) is a better bound than (6.28), we have $UB_1 = \sum_{k=1}^{K} \max_j \log_2(c_{k_j})$.

□

For the purpose of comparison, we propose two sub-optimal greedy algorithms, Algorithm 7 and Algorithm 8 as benchmarks.

Algorithm 7: Greedy Algorithm for User Association

Initialize $\mathcal{K} = \{1, 2, \ldots, K\}$, $L_j, \forall j \in \mathcal{J}$ and x_{k_j} to be an all-zero matrix;
for $k = 1$ *to* K **do**
  for $j = 1$ *to* J **do**
    Compute c_{k_j} in (6.18) ;
  end
end
while $\exists j,\ L_j \neq 0$ **do**
  Find $(k^*, j^*) = \arg\max_{k,j} c_{k,j}$;
  if $L_{j^*} \neq 0$ **then**
    $x_{k^*_{j^*}} = 1$;
    $L_{j^*} = L_{j^*} - 1$;
    $\mathcal{K} = \mathcal{K} \backslash k^*$;
  end
end

Algorithm 8: Greedy Algorithm for User Association

Initialize $\mathcal{K} = \{1, 2, \ldots, K\}$, $L_j, \forall j \in \mathcal{J}$ and x_{k_j} to be an all-zero matrix;
for $k = 1$ *to* K **do**
  for $j = 1$ *to* J **do**
    Compute c_{k_j} in (6.18) ;
  end
end
for $j = 1$ *to* J **do**
  while $L_j \neq 0$ **do**
    Find $(k^*, j) = \arg\max_{k} c_{k,j}$;
    $x_{k^*_j} = 1$;
    $L_j = L_j - 1$;
    $\mathcal{K} = \mathcal{K} \backslash k^*$;
  end
end

The above two greedy algorithms can be directly used for comparison with Problem **P1-1**. To compare with Problem **P2-1**, for Algorithm 7, we need to change step 7 and 8 as "**while** $\exists j,\ L_j \neq 0$ $\&$ $\max_{k,j} \log(c_{k,j}) > 0$ **do**" and "Find $(k^*, j^*) = \arg\max_{k,j} \log(c_{k,j})$".

For Algorithm 8, we need to change step 8 and 9 as "**while** $L_j \neq 0$ $\&$ $\max_{k} \log(c_{k,j}) > 0$" and "Find $(k^*, j) = \arg\max_{k} \log(c_{k,j})$"

6.3.3 Joint resource allocation and user association

In this subsection we take the resource allocation into account. Consider an massive MIMO OFDMA HetNet. The system resources contain time and frequency. In OFDMA system, such as LTE, time-frequency resource is divided into resource blocks (RB). Typical RB consists of 12 subcarriers (180kHz) in the frequency domain and 7 OFDMA symbols in the time domain(0.5 ms). So the system may have up to several hundreds of RB. We normalize it to be a unit number. Every user connecting to a BS gets a portion β_{k_j} of the whole resources. The goal is to maximize the system utility considering both resource allocation and user association. Note, $\log()$ rate utility is considered here. And the problem is formulated as follows.

$$\begin{aligned} \max_{x_{k_j},\beta_{k_j}} \quad & \sum_{k=1}^{K} \log(\sum_{j=1}^{J} x_{k_j} c_{k_j} \beta_{k_j}) \\ \text{s.t.} \quad & \sum_{k=1}^{K} x_{k_j} \leq L_j, j = 1, 2, \ldots, J \\ & \sum_{j=1}^{J} x_{k_j} \leq 1, k = 1, 2, \ldots, K \\ & \sum_{k \in \Phi_j} \beta_{k_j} \leq 1, j = 1, 2, \ldots, J \\ & \text{Constraints (6.5) (6.18).} \end{aligned} \tag{6.30}$$

Note that in (6.30), Φ_j is the user set defined as:

$$\Phi_j = \left\{ k | x_{k_j} = 1 \right\}. \tag{6.31}$$

So problem (6.30) contains two levels of coupled question: (1) select users for each BS, (2) allocate resources to the associated users. We next propose a series of primal decomposition and dual decomposition to optimal solve it. It is worth pointing out that another possible formulation of the problem is as follows.

$$\max_{x_{k_j},\beta_{k_j}} \quad \sum_{k=1}^{K} \log(\sum_{j=1}^{J} x_{k_j} c_{k_j} \beta_{k_j}) \tag{6.32}$$

$$\text{s.t.} \quad \sum_{k=1}^{K} x_{k_j} \leq L_j, j = 1, 2, \ldots, J$$

$$\sum_{j=1}^{J} x_{k_j} = 1, k = 1, 2, \ldots, K$$

$$\sum_{k \in \Phi_j} \beta_{k_j} \leq 1, j = 1, 2, \ldots, J$$

Constraints (6.5) (6.18).

Comparing these two formulations, we have following observations.

1. Problem (6.30) does not require every user must be connected. However, problem (6.32) does require all the users to be connected even under unfavorable conditions.

2. Problem (6.32) has more stringent requirement than problem (6.30). So the optimal value of problem (6.30) is upper bounded by the optimal value of problem (6.30).

3. Since problem (6.30) gives more choices of user association, problem (6.30) is slower in convergence than problem (6.32).

We focus on the harder problem (6.30). Given the algorithm to solve problem (6.30), the solution to problem (6.32) is ready to obtain. Here variables x_{k_j} are integers, while β_{k_j} are real numbers. So problem (6.30) is a mixed integer programming problem, which is general NP-hard. However, next we propose an algorithm to obtain its optimal solution.

We observe that since x_{k_j} are binary numbers and $\sum_{j=1}^{J} x_{k_j} \leq 1$, therefore we have:

$$\sum_{k=1}^{K} \log(\sum_{j=1}^{J} x_{k_j} c_{k_j} \beta_{k_j}) = \sum_{k=1}^{K} \sum_{j=1}^{J} x_{k_j} \log(c_{k_j} \beta_{k_j}) \tag{6.33}$$

Notice that we also define that if $\sum_{j=1}^{J} x_{k_j} = 0$, the $\log$ utility is 0. Also note that the choices of β_{k_j} rely on the values of x_{k_j}. Thus problem (6.30) is in fact the following:

$$\begin{aligned} \max_{x_{k_j}, \beta_{k_j}} \quad & \sum_{k=1}^{K} \sum_{j=1}^{J} x_{k_j} \log(c_{k_j} \beta_{k_j}) \\ \text{s.t.} \quad & \sum_{k=1}^{K} x_{k_j} \leq L_j, j = 1, 2, \ldots, J \\ & \sum_{j=1}^{J} x_{k_j} \leq 1, k = 1, 2, \ldots, K \\ & \sum_{k \in \Phi_j} \beta_{k_j}(x_{k_j}) \leq 1, j = 1, 2, \ldots, J \\ & \text{Constraints (6.5) (6.18).} \end{aligned} \tag{6.34}$$

Given these coupled variables, we firstly apply the Primal Decomposition method [90] to decompose problem (6.34) to the following two levels of problem. Fixing variables x_{k_j}, we have the *lower level problem* as:

$$\begin{aligned} \max_{\beta_{k_j}} \quad & \sum_{k=1}^{K} \sum_{j=1}^{J} x_{k_j} \log(c_{k_j} \beta_{k_j}) \\ \text{s.t.} \quad & \sum_{k \in \Phi_j} \beta_{k_j} \leq 1, j = 1, 2, \ldots, J \end{aligned} \tag{6.35}$$

And the *higher level problem* (or called *master problem*) is given by:

$$\begin{aligned} \max_{x_{k_j}} \quad & \sum_{k=1}^{K} \sum_{j=1}^{J} x_{k_j} \log(c_{k_j} \beta_{k_j}) \\ \text{s.t.} \quad & \sum_{k=1}^{K} x_{k_j} \leq L_j, j = 1, 2, \ldots, J \\ & \sum_{j=1}^{J} x_{k_j} \leq 1, k = 1, 2, \ldots, K \\ & \text{Constraints (6.5) (6.18).} \end{aligned} \tag{6.36}$$

where β_{k_j} are fixed.

Since there are no couplings among these subproblems, for the lower level problem (6.35), we could further decompose it into L subproblems as follows.

$$\begin{aligned} \max_{\beta_{k_j}} \quad & \sum_{k=1}^{K} x_{k_j} \log(c_{k_j} \beta_{k_j}) \\ \text{s.t.} \quad & \sum_{k \in \Phi_j}^{K} \beta_{k_j} \leq 1, j = 1, 2, \ldots, J \end{aligned} \tag{6.37}$$

The Lagrange of problem (6.37) is:

$$\mathcal{L} = \sum_{k=1}^{K} x_{k_j} \log(c_{k_j} \beta_{k_j}) + \lambda (1 - \sum_{k=1}^{K} \beta_{k_j}), \tag{6.38}$$

where λ is the Lagrange multiplier. Applying KKT conditions [45], the optimal solution can be obtained:

$$\beta_{k_j} = \frac{x_{k_j}}{\sum_{k=1}^{K} x_{k_j}}. \tag{6.39}$$

Plug in β_{k_j} to the master problem, we have

$$\begin{aligned} \max_{x_{k_j}} \quad & \sum_{k=1}^{K} \sum_{j=1}^{J} x_{k_j} \log(\frac{c_{k_j}}{\sum_{k=1}^{K} x_{k_j}}) \\ \text{s.t.} \quad & \sum_{k=1}^{K} x_{k_j} \leq L_j, j = 1, 2, \ldots, J \\ & \sum_{j=1}^{J} x_{k_j} \leq 1, k = 1, 2, \ldots, K \\ & \text{Constraints (6.5) (6.18).} \end{aligned} \tag{6.40}$$

Note that we have dropped one x_{k_j} term, since due to constraint (6.5), $(x_{k_j})^2 = x_{k_j}$. Since $\sum_{k=1}^{K} x_{k_j}$ is in the denominator, problem (6.40) has coupled objectives. The key idea of addressing coupled objective is to introduce auxiliary variables and additional equality constraints so that the coupling in the objective function is transferred to coupling in the constraint [90]. So we introduce

a new variable, which is defined as:

$$\Xi_j = \sum_{k=1}^{K} x_{k_j}. \tag{6.41}$$

To solve the above problem, we relax x_{k_j} to be a real number between 0 and 1. However, we will show later that even if we have relaxed the variables, we could still find the optimal solution to the original problem. So the new problem we want to solve is:

$$\begin{aligned} \max_{x_{k_j}} \quad & \sum_{k=1}^{K}\sum_{j=1}^{J} x_{k_j}\log(\frac{c_{k_j}}{\Xi_j}) \\ \text{s.t.} \quad & \Xi_j \leq L_j, j = 1, 2, \ldots, J \\ & \sum_{j=1}^{J} x_{k_j} \leq 1, k = 1, 2, \ldots, K \\ & 0 \leq x_{k_j} \leq 1 \\ & \text{Constraints (6.18) (6.41).} \end{aligned} \tag{6.42}$$

We propose Algorithm 9 to obtain the optimal solution of problem (6.42) [78] [68] [81]. Note that in this algorithm, $\delta^{(t)}$ is the step size at the t-th iteration, given by:

$$\delta^{(t)} = \frac{\vartheta}{t+\gamma}, \tag{6.43}$$

where ϑ and γ are positive numbers.

Theorem 6.2. *Algorithm 9 optimally solves problem (6.42).*

Proof. Let $\mathbf{x}_k^{(t)}$ denotes the solution produced by Algorithm 9 at step t. Let $\partial\mathcal{U}(\mathbf{x}_k^{(t)})$ denotes the subgradient of the objective function in problem (6.42) at step t. We could easily verify that the update direction in step 13 of Algorithm 9 is the subgradient direction. Since Ξ_j is upper bounded by L_j and K, and $\sum_{k=1}^{K} x_{k_j}$ is upper bounded by K, $\partial\mathcal{U}(\mathbf{x}_k^{(t)})$ is bounded. Let κ be a positive number which satisfies $\kappa \leq \inf\left\{\|\partial\mathcal{U}(\mathbf{x}_k^{(t)})\|\right\}, \forall t$.

Denote $\mathcal{U}_a$ as the final result produced by Algorithm 9 and $\mathcal{U}^*$ as the optimal solution of problem (6.42). We prove the theorem by contradiction. Assume that $\mathcal{U}_a$ is not optimal. Then there must exist an $\epsilon > 0$ such that

$$\mathcal{U}_a + 2\epsilon < \mathcal{U}^*. \tag{6.44}$$

Then there must be a solution $\hat{\mathbf{x}}_k$ so that

$$\mathcal{U}_a + 2\epsilon < \mathcal{U}(\hat{\mathbf{x}}_k). \tag{6.45}$$

Let t_0 be sufficiently large so that we have

$$\mathcal{U}(\mathbf{x}_k^{(t)}) \leq \mathcal{U}_a + \epsilon. \tag{6.46}$$

Combining (6.45) and (6.46), we have:

$$\mathcal{U}(\mathbf{x}_k^{(t)}) + \epsilon < \mathcal{U}(\mathbf{x}_k^{(t)}). \tag{6.47}$$

Then we derive:

$$
\begin{aligned}
& \|\mathbf{x}_k^{(t+1)} - \hat{\mathbf{x}}_k\|^2 \qquad (6.48)\\
= \; & \|\mathbf{x}_k^{(t)} - \delta^{(t)}\partial\mathcal{U}^{(t)} - \hat{\mathbf{x}}_k\|^2 \\
= \; & \|\mathbf{x}_k^{(t)} - \hat{\mathbf{x}}_k\|^2 + (\delta^{(t)})^2\|\partial\mathcal{U}^{(t)}\|^2 \\
& -2\delta^{(t)}(\partial\mathcal{U}^{(t)})^H(\mathbf{x}_k^{(t)} - \hat{\mathbf{x}}_k) \\
\geq \; & \|\mathbf{x}_k^{(t)} - \hat{\mathbf{x}}_k\|^2 + (\delta^{(t)})^2\|\partial\mathcal{U}^{(t)}\|^2 - 2\delta^{(t)}(\mathcal{U}(\mathbf{x}_k^{(t)}) - \mathcal{U}(\hat{\mathbf{x}}_k)) \\
\geq \; & \|\mathbf{x}_k^{(t)} - \hat{\mathbf{x}}_k\|^2 + (\delta^{(t)})^2\kappa^2 + 2\delta^{(t)}\epsilon \\
\geq \; & \|\mathbf{x}_k^{(t)} - \hat{\mathbf{x}}_k\|^2 + 2\delta^{(t)}\epsilon \\
\geq \; & \dots \\
\geq \; & \|\mathbf{x}_k^{(t_0)} - \hat{\mathbf{x}}_k\|^2 + 2\epsilon\sum_{j=t_0}^{t}\delta^{(j)}
\end{aligned}
$$

Note that the first inequality is due the property of subgradient. So we finally have $\|\mathbf{x}_k^{(t+1)} - \hat{\mathbf{x}}_k\|^2 \geq \|\mathbf{x}_k^{(t_0)} - \hat{\mathbf{x}}_k\|^2 + 2\epsilon\sum_{j=t_0}^{t}\delta^{(j)}$, which cannot hold for sufficiently large t. Thus Algorithm 9 optimally solves problem (6.42).

□

Theorem 6.3. *The optimal solution to the problem (6.42) is also feasible and optimal for the problem (6.40).*

Proof. From problem (6.42) to (6.40), we relax the variables from binary to real numbers and introduce a equality constraint. The equality constraint is just another representation of the problem and changes nothing. So the optimal values to problem (6.40) provides an upper bound to the problem of (6.42). However it can be observed from Algorithm 9 that the solutions to problem (6.40) are integers rather than fractions. So we could set the solutions to problem (6.42) exactly the same as the solutions to problem (6.40). Since the solutions to problem (6.42) cannot result in higher optimal value than the solutions to problem (6.40), the solutions to problem (6.40) are

Algorithm 9: Two Layer Dual Decomposition Algorithm for Optimization Problem (6.42)

$t = 0$, $\lambda^{(1)} = 0$;
while *the optimization has not converged* **do**
  $t \leftarrow t + 1$;
  for $k = 1, \ldots, K$ **do**
    for $j = 1, \ldots, J$ **do**
      Compute c_{k_j};
    end
    Find $j^* = \arg\max_j \left\{\log(c_{k_j} - \lambda_j^{(t)})\right\}$;
    Let $x_{k_j}^{(t)} = 0$ for $j \neq j^*$;
    Let $x_{k_j^*}^{(t)} = 1$, if $\log(c_{k_j} - \lambda_j^{(t)}) \geq 0$; Otherwise, $x_{k_j^*}^{(t)} = 0$;
  end
  for $j = 1, \ldots, J$ **do**
    Each BS chooses a step size $\delta^{(t)}$ and computes $\Xi_j^{(t+1)} = \min\{L_j, e^{(\lambda_j^{(t)} - 1)}\}$, $\lambda_j^{(t+1)} = \lambda_j^{(t)} - \delta^{(t)}(\Xi_j^{(t)} - \sum_{k=1}^{K} x_{k_j}^{(t)})$.
  end
end

Algorithm 10: Greedy Algorithm for Joint Resource Allocation and User Association

Initialize $\mathcal{K} = \{1, 2, \ldots, K\}$ and $\mathcal{J} = \{1, 2, \ldots, J\}$ x_{k_j} to be an all-zero matrix;
for $k = 1$ *to* K **do**
  for $j = 1$ *to* J **do**
    Compute c_{k_j} in (6.18) ;
  end
end
while $\max_{k,j} \log(c_{k,j}) > 0$ **do**
  Find $(k^*, j^*) = \arg\max_{k,j} \log(c_{k,j})$;
  $x_{k_{j^*}^*} = 1$;
  $\mathcal{K} = \mathcal{K} \backslash k^*$;
  $\mathcal{J} = \mathcal{J} \backslash J^*$;
end

exactly the solutions to problem (6.42) as well. Henceforth, even though we transform problem (6.42) to problem (6.40), the optimal solution does not change. □

To sum up, optimal solution to the problem (6.40) can be find via Algorithm 9. For the purpose of comparison, we propose two greedy algorithms as benchmark. The idea of them are first find a most desirable user-BS pair, then allocation all the resources to that user. Repeat until converge.

Algorithm 11: Greedy Algorithm for Joint Resource Allocation and User Association

Initialize $\mathcal{K} = \{1, 2, \ldots, K\}$, $\mathcal{J} = \{1, 2, \ldots, J\}$ and x_{k_j} to be an all-zero matrix;
for $k = 1$ *to* K **do**
    for $j = 1$ *to* J **do**
        Compute c_{k_j} in (6.18) ;
    end
end
for $j = 1$ *to* J **do**
    if $\max_k \log(c_{k,j}) > 0$ **then**
        Find $(k^*, j) = \arg\max_k c_{k,j}$;
        $x_{k_j^*} = 1$;
        $\mathcal{K} = \mathcal{K} \backslash k^*$;
    end
end

6.4 Distributed User Association

In the previous section, we assume that there is a central controller which has global information and assigns users to the BSs. In this section, we consider distributed user association where there is no central controller. However, the BSs still have all the CSI via uplink training. We further assume that all the base stations including the massive MIMO BS and small cell BS belong to the service provider. And each user make its own decisions based on the broadcast and local information.

We model the behaviors of the service provider and users using repeated game theory. The first key problem is to determine whether the game will terminate. The second key problem is to analyze whether both sides are satisfactory about the outcome of the game, i.e. Nash Equilibrium exists.

Note that throughout this section, we also does not allow fractional connection. Constraint (6.5) is dropped from the problem formuation, but it is enforced.

6.4.1 Service Provider Determines the Prices

In the first subsection, we consider the case that during each round of the game, the service provider determines the price. Users decide whether connect or not, and if connect, connect to

which base station. So the players of the game include the service provider and the users. The strategy of the service provide is to set the price p_{k_j} of each BS for each user, while the strategy of the user k is to determine x_{k_j} is 0 or 1 for $j \in \mathcal{J}$.

The utility of the service provider is defined as $\mathcal{U}_B = \sum_{k=1}^{K} \sum_{j=1}^{J} x_{k_j} p_{k_j}$. However, each BS has its limited loading capacity. Therefore, the service provider tries to solve the following problem:

$$\begin{aligned} \max_{p_{k_j}} \quad & \mathcal{U}_B = \sum_{k=1}^{K} \sum_{j=1}^{J} x_{k_j} p_{k_j} \\ \text{s.t.} \quad & \sum_{k} x_{k_j} \leq L_j \end{aligned} \tag{6.49}$$

The utility of each user is the transmission rate achieved minus its payment. So each user tries to solve the following problem.

$$\begin{aligned} \max_{x_{k_j}} \quad & \mathcal{U}_k = \max \left\{ w_k \log \left(\sum_{j=1}^{J} x_{k_j} c_{k_j} \right) - \sum_{j=1}^{J} x_{k_j} p_{j_k}, 0 \right\} \\ \text{s.t.} \quad & \sum_{j} x_{k_j} \leq 1 \end{aligned} \tag{6.50}$$

Note that $\log()$ function represents the satisfaction of a user towards its achievable rate. w_k is a weight factor used for conversion between the rate satisfaction and monetary measurement. We assume that the weight w_k of each user is drawn from a finite set $\mathcal{W}$ with $|\mathcal{W}|$ members. This assumption is true in real-world practice. For instance, $\$30$ for a wireless service with $60\ Mbps$ data rate is considered to be cheap. $\$45$ is considered to be reasonable. $\$60$ would be thought as acceptable. $\$80$ would be expensive for most people. $\$100$ would be too expensive and $\$150$ or above would not be an option for most people. So the weight of the users has generally finite choices of values based on common sense, and is typically in a range $= (0, W_M)$, where W_M is the maximum possible value for w_k.

Given the plays, their strategies and utilities, we define the NE of the game as: a strategy set $\left\{p_{k_j}^*, x_{k_j}^*\right\},\ \forall k,\ \forall j$ is a NE of the repeated game if $\mathcal{U}_B(p_{k_j}^*, x_{k_j}^*) \geq \mathcal{U}_B(p_{k_j}, x_{k_j}^*),\ \forall p_{k_j}$ and $\mathcal{U}_k(p_{k_j}^*, x_{k_j}^*) \geq \mathcal{U}_k(p_{k_j}^*, x_{k_j}),\ \forall k,\ \forall x_{k_j}$.

Due to the constraint that each user can only connect to one base station, $w_k \log\left(\sum_{j=1}^{J} x_{k_j} c_{k_j}\right) = \sum_{j=1}^{J} x_{k_j} w_k \log(c_{k_j})$. So each user locally optimize the following problem.

$$\begin{aligned} \max_{x_{k_j}} \quad & \mathcal{U}_k = \max\left\{\sum_{j=1}^{J} x_{k_j} w_k \log(c_{k_j}) - \sum_{j=1}^{J} x_{k_j} p_{j_k}, 0\right\} \\ \text{s.t.} \quad & \sum_{j} x_{k_j} \leq 1 \end{aligned} \tag{6.51}$$

Note that the constraint of (6.51) is $\sum_j x_{k_j} \leq 1$, which indicates that $\sum_j x_{k_j}$ could be 0, i.e. a user may choose not to connect to any one of the base stations. On the other hand, if we restrict $\sum_j x_{k_j} = 1$, i.e., a user must connect to a base station, then even if the service provider sets the prices to be infinity, each user will still connect to one of the base station, which is unreasonable.

The repeated game is playing as follows. Initially, the service provider sets a price for each base station for each user. Knowing the prices, users will feedback the service provider their choices based on their own calculations. Then the service provider updates the prices and broadcasts them to all the users. Users again inform the service provider of their choices. The process is repeated until the service provider and users are all satisfied by the price.

Give the utility function and constraint in (6.51). The optimal solution for each user can be found as:

$$j^* = \arg\max_{j \in \mathcal{J}} \left[w_k \log(c_{k_j}) - p_{j_k}\right], \tag{6.52}$$

$$x_{k_j} = \begin{cases} 1, & \text{if } j = j^* \text{ and } w_k \log(c_{k_j^*}) \geq p_{j_k^*}. \\ 0, & \text{otherwise}. \end{cases} \tag{6.53}$$

Users' decision can be interpreted in this way. A user will select out the best connection based on its own evaluation. If the user's evaluation of the connection is greater than equal to the price, then it will connect to this base station. Otherwise, the user will not connect.

For the service provider, it tries to solve (6.49). The variable it controls are p_{k_j}, for $k = 1, 2, \ldots, K$ and $j = 1, 2, \ldots, J$. However, the constraint $\sum_k x_{k_j} \leq L_j$ implicitly contains variable p_{k_j}, since according to the user's choice, $j^* = \arg\max_{j \in \mathcal{J}} \left[w_k \log(c_{k_j}) - p_{j_k} \right]$.

$$\begin{aligned} \max_{p_{k_j}} \quad & \mathcal{U}_B = \sum_{k=1}^{K} \sum_{j=1}^{J} x_{k_j} p_{k_j} \\ \text{s.t.} \quad & \sum_{k} x_{k_{j(p_{k_j})}} \leq L_j \end{aligned} \tag{6.54}$$

Thus, the optimization problem for the service provider is in fact (6.54), which is mixed integer programming in nature and generally NP-hard to solve.

Since problem (6.54) has coupling constraints, one may try to introduce Lagrange multiplier to the constraint and solve the resulting problem using dual decomposition. However, since p_{k_j} is implicitly contained in the constraint, the gradient and subgradient are difficult to find. So we need to resort to other ways. We propose Algorithm 12 for the service provider, and then prove that the algorithm results optimal utility for the service provider and the users.

Proposition 7. *If the service provider adopts Algorithm 12, the game converges and the NE can be achieved.*

Proof. We first notice that the service provider has priority over the wireless users. The users always make decisions based upon the service provider's price setting. Basically, the service provider controls when the repeated game terminates.

In Algorithm 12, the service provider tests out the weight of each user using binary search with $\mathcal{O}(\log_2(|\mathcal{W}|))$ steps. Once the service provider has figured out w_k, $k = 1, 2, \ldots, K$ of each user, it can estimate the users' price evaluation matrix $\mathbf{V}$ as follows.

$$v_{k_j} = c_{k_j} w_k, \tag{6.55}$$

where v_{k_j} is the entry of matrix $\mathbf{V}$ at j-th row and k-th column. Then the service provider is ready to select users for the base stations by solving the following problem.

$$\begin{aligned} \max_{x_{k_j}} \quad & \sum_{k=1}^{K} \sum_{j=1}^{J} x_{k_j} v_{k_j} \\ \text{s.t.} \quad & \sum_{k} x_{k_j} \leq L_j, \ j = 1, 2, \ldots, J \\ & \sum_{j} x_{k_j} \leq 1, \ k = 1, 2, \ldots, K \\ & \text{Constraints (6.5) (6.55).} \end{aligned} \tag{6.56}$$

The optimal solution $x^*_{k_j}$ to the above problem can be solved in similar way of solving problem **P1-2**. Then the optimal price solution to the service provider can be obtained as follows.

$$p^*_{k_j} = \begin{cases} v_{k_j}, & \text{if } x^*_{k_j} = 1; \\ v_{k_j} + \epsilon, & \text{otherwise,} \end{cases} \tag{6.57}$$

where ϵ is any positive number.

So by adopting Algorithm 12, the optimal utility (highest) can be reached for the service provider. Meanwhile, we could see that all the users' utility must be 0 due to the optimal price setting. That means, all the users achieve the optimal utility given the price setting as well. Therefore, the game converges and the NE is met. □

Notice that it is highly possible that the optimal utility of the service provider will be lower than the maximum utility during the game. That's because during the game, the load capacity condition is often violated.

Algorithm 12: Algorithm for Service Provider

Initialize $w_{MAX}, w_{MIN}, t = 0$;
for $k = 1$ *to* K **do**
  for $j = 1$ *to* J **do**
    Compute c_{k_j} in (6.18) ;
  end
end
for $k = 1$ *to* K **do**
  $w_k^u(t) = w_{MAX}$;
  $w_k^l(t) = w_{MIN}$;
end
while *not converged* **do**
  for $k = 1$ *to* K **do**
    $\hat{w}_k(t) = \frac{w_k^u(t)+w_k^l(t)}{2}$;
    for $j = 1$ *to* J **do**
      $p_{k_j}(t) = \max\left\{\hat{w}_k(t)\log(c_{k_j}), 0\right\}$;
    end
  end
  $t = t + 1$;
  for $k = 1$ *to* K **do**
    if $|F_k| > 1$ **then**
      $w_k^u(t) = w_k^u(t-1)$;
      $w_k^l(t) = w_k^l(t-1)$;
    else if $|F_k| = 1$ **then**
      $w_k^u(t) = w_k^u(t-1)$;
      $w_k^l(t) = \hat{w}_k(t)$;
    else
      $w_k^u(t) = \hat{w}_k(t)$;
      $w_k^l(t) = w_k^l(t-1)$;
    end
  end
end
for $k = 1$ *to* K **do**
  for $j = 1$ *to* J **do**
    Calculate v_{k_j} in (6.55) using $\hat{w}_k$;
  end
end
Solve (6.56) and find optimal price in (6.57);

6.4.2 Users Bid

In this subsection, we consider the case that before service, users bid to the service provider according to its predicted satisfaction towards each BS. And service provider determines whether

or not accept a user's bid and feedback the decisions to users. Then the users make another round of bids according to its predicted satisfaction and the service provider's decision history. The service provider again decides whether or not accept a user's bid and feedback the decision.

Here we consider the users to be data-hungry and strive for as high data rate as possible. Considering that a user will not bid to a BS with satisfaction less than 0, each user solves the following problem:

$$\begin{aligned} \max_{p_{k_j}} \quad & \mathcal{U}_k = \max\left\{\sum_{j=1}^{J} x_{k_j} w_k \log(c_{k_j}), 0\right\} \\ \text{s.t.} \quad & \sum_{j} x_{k_j(p_{k_j})} \leq 1 \end{aligned} \tag{6.58}$$

On the other hand, the utility of the service provider is the total payment made by all the users. So it tries to maximize:

$$\begin{aligned} \max_{x_{k_j}} \quad & \mathcal{U}_B = \sum_{k=1}^{K}\sum_{j=1}^{J} x_{k_j} p_{k_j} \\ \text{s.t.} \quad & \sum_{k} x_{k_j} \leq L_j \end{aligned} \tag{6.59}$$

To sum up, the players of the game include the service provider and the users as well. The strategy of the user is to make payment 0 or the satisfactory level to a BS. The strategy of the service provider is to determine whether or not accept a user's bid. The utility of each user is given in (6.58) and the utility of the service provider is given in (6.59).

We assume that $K \geq \sum_{j=1}^{J} L_j$. The optimal solution for each user is simple. In order to have the greatest level of satisfaction, it makes highest possible payment. So the payment made by each user is:

$$p_{k_j} = \max\left\{\sum_{j=1}^{J} x_{k_j} w_k \log(c_{k_j}), 0\right\} \tag{6.60}$$

The optimal strategy for the service provider is summarized in Algorithm .

Algorithm 13: Algorithm for the Service Provider

```
while not converged do
    for j = 1 to J do
        if j is bidden by ≤ L_j users then
            Keep all the users in BS j's waiting list;
        else
            Keep L_j users with highest bids and reject other users;
        end
    end
end
```

At the first stage of the game, each user bids a price to its most desirable base station. Then Algorithm 13 indicates if the j-th base station receives more than L_j bids, the service provider only puts L_j users on BS-j's waiting list based on the prices the users offer, and rejects all other users. If the j-th BS receives less than or equal to L_j bids, the service provider puts all these users on its waiting list.

At the second stage of the game, if a user gets a position in a BS's waiting list in the previous round, it will keep bidding the same BS with the same price to guarantee the highest utility. However, if a user gets rejected in the previous round, being selfish, it will exclude the base stations which have rejected him before and bids a price to its most desirable base station among the remaining base stations. For the service provider, it adopts the same strategy. If the number of bids received for a BS outnumbers the loading capacity of that BS, the service provider only keeps the L_j most desirable users on the waiting list and reject the others. It keeps all users on the waiting list if the number of bids received is less than a BS's loading capacity.

Game repeats until it converges.

Lemma 14. *The sequence of bidding made by a user is non-increasing in the user's preference list.*

Proof. Before a user offers bidding, it will calculate the satisfaction of all the base stations and have a preference list in its mind. Since a user tries to maximize its utility, it will firstly propose to the base station with the highest satisfaction. If that base station rejects it, it will propose to the base station with the second highest satisfaction. Note that even if a user may be put on the waiting

list of a base station, he may be removed from that waiting list later. If that happens, this user will start bidding to other base station again. A user will repeat this process until he is finally in a base station's serving list or he will be rejected by all base stations. So the sequence of bidding made by a user is non-increasing in the user's preference list. □

Lemma 15. *The sequence of bidding a base station put on the waiting list is non-decreasing in its preference list.*

Proof. Given the fact any base station has finite loading capacity and $K \geq \sum_{j=1}^{J} L_j$, all the base station will have at least one user bids to it at some stage of this game. Since a base station tries to maximize its utility, it puts all the users who offer bids on the waiting list. On the condition that there are too many users, it will reject the users who will never be served by it. In the next round of game, the base station will often have more or at least the same amount of bids compared to the size of its current waiting list. That means the base station has more choices. The base station again only keeps the most profitable ones and reject or remove the others from the waiting list. So the sequence of bidding a base station put on the list is non-decreasing in its preference list. □

Theorem 6.4. *The above repeated game converges.*

Proof. Given observations in **Lemma** 14 and **Lemma** 15, we prove this theorem by contradiction. Suppose that this repeated game does converge. Then there must be a stage of the game that there is a user k and BS j pair so that user k is connected to another BS j' or is not connected to any BS, while user k prefers BS j to BS j' or prefers BS j to be not connected; and BS j prefers user k to a user k' who is on its serving list. Let's firstly consider user k is now served by BS j'. If this happens, since the sequence of bidding a base station put on the list is non-decreasing in its base station, it must be that user k has never bidden to BS j during the game. Because if user k has bidden to BS j, BS j would not have ended up with choosing k' over k. So user k must have never bidden to BS j. In this case, user k would never have bidden to BS j' either, since user k prefers j to j'. However, user k is now served by BS j', user k must have bidden to BS j', which contradicts that user k would never have bidden to BS j'. Same reasoning holds for the case under which user

k is not connected to any base station. If BS j prefers k to k' on the serving list, BS j would never reject user k but meanwhile keep user k'.

Therefore, the repeated game must converge. And the game converges when every user is either on a waiting list or has been rejected by every BS. □

From the proof above, we can actually see that the game terminates when the least popular base station becomes fully loaded.

Theorem 6.5. *The outcome of the above repeated game is optimal for the users and service provider.*

Proof. Suppose that the outcome of the game is not optimal for a user k, who is connected to BS j. Then there must be another BS j', which has higher ranking than BS j in the preference list of user k and has a serving list of user $\left\{j'_1, j'_2, \ldots, j'_{L_{j'}}\right\}$. Since BS j' serves user $j'_1, j'_2, \ldots, j'_{L_{j'}}$, that means BS j' prefer these users to user k and BS j' is at the top of the preference list of these users. If at some stage user k is or we insert user k by force to the waiting list of BS j', the game must have not terminated. Since user k is in the waiting list, then one of the final users $j'_1, j'_2, \ldots, j'_{L_{j'}}$ must be currently off the list. Say user $j'_{L_{j'}}$ is out of the list. User $j'_{L_{j'}}$ will immediately bids for BS j' since BS j' is at the top of its preference list among the remaining base stations. And BS j' will remove k from the waiting list, since user k has lowest ranking in the preference list of BS j'. Thus, when the repeated game terminates, the outcomes are optimal for each user. It is obvious that the outcome is optimal for the service provider. □

From Theorem 6.4 and Theorem 6.5, we know that the game converges and the NE is met when the game terminates.

6.5 Simulation Study

In this section, we conduct numeric simulations to verify the efficacy of our proposed schemes.

Throughout the simulation, we assume $l_{j,k} = 1/(1+(\frac{d_{j,k}}{40})^{3.5})$ for the path loss between a user and the massive MIMO BS, and $l_{j,k} = 1/(1+(\frac{d_{j,k}}{40})^{4})$ for the path loss between a user and a small

Table 6.1: System Configuration

Parameter	**Value**	**Parameter**	**Value**
$M_{massive}$	100	M	4
$L_{massive}$	10	L	4
$P_{massive}$	40 dBm	P	40 dBm
Area	1000×1000	J	11

cell BS [75]. For the small scale fading, we assume the power of the small scale fading following a uniform distribution from $[0.8, 1]$.

For the geometry of the base stations, we fix the location of the massive MIMO BS at the center of the map. Other BSs are randomly placed across the map. Users are randomly dropped across the map. More parameter settings are listed in Table 6.1.

Fig. 6.2 represents the comparison among the rate maximization of the optimal solution and the two proposed greedy algorithms. Fig. 6.3 depicts the comparison among the rate maximization considering proportional fairness of the optimal solution and the two proposed greedy algorithms. We can see from both figures that the optimal solution achieves the highest network utility. We also notice that as the number of users increase, the gaps between the optimal utility and the greedy solutions become more and more narrower. This is because that as there are more users, the user diversity effect becomes stronger. So the greedy algorithm and the optimal user association tend to produce similar solutions.

Throughout this chapter, the constraint for each user is $\sum_{j=1}^{J} x_{k_j} \leq 1$. It should provides upper bounds for the problem with the constraint $\sum_{j=1}^{J} x_{k_j} = 1$. Fig. 6.4 illustrates this comparison. Here for fair comparison. We have exactly the same number of active users as the loading capacity of all BSs. For instance, when the system loading capacity is 250, we have $J = 51$ BSs and $K = 250$. We can see that the inequality constraint problem indeed upper bounds the equality constraint problem. This is because the inequality constraint problem could eliminate the users whose rate is too low with negative utility.

Fig. 6.5 illustrates the comparison among the optimal joint resource allocation and user association and two proposed greedy algorithms. We could see that the optimal scheme achieves

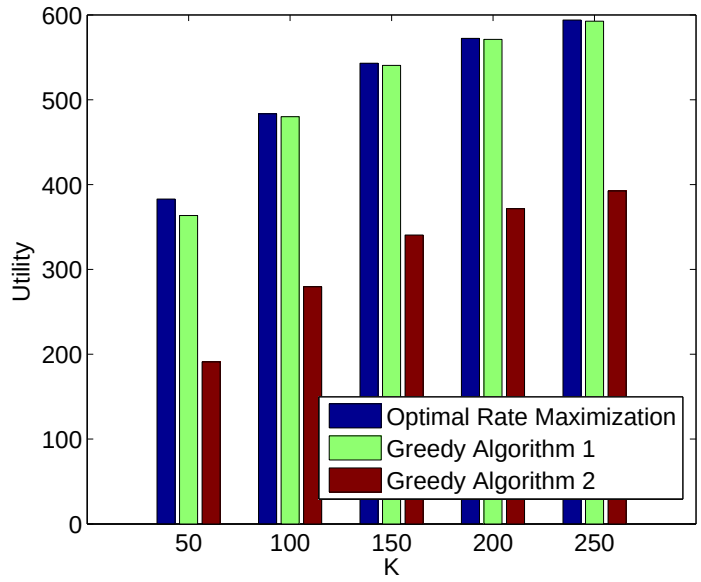

Figure 6.2: Rate Maximization of Centralized Control.

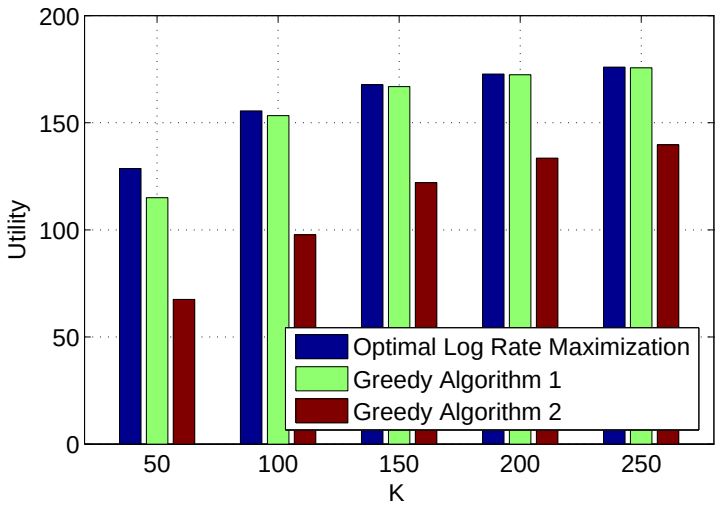

Figure 6.3: Log Rate Utility of Centralized Control.

the highest utility. Moreover, the gap between the optimal scheme and the greedy schemes is very large. We also consider the equality constraint problem as a benchmark for comparison, which is shown in Fig. 6.6 and Fig. 6.7. For fair comparison, we set the sum capacity of this system being equal to the number of users. So there are totally $K = 50$ users active in the system. Fig. 6.6 illustrates the optimal solution of problem (6.32), with optimal network utility as -59.8462. Fig. 6.7 illustrates the optimal solution of problem (6.30), with optimal network utility as 29.5433,

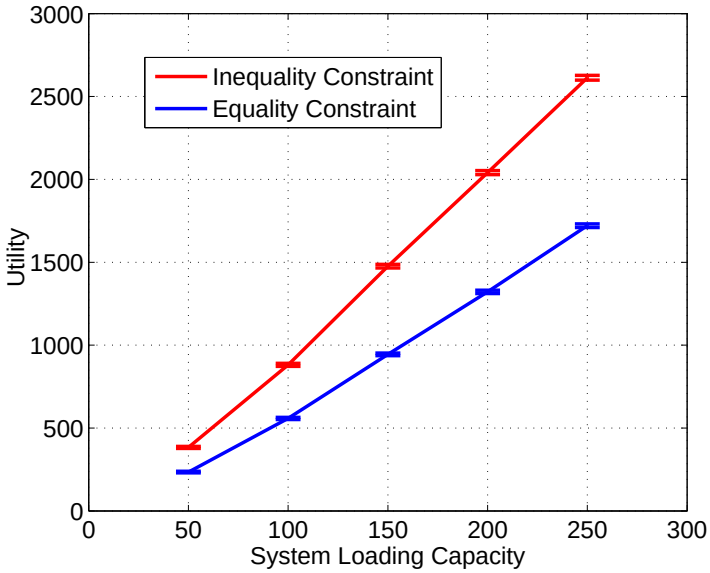

Figure 6.4: Log Rate Utility of Centralized Control.

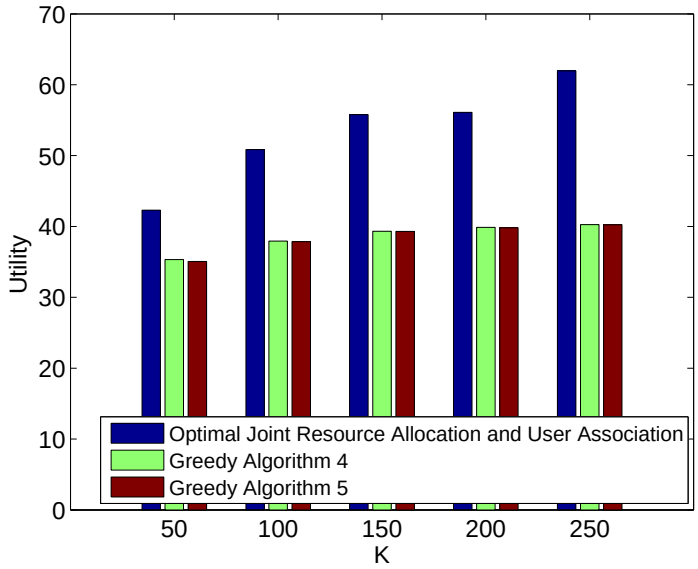

Figure 6.5: Joint Resource Allocation and User Association.

which is much higher than -59.8462. We can also see that if we connect every user. Some edge user with low rate will be harmful for the network utility.

Fig. 6.8 shows the utility of the service provider and all users when the service provider sets the price. We could see that the repeated game converges after 8 round of games. It can also be observed that the utility of all users is monotonically decreasing. That is because once a user's

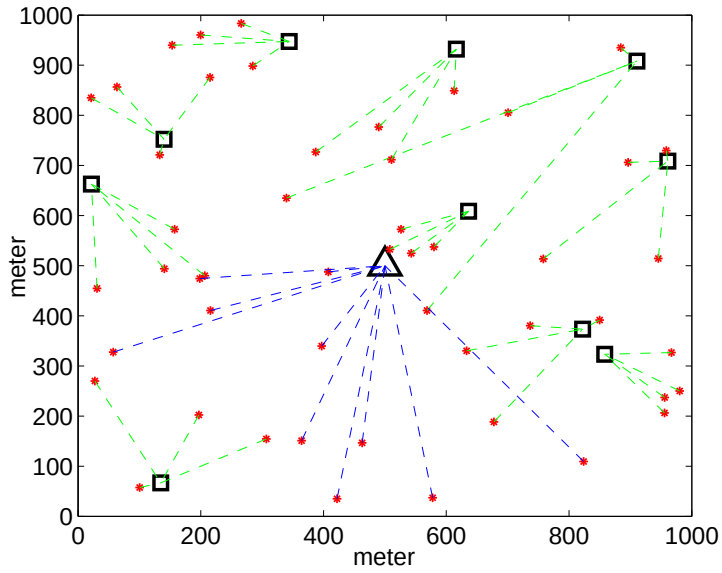

Figure 6.6: Optimal joint resource allocation and user association with equality constraint.

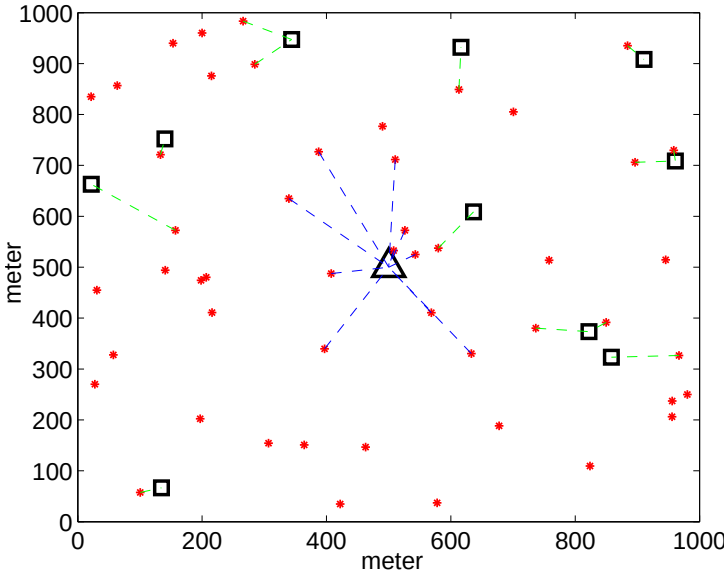

Figure 6.7: Optimal joint resource allocation and user association with inequality constraint.

evaluation is known to the service provider, the service provider will sets price for highest profit, which results in 0 utility for that user. As discussed before, the utility for the service provider is not monotonically increasing, since during the game, the load capacity constraint may be violated. Fig. 6.9 represents the utility of the service provider and users versus the number of users. We can see that as the number of user increases, utility of the service providers increases, which is also

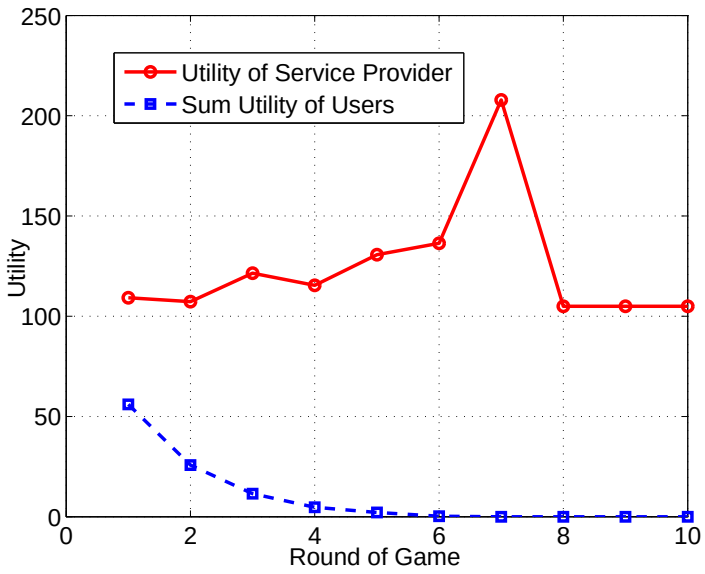

Figure 6.8: Convergence of the repeated game when service provider sets the price and $K = 100$.

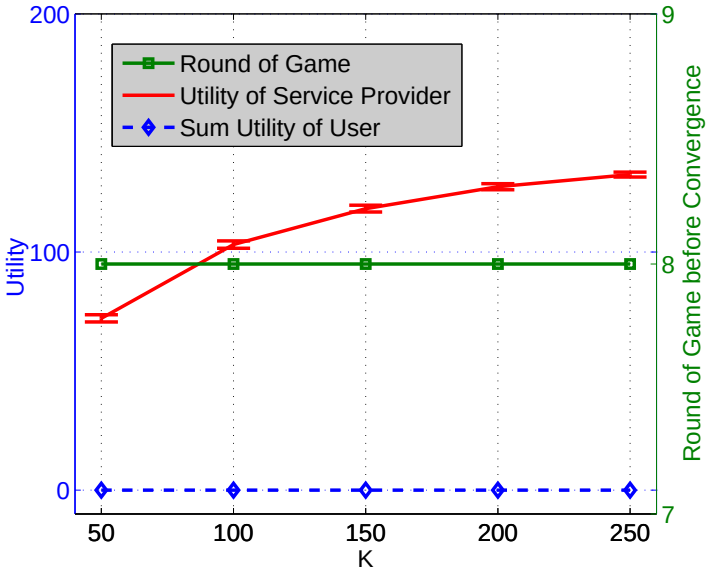

Figure 6.9: Convergence of the repeated game when service provider sets the price and $K = 100$.

mainly due to multi-user diversity gain. We can also observe that the game terminates after about 8 round of games no matter how many users are active.

Fig. 6.10 depicts the process of the game when users bid for base stations. Here we deploy $J = 41$ BSs in the system, equip the massive MIMO BS with $M_{massive} = 400$ antennas and drop $K = 350$ users. The left axis represents the loading of these 41 BSs. The right axis represents the

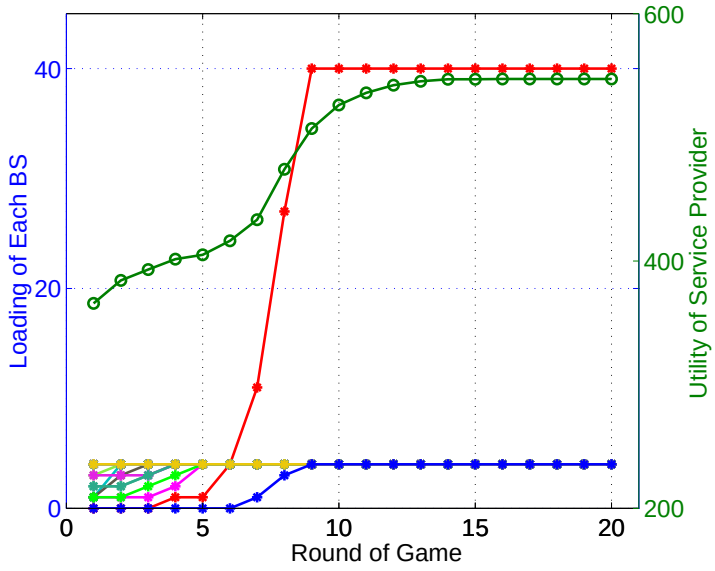

Figure 6.10: Convergence of the repeated game when users bid.

utility of the service provider. We could see that the game converges about 10 round of games. We also note that the utility of the service provider is monotonically increasing as the game continues.

To encourage offloading, rate bias of the BS is considered here. We manually multiple the rate of the massive MIMO BS by a factor of 0.5. Fig. 6.11 shows the result. Here we set the parameters according to Table 6.1. It can be observed that the utility of rate bias is higher than the utility without considering rate bias, which demonstrate the efficacy of rate bias and load balancing. We could also see that the games terminate less than 8 rounds of game.

6.6 Conclusions

In this chapter, we have investigated the user association problem in massive MIMO HetNet from the centralized and distributed perspectives. Particularly, by leveraging totally unimodularity we have obtained the optimal solution to the rate maximization and rate maximization with proportional fairness problems. By applying primal decomposition and dual decomposition we have obtained the optimal solution to the joint resource allocation and user association problem. Modeling the behaviors of the service provider and users using repeated games, we have proven that the games when the service provider sets the price or users bid for connection would converge

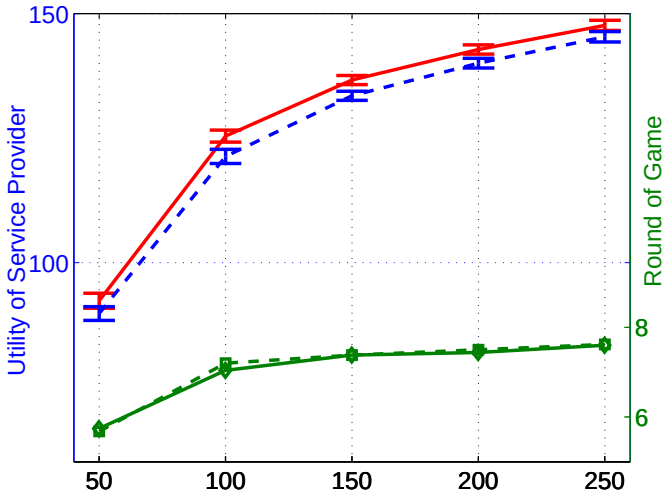

Figure 6.11: Utility sum from all the BSs of the repeated game when users bid.

to the Nash Equilibrium. We have compared the proposed schemes to some heuristic schemes. Simulation results verify the efficacy of our proposed schemes.

Chapter 7

Conclusions

In this dissertation work, several advanced physical layer techniques (MIMO, massive MIMO, OFDM, IA, IDMA) and novel network work level technology (femtocell and CRN), have been reviewed. Overall speaking, all of these techniques are helpful for system throughput enhancement. However, there are many technical challenges for incorporating these techniques to existing wireless networks. For instance, how to adopt IDMA for femtocell network, how to incorporate interference alignment in (MIMO) OFDM network, how will the primary and secondary user behave in future wireless network, how to introduce massive MIMO in FDD systems. To address these challenges motivates this dissertation work.

In Chapter 2, how to manage interference in the uplink of two-tier femtocell networks was investigated. IDMA was adopted to allow concurrent transmissions from all users and cancel the intra- and cross-tier interference with iterative decoding and interference cancellation, while utilizing all the time and frequency resources. Three IDMA based schemes were proposed considering the processing capability of femtocells. Simulation results verified that considerable throughput gains can be achieved at comparatively low costs.

In Chapter 3, how to exploit interferences in OFDM systems to enhance the system throughput was discussed. Since the channel of OFDM system is highly structured, the challenge is how to overcome the difficulty of precoding over dependent subcarriers. With an integer programming formulation, we derived the upper bounds for the multi-user (MIMO) OFDM interference alignment system, and proposed effective algorithms to approach these bounds.

In Chapter 4, how will the primary user and secondary users behave in a MIMO CR network was modeled and investigated. A three-phase cooperative spectrum leasing scheme with distributed interference alignment was proposed. Given the framework, the system was analyzed

using Stackelberg game theory. With backward induction, the unique Stackelberg equilibrium was derived. Simulation results demonstrated that the proposed scheme outperformed a no-spectrum-leasing scheme and a cooperative scheme from prior work. Through analysis, the best strategies for the primary user and secondary users under different configurations were found. Another important insight obtained was, leasing spectrum to secondary users was always helpful for enhancing the primary user utility.

In Chapter 5, user grouping and scheduling problems were studied under the context of massive MIMO system operating in the FDD mode. Typically, weighted likelihood similarity measure, subspace projection based similarity measure, Fubini Study based similarity measure, hierarchical clustering, and K-medoids clustering for user grouping were investigated. A dynamic user scheduling scheme was proposed as well. The load balancing problem when the number of users was small was also investigated. Efficient algorithm for solving the load balancing problem was proposed and validated.

In Chapter 6, user association problem in massive MIMO heterogeneous networks were studied from both centralized and distributed perspectives. Particularly, with a centralized perspective, the rate maximization problem and rate maximization with proportional fairness problem were optimally solved by leveraging totally unimodulairty. Through a series of primal and dual decomposition, the optimal solution to the joint resource allocation and user association problem were also obtained. With a distributed perspective, the behaviors of the service provider and the users were firstly modeled as a repeated game. It was proved that the game would converge and the Nash Equilibrium was obtained.

Although considerable progresses have been made throughout this dissertation work, there are many remaining open problems to explore. Some of them are listed here.

1. The performance of IDMA system depends on the specific coding and decoding scheme. To obtain analytical expressions for each scheme could enable optimizations of throughput or interference control for IDMA system.

2. Joint design of IDMA, (massive) MIMO and OFDM has the potential of further enhance the system throughput.

3. Contents related research could be conducted for CRN with distributed interference alignment. For instance, in the future, video transmissions would consume most of the bandwidth. How to deliver high quality videos considering the QoE (quality of experience) of the primary and secondary user is of great significance.

4. Implementation of MIMO OFDM system with interference alignment could ultimately demonstrate the benefits brought by interference alignment.

5. Investigate the system in which users are also equipped with multiple antennas for massive MIMO system is of great importance, theoretically and practically.

Bibliography

[1] Federal Communications Commission, “Spectrum Policy Task Force,” Rep. ET Docket no. 02-135, Nov. 2002.

[2] A. Goldsmith, S. A. Jafar, I. Maric and S. Srinivasa , “Breaking spectrum gridlock with cognitive radios: an information theoretic perspective,” *Proc. of The IEEE*, vol. 97, no. 5, pp. 894 – 914, May 2009.

[3] V. Chandrasekhar, J. Andrews, and A. Gatherer, “Femtocell networks: A survey,” *IEEE Commun. Mag.*, vol. 46, no. 9, pp. 59 – 67, Sept. 2008.

[4] V. Chandrasekhar and J. Andrews, “Uplink capacity and interference avoidance for two-tier femtocell networks,” *IEEE Trans. Wireless Commun.*, vol. 8, no. 7, pp. 3498 – 3509, July 2009.

[5] T. Alade, H. Zhu and J. Wang, “Uplink Co-Channel Interference Analysis and Cancellation in Femtocell Based Distributed Antenna System,” in *Proc. IEEE ICC’10*, Cape Town, South Africa, May 2010, pp. 1 – 5.

[6] H.-S. Jo, C. Mun, J. Moon, and J.-G. Yook, “Interference mitigation using uplink power control for two-tier femtocell networks,” *IEEE Trans. Wireless Commun.*, vol. 8, no. 10, pp. 4906 – 4910, Oct. 2009.

[7] H.-C. Lee, D.-C. Oh, and Y.-H. Lee, “Coordinated user scheduling with transmit beamforming in the presence of inter-femtocell interference,” in *Proc. ICC’11*, Kyoto, Japan, June 2011, pp. 1 – 5.

[8] D. Hu and S. Mao, “Resource allocation for medium grain scalable videos over femtocell cognitive radio networks,” in *Proc. IEEE ICDCS’11*, Minneapolis, MN, June 2011, pp. 258 – 267.

[9] D. Hu and S. Mao, “Multicast in femtocell networks: A successive interference cancellation approach,” in *Proc. IEEE GLOBECOM’11*, Houston, TX, Dec. 2011, pp. 1 – 6.

[10] P. Li, L. Liu, K. Wu, and W. K. Leung, “Interleave division multipleaccess,” *IEEE Trans. Wireless Commun.*, vol. 5, no. 4, pp. 938 – 947, Apr. 2006.

[11] K. Li, X. Wang, and P. Li, “Analysis and optimization of interleavedivision multiple-access communication systems,” *IEEE Trans. Wireless Commun.*, vol. 6, no. 5, pp. 1973 – 1983, May 2007.

[12] S. M. Perlaza, L. Cottatellucci, and M. Debbah, "A game theoretic framework for decentralized power allocation in IDMA systems," in *Proc. IEEE PIMRC'08*, Cannes, France, Sep. 2008, pp. 1 – 5.

[13] X. Wang and H. V. Poor, "Iterative (turbo) soft interference cancellation and decoding for coded CDMA," *IEEE Trans. Commun.*, vol. 47, no. 7, pp. 1046 – 1061, Jul. 1999.

[14] M. Xiao, N. B. Shroff, and E. K. P. Chong, "A utility-based powercontrol scheme in wireless cellular systems," *IEEE/ACM Trans. Netw.*, vol. 11, no. 2, pp. 210 – 221, Apr. 2003.

[15] Q. Huang, S. Chan, K.-T. Ko, P. Li, and P. Wang, "A QoS architecture for IDMA-based multiservice wireless networks," in *Proc. IEEE ICC'07*, Glasgow, Scotland, Jun. 2007, pp. 5070 – 5075.

[16] Z. Rosberg, "Optimal transmitter power control in interleave division multiple access (IDMA) spread spectrum uplink channels," *IEEE Trans. Wireless Commun.*, vol. 6, no. 1, pp. 192 – 201, Jan. 2007.

[17] T. Yang, J. Yuan, and Z. Shi, "Rate optimization for IDMA systems with iterative joint multiuser decoding," *IEEE Trans. Wireless Commun.*, vol. 8, no. 3, pp. 1148 – 1153, Mar. 2009.

[18] T. Hwang, C. Yang, G. Wu, S. Li, and Y. G. Li,"OFDM and its wireless applications: A survey," *IEEE Trans. Vehi. Technol.*, vol.58, no.4, pp. 1673 – 1694, May 2009.

[19] V. R. Cadambe and S. A. Jafar, "Interference alignment and degrees of freedom of the K-user interference channel," *IEEE Trans. Inform. Theory*, vol. 54, no. 8, pp. 3425 – 3441, Aug. 2008.

[20] C. M. Yetis, T. Gou, S. A. Jafar, and A. H. Kayran,"On feasibility of interference alignment in MIMO interference networks," *IEEE Trans. Signal Process.*, vol.58, no.9, pp.4771 – 4782, Sept. 2010.

[21] M. Shen, C. Zhao, X. Liang, and Z. Ding, "Best-effort interference alignment in OFDM systems with finite SNR," in *Proc. IEEE ICC'11*, Kyoto, Japan, June 2011, pp. 1 – 6.

[22] C. Shi, R. A. Berry, and M. L. Honig, "Interference alignment in multi-carrier interference networks," in *Proc. IEEE ISIT'11*, Saint Petersburg, Russia, July 2011, pp. 1 – 5.

[23] J. Mietzner, R. Schober, L. Lampe, W. H. Gerstacker, and P. A. Hoeher,"Multiple-antenna techniques for wireless communications - A comprehensive literature survey," *IEEE Commun. Surveys & Tutorials*, vol.11, no.2, pp. 87 – 105, Second Quarter, 2009.

[24] Y. Xu and S. Mao, "On interference alignment in multi-user OFDM systems," in *Proc. IEEE GLOBECOM 2012*, Anaheim, CA, Dec. 2012, pp.5339–5344.

[25] V. Kafedziski and T. Javornik, "Frequency-space interference alignment in multi-cell MIMO OFDM downlink systems," *Proc. IEEE VTC Spring*, Dresden, Germany, June 2013, pp. 1–5.

[26] Q. Zhang, Q. Yong, J. Qin, A. Nallanathan, "On the Feasibility of the CJ Three-User Interference Alignment Scheme for SISO OFDM Systems," *IEEE Communications Letters*, to appear.

[27] O. E. Ayach, S. W. Peters and R. W. Heath, Jr., "The feasibility of interference alignment over measured MIMO-OFDM channels," *IEEE Transactions on Vehicular Technology*, vol. 59, no. 9, pp. 4309–4321, Nov. 2010.

[28] M. Maso, M. Debbah, L. Vangelista, "A Distributed Approach to Interference Alignment in OFDM-Based Two-Tiered Networks," *IEEE Transactions on Vehicular Technology*, vol.62, iss.5, pp. 1935–1949, Jun. 2013.

[29] Y. Xu and S. Mao, "Distributed interference alignment in cognitive radio networks," in *Proc. IEEE ICCCN*, Nassau, Bahamas, July/August 2013, pp. 1–7.

[30] Y. Xu and S. Mao, "Stackelberg game for cognitive radio networks with MIMO and distributed interference alignment," *IEEE Transactions on Vehicular Technology*, to appear.

[31] Y. Jin, X.-G. Xia, "An interference alignment based precoder design using channel statistics for OFDM systems with insufficient cyclic prefix," in *Proc. IEEE GLOBECOM*, Anaheim, CA, Dec. 2012, pp. 3778–3782.

[32] L. E. Li, R. Alimi, D. Shen, H. Viswanathan, and Y. R. Yang, "A General Algorithm for Interference Alignment and Cancellation in Wireless Networks," in *Proc. IEEE INFOCOM*, San Diego, CA, Mar. 2010, pp. 1–9.

[33] S. Gollakota, S. D. Perli and D. Katabi, "Interference alignment and cancellation," in *Proc. ACM SIGCOMM*, Barcelona, Spain, Aug. 2009, pp. 159–170.

[34] M. El-Hadidy, M. El-Absi, L. Sit, "Improved Interference Alignment Performance for MIMO OFDM Systems by Multimode MIMO Antennas," in *Proc. IEEE InOWo*, Essen, Germany, Aug. 2012, pp. 1–5.

[35] C. Le, E. Dimitrov, A. Anggraini, J. Peissig, and H.-P. Kuchenbecker, "Effect of spatial correlation on MMSE-based interference alignment in a multiuser MIMO MB-OFDM system," in *Proc. IEEE WiMob*, Barcelona, Spain, Oct. 2012, pp. 739–744.

[36] S. Jafar, "Interference Alignment: A New Look at Signal Dimensions in a Communication Network," *Foundations and Trends in Communications and Information Theory*, vol.7, no.1, pp. 1–136, 2010.

[37] Y. Xu and S. Mao, "On interference alignment in multi-user OFDM systems," in *Proc. IEEE GLOBECOM*, Anaheim, CA, Dec. 2012, pp. 5339–5344.

[38] H. Li, T. Jiang and Y. Zhou,"A novel subblock linear combination scheme for peak-to-average power ratio reduction in OFDM systems," *IEEE Transactions on Broadcasting*, vol. 58, iss. 3, pp. 360–369, Sep. 2012.

[39] V. Dalakas, P. T. Mathiopoulos, F. Di Cecca, G. Gallinaro, "A comparative study between SC-FDMA and OFDMA schemes for satellite uplinks," *IEEE Transactions on Broadcasting*, vol. 58, iss. 3, pp. 370–378, Sep. 2012.

[40] Jong-Seob Baek and Jong-Soo Seo, "Efficient pilot patterns and channel estimations for MIMO-OFDM systems," *IEEE Transactions on Broadcasting*, vol. 58, iss. 4, pp. 648–653, Dec. 2012.

[41] K. Gomadam, T. Gou, V. R. Cadambe and S. A. Jafar,"A distributed numerical approach to interference alignment and applications to wireless interference networks," *IEEE Trans. Inf. Theory*, vol. 57, no. 6, pp. 3309 – 3322, June 2011.

[42] D. Fudenberg and J. Tirole, *Game Theory*. Cambridge, MA: MIT Press, 1993.

[43] S. Haykin, "Cognitive Radio: Brain-Empowered Wireless Communications," in *IEEE Journal on Selected Areas in Communications*, vol. 23, no. 2, pp. 201 – 220, Feb. 2005.

[44] Q. Li, G. Li, and W. Lee et al, "MIMO techniques in WiMAX and LTE: a feature overview" *IEEE Communications Magazine*, vol. 48, pp. 86 – 92, May 2010.

[45] S. Boyd and L. Vandenberghe, *Convex Optimization*. Cambridge, UK: Cambridge University Press, 2004.

[46] D. Tse and P. Viswanath, *Fundamentals of Wireless Communication*. Cambridge, UK: Cambridge University Press, 2005.

[47] J. Zhang and Q. Zhang, "Stackelberg game for utility-based cooperative cognitive radio networks," in *Proc. ACM MobiHoc'11*, New Orleans, LA, May 2011, pp. 23 – 31.

[48] Y. Xu and S. Mao, "On interference alignment in multi-user OFDM systems," in *Proc. IEEE GLOBECOM'12*, Anaheim, CA, Dec. 2012, pp. 1 – 6.

[49] A. A. Daoud, T. Alpcan, S. Agarwal and M. Alanyali, "A Stackelberg game for pricing uplink power in wide-band cognitive radio networks," in *Proc. IEEE CDC'08*, Cancun, Mexico, Dec. 2008, pp. 1422 – 1427.

[50] Y. Xiao, G. Bi and D. Niyato, "Distributed optimization for cognitive radio networks using Stackelberg game," in *Proc. IEEE ICCS'10*, Singapore, Nov. 2010, pp. 77 – 81.

[51] D. Niyato, E. Hossain and Z. Han, "Dynamics of Multiple-Seller and Multiple Buyer Spectrum Trading in Cognitive Radio Networks: A Game Theoretic Modeling Approach," *IEEE Trans. Mobile Comput.*, vol. 8, no. 8, pp. 1009 – 1022, Aug. 2009.

[52] M. Amir, A. El-Keyi and M. Nafie, "Opportunistic Interference Alignment for Multiuser Cognitive Radio," in *Proc. IEEE ITW*, Dublin, Ireland, Aug.-Sep. 2010, pp. 1 – 5.

[53] H. Zhou, T. Ratnarajah and Y. Liang, "On Secondary Network Interference Alignment in Cognitive Radio," in *Proc. IEEE DySPAN*, Aachen, Germany, May. 2011, pp. 637 – 641.

[54] D. Hu and S. Mao, "Cooperative relay with interference alignment for video over cognitive radio networks, " in *Proc. IEEE INFOCOM'12*, Orlando, FL, Mar. 2012, pp. 2014 – 2022.

[55] K.-H. Park and M.-S.Alouini, "Alternate MIMO AF Relaying Networks With Interference Alignment: Spectral Efficient Protocol and Linear Filter Design," IEEE Transactions on Vehicular Technology, vol. 62, no. 2, pp. 914 – 920, Feb. 2013.

[56] T.-W. Tang, M.-k. Chen and H.-F. Lu, "Improving the DMT Performance for MIMO Communication With Linear Receivers," IEEE Transactions on Vehicular Technology, vol. 62, no. 3, pp. 1189 – 1200, Mar. 2013.

[57] K. T. Truong and R. W. Heath Jr., "Joint Transmit Precoding for the Relay Interference Broadcast Channel," IEEE Transactions on Vehicular Technology, vol. 62, no. 3, pp. 1201 – 1215, Mar. 2013.

[58] E. G. Larsson, F. Tufvesson, O. Edfors, and T. L. Marzetta, "Massive MIMO for Next Generation Wireless Systems", *IEEE Communications Magazine*, vol. 52, no. 2, pp. 185–195, Feb. 2014.

[59] F. Rusek, D. Persson, B. K. Lau, E. G. Larsson, T. L. Marzetta, O. Edfors, and F. Tufvesson, "Scaling Up MIMO Opportunities and challenges with very large arrays," *IEEE Signal Processing Magazine*, vol. 30, iss. 1, pp. 40–60, Jan. 2013.

[60] C. Shepard, H. Yu, N. Anand, L. E. Li, T. L. Marzetta, R. Yang, and L. Zhong, "Argos: Practical Many-Antenna Base Stations", in Proc. *ACM MobiCom'12*, Istanbul, Turkey, pp. 53-64, Aug. 2012.

[61] C. Shepard, H. Yu, and L. Zhong, "ArgosV2: A Flexible Many-Antenna Research Platform," to appear in *ACM Mobicom'13*, Miami, FL, Sep. 2013.

[62] J. Jose, A. Ashikhmin, T. L. Marzetta, and S. Vishwanath, "Pilot Contamination and Precoding in Multi-cell TDD Systems," *IEEE Transactions on Wireless Communications*, vol. 10, no.8, pp. 2640–2651, Aug. 2011.

[63] F. Fernandes, A. Ashikhmin, and T. L. Marzetta, "Inter-Cell Interference in Noncooperative TDD Large Scale Antenna Systems", *IEEE Journal on Selected Areas in Communications*, vol. 31, no. 2, pp. 192–201, Feb. 2013.

[64] J. Hoydis, K. Hosseini, S. ten Brink, and M. Debbah, "Making Smart Use of Excess Antennas: Massive MIMO, Small Cells, and TDD," *Bell Labs Technical Journal*, vol. 18, no. 2, pp. 5–21, Sep. 2013.

[65] "List of LTE networks," http://en.wikipedia.org/wiki/List of LTE networks

[66] A. Adhikary, J. Nam, J.-Y. Ahn, and G. Caire, "Joint spatial division and multiplexing-the large-scale array regime," *IEEE Transactions on Information Theory*, vol. 59, no. 10, pp. 6441–6463, Oct. 2013.

[67] A. Adhikary and G. Caire, “Joint spatial division and multiplexing: opportunistic beamforming and user grouping”, available online: http://arxiv.org/abs/1305.7252.

[68] Y. Xu, G. Yue, N. Prasad, S. Rangarajan, and S. Mao, “User grouping and scheduling for large scale MIMO systems with two-stage precoding,” in Proc. *IEEE ICC*, Sydney, Australia, pp. 5208-5213, Jun. 2014.

[69] J. Choi, D. J. Love, and P. Bidigare, “Downlink Training Techniques for FDD Massive MIMO Systems: Open-Loop and Closed-Loop Training with Memory,” to appear in *IEEE Journal of Selected Topics in Signal Processing*.

[70] J. Choi, Z. Chance, D. Love, and U. Madhow, “Noncoherent Trellis Coded Quantization: A Practical Limited Feedback Technique for Massive MIMO Systems,” *IEEE Trans. Commun.*, vol. 61, no. 12, pp. 5016–5029, Dec. 2013.

[71] S. Noh, M. Zoltowski, Y. Sung, and D. Love, “Pilot Beam Pattern Design for Channel Estimation in Massive MIMO Systems,” to appear in *IEEE Journal of Selected Topics in Signal Processing*.

[72] H. Noh, Y. Kim, J. Lee, and C. Lee, “Codebook Design of Generalized Space Shift Keying for FDD Massive MIMO Systems in Spatially Correlated Channels,” to appear in *IEEE Transactions on Vehicular Technology*.

[73] X. Rao, V. Lau, “Distributed Compressive CSIT Estimation and Feedback for FDD Multi-User Massive MIMO Systems,” *IEEE Transactions on Signal Processing*, vol. 62, no. 12, pp. 3261–3271, Jun. 2014.

[74] J. Chen, V. Lau, “Two-Tier Precoding for FDD Multi-cell Massive MIMO Time-Varying Interference Networks,” to appear in *IEEE Journal on Selected Areas in Communications*.

[75] D. Bethanabhotla, O.Y. Bursalioglu, H.C. Papadopoulos, and G. Caire, “User association and load balancing for cellular massive MIMO,” in Proc. *IEEE Information Theory and Applications Workshop*, San Diego, CA, pp. 1–10 Feb. 2014.

[76] T. L. Marzetta, “Noncooperative cellular wireless with unlimited numbers of base station antennas,” *IEEE Transactions on Wireless Communications*, vol. 9, no. 11, pp. 3590–3600, Nov. 2010.

[77] C. Shepard, N. Anand, and L. Zhong, “Practical Performance of MU-MIMO Precoding in Many-Antenna Base Stations,” in Proc. *ACM CellNet*, Taipei, Taiwan, pp. 13–18, Jun. 2013.

[78] Q. Ye, B. Rong, Y. Chen, M. A.-Shalash, C. Caramanis, and J. G. Andrews, “User association for load balancing in heterogeneous cellular networks,” *IEEE Transactions on Wireless Communications*, vol. 12, no. 6, pp. 2706–2716, Jun. 2013.

[79] Cisco Visual Networking Index: Global Mobile Data Traffic Forecast Update, 2012-2017, Cisco White Paper, Feb.6 2013, [online] Available: `http://www.cisco.com/en/US/solutions/collateral/ns341/ns525/ns537/ns705/ns827/white_paper_c11-520862.html`.

[80] J. Andrews, S. Buzzi, et al, "What will 5G be?," *IEEE Journal on Selected Areas in Communications*, vol. 32, no. 6, pp. 1065–1082, Jun. 2014.

[81] Y Xu, G. Yue, and S. Mao, "User grouping for Massive MIMO in FDD systems: New design methods and analysis," *IEEE Access Journal, Special Section on 5G Wireless Technologies: Perspectives of the Next Generation Mobile Communications and Networking*, vol.2, no.1, pp. 1-13, Dec. 2014.

[82] S. Bayat, R. Louie, et al, "Distributed user association and femtocell allocation in heterogeneous wireless networks," *IEEE Transactions on Communications*, vol. 62, no. 8, pp. 3027–3043, Aug. 2014.

[83] A. Gupta, H. Dhillon, S. Vishwanath, and J. Andrews, "Downlink Multi-Antenna Heterogeneous Cellular Network with Load Balancing," *arXiv:1310.6795v2*.

[84] E. Björnson, M. Kountouris, and M. Debbah, "Massive MIMO and Small Cells: Improving Energy Efficiency by Optimal Soft-Cell Coordination," *arXiv:1304.0553v3* .

[85] A. Damnjanovic, J. Montojo, et al,"A survey on 3GPP heterogeneous networks," *IEEE Wireless Communications*, vol. 18, iss. 3, pp. 10–21, Jun. 2011.

[86] L. Lu, G. Li, A. Swindlehurst, A. Ashikhmin, and R. Zhang, " An overview of massive mimo: benefits and challenges," *IEEE Journal on Selected Topics in Signal Processing*, vol. 8, no. 5, pp. 742–758, Oct. 2014.

[87] R. Karp, "Reducibility among Combinatorial Problems," *Complexity of Computer Computations*, pp. 85–103, Mar. 1972.

[88] A. Schrijver, "Theory of linear and integer programming," John Wiley & Sons, Jun. 1998.

[89] C. Berenstein and R. Gay, "Complex Variables: An Introduction," Springer, 1997.

[90] D. Palomar and M. Chiang, "A tutorial on decomposition methods for network utility maximization," *IEEE Journal on Selected Areas in Communications*, vol. 24, no.8, pp. 1439–1451, Aug. 2006.

Appendices

Appendix A

Publication

A.1 JOURNAL PUBLICATIONS

1. **Yi Xu** and Shiwen Mao, "User Association in Massive MIMO System with Small Cells," under review (12 pages).

2. **Yi Xu**, Shiwen Mao and Xin Su, "Interference Alignment Improves the Capacity of OFDM Systems," accepted to appear in *IEEE Transactions on Vehicular Technology* (12 pages).

3. **Yi Xu**, Guosen Yue, and Shiwen Mao, "User grouping and load balancing for FDD massive MIMO systems," invited paper, *E-Letter of IEEE Communications Society Multimedia Communications Technical Committee (MMTC)*, Special Issue on Large-Scale MIMO, vol. 9, no. 6, pp.28-31, Nov. 2014.

4. **Yi Xu**, Donglin Hu and Shiwen Mao, "Relay-assisted multi-user video streaming in cognitive radio networks," *IEEE Transactions on Circuits and Systems for Video Technology*, vol.24, no.10, pp.1758-1770, Oct. 2014.

5. **Yi Xu**, Guosen Yue, and Shiwen Mao, "User grouping for Massive MIMO in FDD systems: New design methods and analysis," *IEEE Access Journal, Special Section on 5G Wireless Technologies: Perspectives of the Next Generation Mobile Communications and Networking*, vol.2, no.1, pp.947-959, Sep. 2014.

6. **Yi Xu** and Shiwen Mao, "Stackelberg game for cognitive radio networks with MIMO and distributed interference alignment," *IEEE Transactions on Vehicular Technology*, vol.63, iss.2, pp.879-892, Feb. 2014.

7. **Yi Xu** and Shiwen Mao, "A survey of mobile cloud computing for rich media applications," *IEEE Wireless Communications, Special Issue on Mobile Cloud Computing*, vol.20, no.3, pp.46-53, Jun. 2013.

A.2 CONFERENCE PUBLICATIONS

1. **Yi Xu**, Guosen Yue, Narayan Prasad, Sampath Rangarajan, and Shiwen Mao, "User grouping and scheduling for large scale MIMO systems with two-stage precoding," in *Proceedings of IEEE ICC 2014*, pp. 5197-5202, Sydney, Australia, Jun. 2014.

2. **Yi Xu** and Shiwen Mao, "Distributed interference alignment in cognitive radio networks," in *Proceedings of IEEE ICCCN 2013*, pp. 1-7, Nassau, Bahamas, July/August 2013.

3. **Yi Xu** and Shiwen Mao, "On interference alignment in multi-user OFDM systems," in *Proceedings of IEEE GLOBECOM 2012*, pp. 5339-5344, Anaheim, CA, Dec. 3-7, 2012.

4. **Yi Xu**, Shiwen Mao, and Xin Su, "On adopting interleave division multiple access to two-tier femtocell networks: the uplink case," in *Proceedings of IEEE ICC 2012*, pp. 591-595, Ottawa, Canada, Jun. 10-15, 2012.

A.3 BOOK CHAPTER

1. **Yi Xu** and Shiwen Mao, "Mobile cloud media: State of the art and outlook," in *Mobile Computing over Cloud: Technologies, Services, and Applications*, Chapter 2, pp.18-38, J. Rodrigues, K. Lin, and J. Lloret (Editors), IGI Global: Hershey, PA, 2013. ISBN13: 9781466647817; DOI: 10.4018/978-1-4666-4781-7.ch002.